Exploration of signalling molecule interactions to protect against a heart attack and heart failure, using STAT3 deficient & PKCε over-expressing mice

Presented for M.Sc. (Medicine)

Submitted by:

Ageela Imamdin

Hatter Institute for Cardiovascular Research in Africa,

Department of Medicine

Faculty of Health Science

University of Cape Town

February 2013

Supervisors

Dr Joy McCarthy

(Department of Chemical Pathology, Division of Lipidology, UCT)

Associate Professor Sandrine Lecour

(Hatter Institute for Cardiovascular Research in Africa, UCT)

Declaration

1. I know that plagiarism is wrong. Plagiarism is to use another's work and pretend that it is one's own.

2. I have used the Journal of Biochemistry convention for citation and referencing. Each contribution to, and quotation in, this proposal from the work(s) of other people has been attributed, and has been cited and referenced.

3. This submission is my own work.

4. I have not allowed, and will not allow, anyone to copy my work with the intention of passing it off as his or her own work.

5. I acknowledge that copying someone else's assignment or essay, or part of it, is wrong, and declare that this is my own work.

Signature _____ Date_____

Acknowledgements:

I would like to acknowledge and thank the National Research Foundation for funding my studies for two years of this project.

I would like to thank the Medical Research Council and Cape Heart group for funding parts of my project.

I would like to acknowledge and thank Professor Karen Sliwa as head of the Hatter Institute for Cardiovascular Research in Africa for financial and moral support throughout this project, and I would like to thank everybody in the lab that had assisted me with all elements of it.

I would like to acknowledge and thank Dr Neil Davies and his group at the Cape Heart Centre who assisted with the histology sections of this project.

I would like to acknowledge and thank Dr Ben Loos and his team in the Department of Physiology at the University of Stellenbosch for their assistance in the staining and fluorescence imaging section of this project.

I would like to make special mention of Gaurang Deshpande and thank him for all his efforts and help, especially when it came to discussing heart failure, and for keeping me company in the lab at odd hours when "I think someone else is on the other side" (in fact, these were the freezer fans switching on in the freezer room).

I would like to thank my parents, Zubeida and Shamsuddin Imamdin, and my brother, Mohammed Irfaan Imamdin, for their support always.

I would like to thank my co-supervisor Associate Professor Sandrine Lecour for everything she has done to help me through this project and for her support and encouragement.

I would like to thank my supervisor Dr Joy McCarthy for absolutely everything she has done for me, for having unwavering faith in me, and for being the best and most awesome supervisor I could have asked for.

Summary

Introduction: Heart failure (HF) is the inability of the left ventricle to fill with or eject blood. It often occurs as a side-effect of cardiovascular complications such as ischemia. At the molecular level, Signal Transducer and Activator of Transcription 3 (STAT3) is linked to the heart and HF, as STAT3 deficient (STAT3 KO) mouse models have shown development of HF with age. STAT3 is well known for its pro-survival effect in many instances of injury in the heart, and these effects are remarkably similar to PKCε, another known pro-survival molecule in the heart

Aims and objectives: We investigated the possibility of an interaction between STAT3 and PKCε in the induction of cardioprotection in the heart.

Methods: A specific PKCε-activator was administered via intra-peritoneal injection in mice to mimic a PKCε over-expressing mouse model. These mice were sacrificed, hearts excised and fibres permeabilized and simultaneously treated with a STAT3 inhibitor (or vehicle control) to determine whether inhibition of STAT3 would affect the recovery in respiration after a 25 minute hypoxic insult , compared to saline-treated wildtype (WT) controls. This procedure was repeated with STAT3 KO mouse permeabilized heart fibres which were treated with a PKCε-activator to determine whether activation of PKCε could counter the STAT3 KO and improve the recovery in respiration. As STAT3KO is associated with heart failure with age, aged STAT3 KO mice were sacrificed and heart fibres permeabilized for respiration studies, to determine whether mitochondrial respiration would be impaired with a fatty acid substrate compared to a control substrate, as inability to respire with a fatty acid substrate is typical of the failing heart. Histological staining (picro-sirius stain) was also performed on these aged mouse hearts to quantify fibrosis, a marker for heart failure. Fluorescence imaging was performed on these hearts to observe patterns of colocalization of PKCε and STAT3.

Results: No significant differences detected in mitochondrial respiration for PKCε-activated heart fibres with STAT3 inhibitor treatment when compared to control. No significant differences were detected in

STAT3 KO fibres when treated with a PKCε-activator when compared to control. Fatty acid oxidation was unimpaired in aged STAT3 KO hearts compared to wildtype control hearts, and histology staining showed no significant difference in the amount of fibrosis between the STAT3 KO group compared to the wildtype control group. Fluorescence imaging in aged hearts showed presence of STAT3 in the hearts of STAT3 KO mice, and no difference in the areas colocalization of PKCε and STAT3 in STAT3 KO hearts compared to wildtype controls.

Conclusion: Our findings here suggest that the model we have used to mimic PKCε over-expressing mice was not as effective as the genetic overexpressing mouse model it has been designed to mimic. The STAT3 KO model established in our laboratory was also not displaying the expected phenotype found in the original mice, possibly as a result of incorrect genotyping and /or breeding. From the findings in our model, we cannot categorically support or deny the possibility of an interaction between the signalling of PKCε and STAT3.

Abbreviations:

ACE	Angiotensin converting enzyme, a circulating peptidase enzyme regulating blood pressure
AG490	JAK inhibitor
AKT1	Serine-threonine protein kinase
p-AKT1	AKT1 phosphorylated at serine reside 473
t-AKT1	total AKT1
ANF	Atrial naturetic factor, a hormone released by atrial tissue which increases elimination of sodium by the kidney
AngII	Angiotensin II, a potent vasopressor stimulating the production and release of aldosterone from the adrenal cortex
AP-1	Activator protein-1, a transcription factor regulating gene expression in response to stimuli, controlling cellular processes including differentiation, proliferation, and apoptosis
ARB	AT1 agonist
AT1	Angiotensin II type 1 receptor, a vasopressor affecting the release of aldosterone
ATP	Adenosine triphosphate
BAD	Bcl-2-associated death promoter, a pro-apoptotic protein
BalbC	Inbred albino laboratory mice
Bcl-xL	Follicular B cell lymphomas xL, a pro-survival protein
cGMP	Cyclic guanosine-3', 5'-monophosphate, a cyclic nucleotide of guanosine that regulates various metabolic processes
COX-2	Cyclooxygenase-2, an enzyme mediating inflammation and pain
CT-1	Cardiotrophin-1, a cytokine involved in the pathophysiology of heart disease
CVD	Cardiovascular diseases
Cx43	Connexin 43, an integral membrane protein which aggregate together to form gap junctions, through which ions diffuse to a neighbouring cell
DAG	Diacylglycerol
DMSO	Dimethyl Sulfoxide
DNA	Dexyribo nucleic acid
Dox	Doxorubicin, a drug used in anti-cancer therapy, also used to induce heart failure
ECL	Enhanced chemiluminescent agent
ERK	Extracellular signal-regulated kinase1 and 2, members of the mitogen-activated protein

	kinase super family that can mediate cell proliferation and apoptosis
p-ERK1/2	ERk1/2 phosphorylated at threonine residue 202 / tyrosine residue 204
t-ERK1/2	Total ERK1/2
GAPDH	Glyceraldehyde 3-phosphate dehydrogenase
G-CSF	Granulocyte colony stimulating factor, a blood growth factor which stimulates bone marrow to produce white blood neutrophils
gp130	Glycoprotein 130, a transmembrane protein and cytokine receptor which works in conjunction with other cell surface receptors
GPCR	G-protein coupled receptor, cell surface receptors which transduce external signals to produce cellular responses
GSK3β	glycogen synthase kinase 3 β, a serine-threonine kinase initially identified to phosphorylate glycogen synthase, thereby inactivating it
HF	Heart failure
HIF-1α	Hypoxia-induced factor 1 alpha, a transcription factor found in mammalian cells growing at low oxygen concentrations
I/R	Ischemia / reperfusion
IL	Interleukin, a group of cytokines which regulate cellular processes such as cell growth, differentiation and motility
IPC	Ischemic preconditioning, short bursts of ischemia and reperfusion prior to an extended ischemic insult
IPostC	Ischemic postconditioning, short bursts of ischemia and reperfusion after an extended ischemic insult
JAK	Janus kinase, self-phosphorylating of cell-surface receptors which recruit and phosphorylate STAT proteins
JNK	c-Jun N-terminal protein kinase, members of the mitogen-activated protein kinase family that bind and phosphorylate c-Jun. They respond to stress stimuli, such as cytokines. Also plays a role in T cell differentiation and apoptosis
KATP channel	ATP-gated potassium-sensitive channel
KCl	Potassium chloride
Lck	lymphocyte-specific protein kinase, a tyrosine kinase found in lymphocyte cells involved in signal transduction
LIF	Leukaemia inhibitory factor, an interleukin 6-typecytokineaffecting cellular growth by inhibiting differentiation

LV	Left ventricle of the heart
LVDP	Left ventricular developed pressure, a typical measure of cardiac function
MAP 42/44	ERK1/2
MAPK	Mitogen-activated protein kinase, a family of serine/ threonine protein kinases involved in signal transduction for cellular processes including cell proliferation, differentiation and migration
Mcl-1	myeloid cell leukemia-1, an anti-apoptotic protein
αMHC	Alpha myosin heavy chain, a contractile protein dominantly expressed in adult mammalian hearts
βMHC	Beta myosin heavy chain, a contractile protein dominantly expressed in foetal mammalian hearts
MI	Myocardial infarction, a scar on the heart formed as a result of a lack of oxygen, causing myocyte death and formation of a fibrotic scar tissue
mitoKATP	Mitochondrial ATP-gated potassium ion channel
MLC2V	A form of myosin specific for the ventricle of the mammalian heart
MnSOD	Manganese superoxide dismutase, enzymes catalysing dismutation of superoxide into hydrogen peroxide and oxygen
mPTP	Mitochondrial permeability transition pore, a calcium dependent pore in the mitochondrial membrane
NAC	N-acetyl-l-cysteine, a reactive oxygen species scavenger
NFκβ	Nuclear factor kappa beta, a transcription factor involved in immune and inflammatory responses
NIH	National institute of health
NO	Nitric oxide, an oxygen free-radical
NOS	Nitric oxide synthase, an enzyme which catalyses production of nitric oxide from L-arginine
PBS	Phosphate buffered saline
PKCε	Protein kinase C epsilon
aPKCε	Activated Protein Kinase C epsilon
PKCε WT	Protein Kinase C epsilon wildtype
PLC	Phospholipase C, a family of enzymes which cleave phospholipids in the initial phases of cellular signal transduction
PMA	Phorbol 12-myristate 13-acetate, a broad-spectrum Protein Kinase C inhibitor

PVDF	Polyvinylidene difluoride, a non-reactive thermoplastic membrane
ψεRACK	Receptor for activated C-kinase, PKCε -specific activator
RAS	Renin-angiotensin system, a hormone system which regulates fluid balance and blood pressure
RISK	Reperfusion injury salvage kinase pathway, a pro-survival pathway involving PKCε
ROS	Reactive oxygen species
RPC	Remote preconditioning, short bursts of ischemia and reperfusion in remote organs prior to an extended ischemic incident
SAFE	Survival-activating factor enhancement pathway, a pro-survival pathway involving STAT3
Src	Sarcoma, tyrosine kinases transmitting integrin-dependent signals affecting cell proliferation and movement
STAT3	Signal transducer and activator of transcription 3
p-ser STAT3	STAT3 phosphorylated at serine residue 727
p-tyr STAT3	STAT3 phosphorylated at tyrosine residue 705
STAT3 KO	STAT3 deficient mice
STAT3 WT	STAT3 wildtype mice
STATTIC	STAT3 inhibitory compound
TBS-T	Tris buffered saline containing tween
TGFβ1	Transforming growth factor beta-1, a secreted protein affecting cell proliferation, growth and differentiation
TNFα	Tumor necrosis factor alpha, a cytokine inducing inflammation. Its primary role is in the regulation of immune cells
WT	Wildtype

Table of Contents Page no.

Chapter 2 – Materials and Methods

Chapter 3 – Results

A: Introduction:

1.1) Cardiovascular disease

Cardiovascular disease (CVD) is a group of disorders affecting the heart and blood vessels and is the number one cause of death worldwide, with more people dying of CVDs annually than of any other cause. In 2008 alone, 17.3 million people died of cardiovascular complications, accounting for one third of all deaths [1], [2]. Stereotypically, heart conditions supposedly exclusively affect wealthy people with a taste for rich foods and who live sedentary, luxurious lives. In reality 80% of cardiovascular deaths take place in low- and middle-income households. The burden of CVDs is closely linked to the national income of the countries where statistics have been obtained (see fig. 1) [3]. It is projected that 23.6 million people will die from CVD's by 2030, and it will continue to be the single leading cause of morbidity internationally [1]. In South Africa alone, 195 people die every day due to heart attacks, strokes and heart failure (HF) [4].

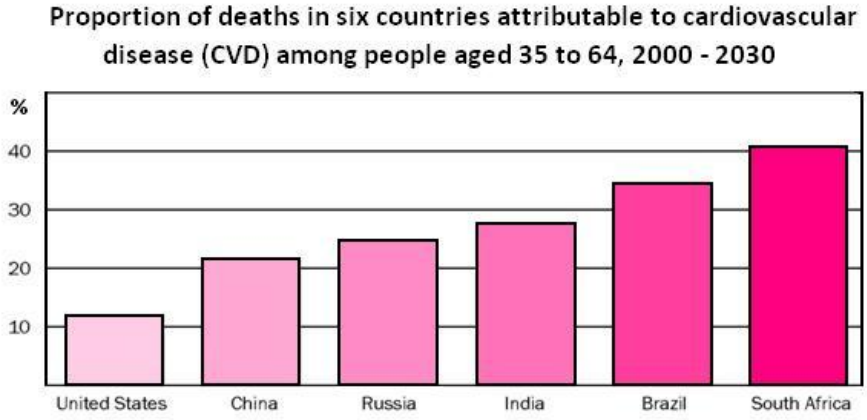

Figure1: Percentage of deaths due to CVD per 100 000 predicted for five developing countries and one comparator country (USA) for the period 2000 - 2030, assuming current CVD rates. [5]

B: Heart failure

1.2.1) Development and increase in incidence of heart failure

Treatments for heart conditions have been drastically improved in recent years. More people are surviving conditions like myocarditis (inflammation of the heart muscle tissue) and heart attacks. Myocardial Infarction, or a heart attack, is the occurrence of cell death in part of the heart tissue when a coronary artery has been occluded for a period of time [6]. Blood flow and oxygen cannot reach a portion of the heart muscle (ischemia), leading to localised cell death and ultimately the formation of fibrous scar tissue in the heart which impairs contractility [7]. While life expectancy and survival has tremendously improved, there are sequelae for the resultant chronic conditions – with time, the onset of heart failure (HF) may occur [8]. HF is one of the CVDs prevalent in poorer communities right across the globe. For centuries it was known as 'dropsy'. It was described by Hippocrates more than two millennia ago and was identified as a shortness of breath with peripheral swelling in the body. HF presented as an enlarged ventricular chamber with an increased heart mass in patients from autopsies performed in the 17th and 18th centuries. [7]. There is no set criteria that defines HF. It can stem from an array of pre-existing medical conditions and display many different physical symptoms, the most common of which are exercise intolerance and muscle fatigue [9]. There are multiple specific types of HF including right-, left-, congestive- and dilated HF, all displaying different physical attributes. For the purposes of this project, we will consider heart failure as characterised by Cohn et al to be the inability of the left ventricle to fill with or eject blood, thereby failing to meet the body's demand for nutrients and oxygen (see fig. 2) [10]. It is estimated that two thirds of all cases of heart failure stem from ischemic heart disease resulting from altered coronary artery circulation or myocardial infarction. Each year, about one million people suffer from acute myocardial infarction and within 6 years, just less than one third of these patients develop HF [11], [12].

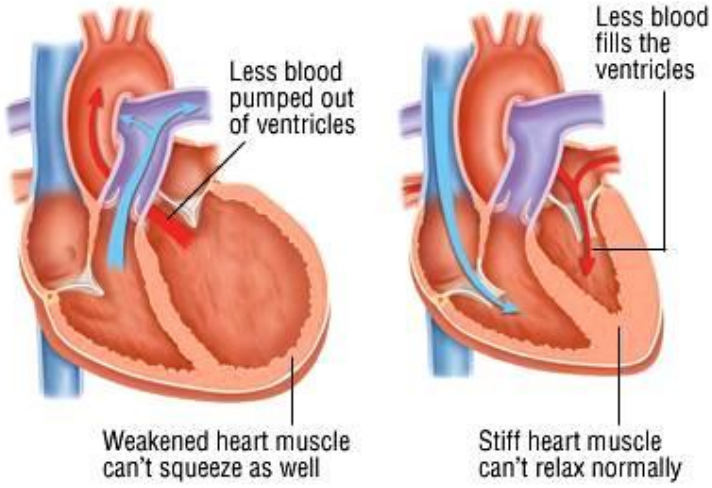

Figure2: Heart failure, as defined by Cohn et al is the inability of the left ventricle to fill with or eject blood. This is not due to a single physical property, but rather many different ones that bring about the same outcome. One such example is a dilated heart chamber with a weakened heart muscle (left) which cannot effectively eject blood, and a second (right) is a hypertrophied, stiffened chamber wall which cannot fully relax to allow the ventricle to fill with blood. Picture taken from: [13]

The remaining third of HF cases can have multiple origins including pressure overload, cardiomyopathies and defects in genes encoding an array of proteins with cellular functions, such as cytoskeleton, intercellular matrix, contractile apparatus and mitochondrial proteins. These conditions can lead to complications where the heart is unable to eject blood sufficiently for the body's needs, or where structural changes are brought on to compensate for impeded function. In heart failure, structural remodelling and alterations give rise to a weaker contractile force which has implications for energy consumption and the coupling of oxidative phosphorylation in mitochondria.

1.2.2) How does heart failure manifest?

The onset of symptoms classified as HF triggers downstream effects which include retention of salt and water by the kidneys, stimulation of the organs by neurohormones and the activation of intracellular cascades in the heart and vascular system that alter the function and morphology of

the ventricles so as to compensate for the lack of pressure and blood flow [11], [12]. Structural and biochemical anomalies associated with HF are a result of defunct mitochondria and adrenergic signalling gone awry. Contractility in the heart is stimulated by means of β_1-adrenergic receptors downstream of catecholamines. Certain polymorphisms in β_1-adrenergic receptors are associated with heart failure. Cardiac-specific modification of β_1-adrenergic receptors to mimic a human polymorphism presented with abnormal expression of hypertrophy and foetal genes, decreased G-protein expression and adenylyl cyclase as well as fibrosis with heart failure. This is consistent with the outcome in human patients with the same polymorphism in end-stage heart failure [14].

A low, but marked level of programmed cell death (apoptosis) in cardiomyocytes seems to contribute to the heart failure phenotype [15], [16]. Apoptosis is described as the fragmentation of nuclear deoxyribo nucleic acids (DNA) into multiples of 180 base pairs in length [17]. Their separation by electrophoreses results in a ladder-like pattern. Autophagy also affects the development of HF. Autophagy is the bulk degradation of organelles of cytoplasmic proteins by formation of a double-membraneous structure known as an autophagosome [18], [19]. This fuses with a lysosome to form an autophagolysosome where the contents are degraded by acid lysosomal hydrolases. Autophagy serves as a survival mechanism in starving cells and is commonly observed in dying cells placing it in category with the other forms of cell death. It affects HF as mice lacking the protein ATG5 which is required for autophagy develop dilated cardiomyopathy [20]. A cardiac-specific deletion of this gene required for autophagy in mice showed exacerbated hypertrophy in hearts in response to a pressure overload [21].

Age is an apparent link to heart failure. With time, the contractile properties of the heart, the left ventricular (LV) chamber size and cardiac mitochondrial function are all affected by age, independently of HF. Myocardial substrate metabolism alters in response to stressors like age, and

heart failure. In humans, the heart decreases uptake and oxidation of fatty acids but not glucose under these conditions [22], [23]. In the late stages of HF, the myocardium presents with low levels of ATP due to abnormal oxidative metabolism and inefficient transfer of energy from carbon–based fuels to ATP for the heart's contractile requirements [7].

1.2.3) Metabolic changes in the failing heart

There is much evidence to suggest that impaired metabolic processes contribute to the contractile dysfunction and LV remodelling displayed in HF. The general observation is that the substrate selection is close to normal during the early stages of HF, and with time, it changes to favour glycolysis and glucose oxidation, down-regulating fatty acid oxidation and reducing electron transport chain activity, thereby impairing cardiac energy efficiency [22], [23], [7]. This process is known as 'mechanoenergetic uncoupling', where energy consumption in the heart increases, while contractile force does not. In failing hearts this is as a result of enhanced oxidative stress from mitochondrial and cytosolic free-radical generating sources [24]. In these systems, nitric oxide synthase (NOS) activity plays a role in the uncoupling, as the ratio between nitric oxide and reactive oxygen species (ROS) is unbalanced, and an excess of ROS is produced [24].

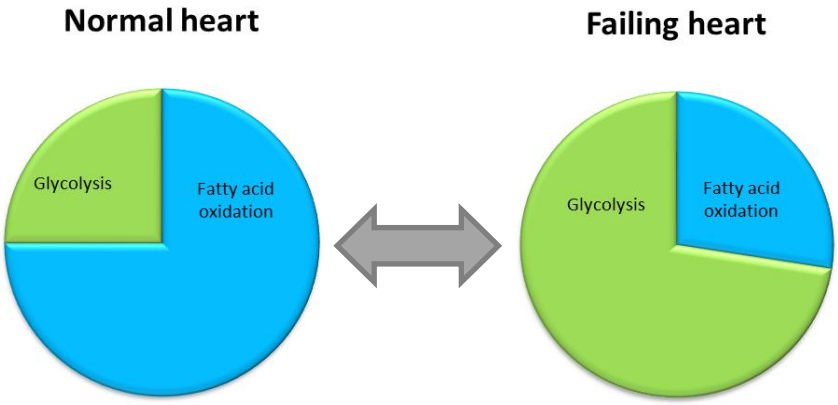

Figure 3: There is a preferential switch in substrate between the normal and failing heart. The normal heart uses 70 – 90% fatty oxidation to produce energy, while in the late stages of the failing heart glycolysis is favoured, while fatty acid oxidation is depressed [25], [26].

Heart mitochondria are designed to generate high energy output in the form of adenosine triphosphate (ATP) to cope with the demand of the contracting muscle. At a maximum, the mitochondrion works at 80 – 90% of its total capacity, compared to at rest where it only uses 15 – 25% of its total capacity for electron transport [27]. Metabolic enzymes in the cell can be rapidly modified to be functional or non-functional by means of allosteric modification, and these enzymes, along with changes in metabolites that have an inhibitory or stimulatory effect allow for the rapid adaptation to stresses such as fasting, ischemia or exercise. In the normal resting heart, fatty acid oxidation (~70 - 90%) is favoured over the oxidation of pyruvate (which comes from glycolysis, ~15 – 35%) for the production of ATP [25], [28]. In the later stages of the failing heart, ATP is generated preferentially through the oxidation of pyruvate (see fig. 3), which has been shown by Lei et al (2004) to increase 2.5 fold in a model of end stage induced heart failure in dogs [26]. This preferential shift occurs as fatty acid oxidation requires more oxygen to produce energy and oxygen is a limiting factor when the heart is not functioning optimally. In HF, mitochondria exhibit membrane disruption, decreased capacity for oxidative phosphorylation and a lower capacity for respiration with substrates such as fatty acids. [7]. Errors in the mitochondrial metabolism and electron transport chain may also manifest as part of the HF phenotype [22].

In the failing canine myocardium, enzymes which deliver ATP and remove ADP were depressed including the activities of creatine kinase, adenylate kinase, 3-phosphoglycerate kinase and pyruvate kinase [30]. These enzymes as part of the phosphotransfer pathway in the myocardium are required for efficient delivery of high energy phosphates to cellular ATPases and removal of

metabolites from these ATPases. Their reduced activities may provide a basis for the impaired contraction-relaxation in the failing heart.

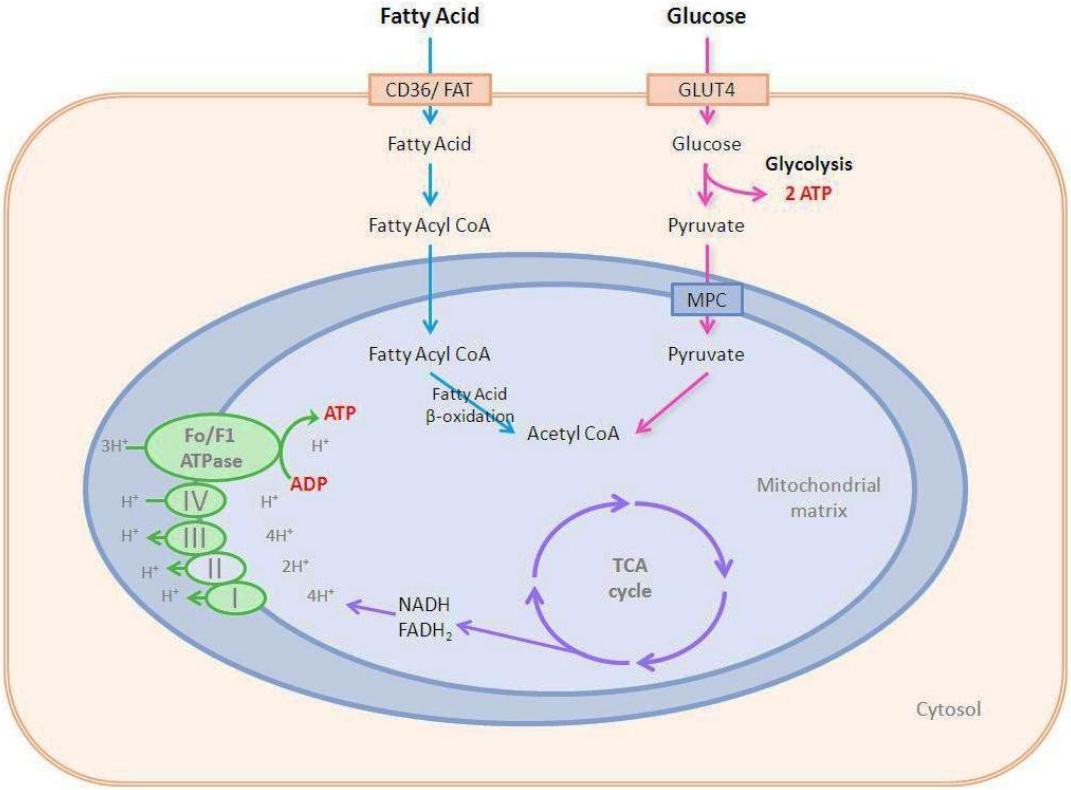

Figure 4: Pathways for glucose and fatty acid metabolism to produce ATP in the heart. Generally in the late stages of the failing heart the glycolytic pathway (right) is favoured over fatty acid oxidation (left) as it requires les oxygen to produce energy [29].

The shift in preference for substrates in the failing heart down-regulates some of the adult heart gene transcription to favour the foetal metabolic profile [31]. In the foetal heart, glucose is the primary source of fuel for cellular processes with very low level of fatty acid oxidation [9]. The similarity between the foetus and the failing heart is the limit of oxygen for respiration, and this may explain the shift to glucose as a fuel, as it requires less oxygen to transfer energy to ATP per molecule that fatty acids do. Both of these are hypoxic systems, but in the foetus this hypoxia is global and is not detrimental as end-stage metabolites are removed, whereas in the failing heart hypoxia is localised and the removal of end-stage metabolites decreases, causing toxicity [32].

Metabolism may not be the only thing that shifts from a normal adult state to a foetal state with hypoxia. The adult rodent heart normally has more α-myosin, which has less tension and faster crossbridge kinetics than β-myosin heavy chain which is expressed in the foetus. In HF and hypertrophy, the β-myosin isoform is re-expressed [33]. In rodent models of HF, the expression of myosin shifts from α-myosin heavy chain to β-myosin heavy chain which may contribute to the altered contractile phenotype [14]. The β-myosin isoform confers a slower, more powerful and oxygen-sparing contraction, and re-expression may be an adaptive mechanism which with time disadvantages the heart [34], [35]. The expression of these isoforms is different in large mammals (including humans) which also shift to favour one form over the other to contribute to the phenotype. Infant human and rabbit hearts manage to adapt to hypoxia through signal transduction pathways involving protein kinase C epsilon (PKCε), p38 mitogen-activated protein kinase and JUN amino-terminal kinase [36]. These pathways may be responsible for cardioprotection in chronic hypoxia.

1.2.4) Signals contributing to heart failure

In the initial phases of HF, compensatory mechanisms are activated such as the Renin-Angiotensin System (RAS), sympathetic nervous activity and cardiac hypertrophy [37], [38]. These systems contribute to the progression of HF through ventricular modelling in which chamber walls become thinner in the heart, the left ventricular (LV) chamber dilates, and fibrosis occurs in the walls of the heart [39], [7].

High circulating levels of cytokines have been reported in cases of HF, implicating them as players in the pathogenicity thereof [40]. Focus on cytokines has been specific to a few, with more of an interest in the soluble cytokine receptors transducing cellular signals that promote and prevent

inflammation. Patients with heart failure have shown elevated plasma levels of tumour necrosis factor α (TNFα) and its soluble receptor, interleukin 6 and its soluble receptor, as well as glycoprotein 130 (gp130) [41], [42], [43]. In combination these molecules produce a net inflammatory effect. Anti-inflammatory cytokines were also found to be depressed in plasma of HF patients with decreased levels of Transforming Growth Factor β1 (TGFβ1) and interleukin 10 [44], [45], [46]. Plasma levels of gp130 in particular were closely correlated to parameters which indicate a deranged hemodynamic load [46]. These changes in cytokines indicate an elevated inflammatory state in HF.

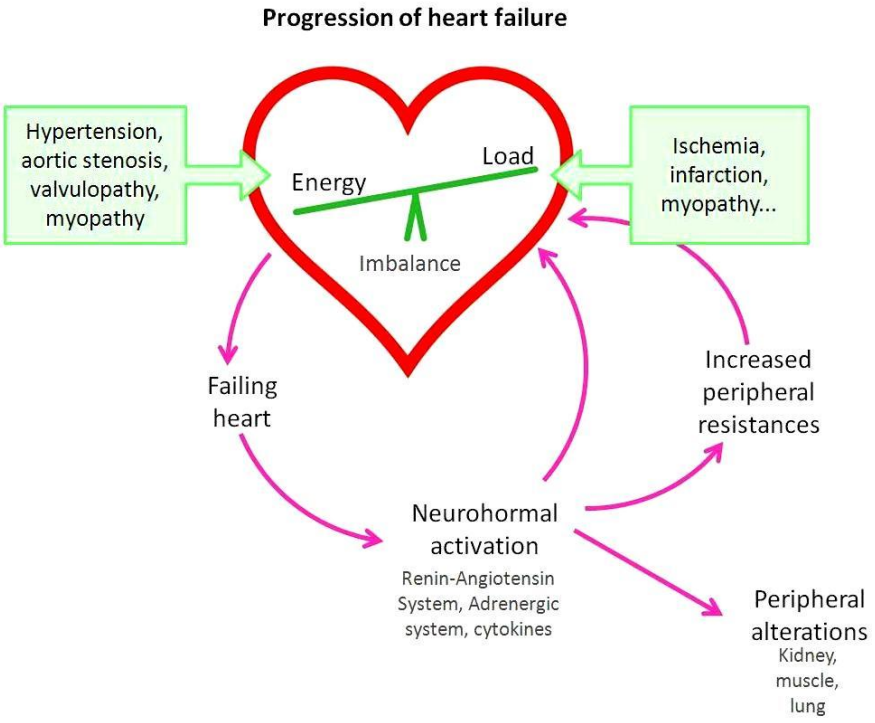

Figure 5: Progression of heart failure. An imbalance between the energy required by the heart to meet the applied load can occur as a result of mechanical and/or metabolic dysfunction. Certain instances of HF can increase peripheral resistance and induce harmful cardiac (and skeletal muscle) remodelling. These in turn aggravate HF. [9]

Alongside inflammation, low but marked levels of apoptosis have also been associated with HF [15], [16]. Two prominent, well known cell survival pathways which assist in preventing apoptosis are the Survivor Activating Factor Enhancement (SAFE) pathway involving signal transducer and

activator of transcription 3 (STAT3) [47], [48], and the Reperfusion Injury Salvage Kinase (RISK) pathway involving protein kinase C ε (PKCε) [49]. These pathways suppress the apoptosis of cardiomyocytes by blocking the activation of caspases (a family of calcium-dependent proteases central to apoptosis) or by activating Akt, a cell signalling factor which promotes cell survival [50], [51], [12]. Here we will examine these two pathways and their contribution to the heart and heart failure.

C: Signal Transducer and Activator of transcription 3 (STAT3)

One of the pathways closely linked to the protection of the heart in heart failure and ischemia/reperfusion is the Survival Activating Factor Enhancement (SAFE) pathway involving Janus kinase (JAK) - signal transducer and activator of transcription 3 (STAT3) signalling. STAT3 protects the heart by reducing apoptosis via a number of cellular pathways, including those activated by reactive oxygen species (ROS), sympathetic stimulation, or cytokine cascades.

1.3.1) The STAT family

The Signal Transducer and Activator of Transcription (STAT) family is composed of regulatory proteins involved in signal transduction pathways downstream of an array of ligands. The family consists of six members (STAT1, 2, 3, 4, 5a and 5b) that are known to play a role in cytokine signalling. Cytokines bind to their specific Janus Kinase (JAK) receptors at the cell surface to which STAT proteins are recruited for modification to effect stress-response pathways and transmit signals from the cell surface to the nucleus where gene expression is altered. The JAK-STAT signalling often involves working with co-receptors to achieve specificity of the signal and STAT

protein that is activated. The JAK-STAT pathway has been shown to play a role in hypertrophy, apoptosis, angiotensin signalling, ischemia/reperfusion injury and ischemic preconditioning [52]. [53]. Once STAT3 binds to the JAK receptor, it is phosphorylated at tyrosine residue 705, after which it dimerizes with a fellow tyrosine-phosphorylated STAT3 molecule and moves off to the nucleus to promote transcription of survival-related genes (see fig. 5) [54], [55]. STAT3 can also be phosphorylated at a second position while in the cytoplasm, at serine residue 727, in response to growth factors by an extracellular signal-regulated kinase (ERK) family of mitogen activated protein kinases (MAPK) excluding c-Jun N-terminal protein kinase (JNK) and p38 [56].

STAT3, in particular, has been identified as a key player in processes such as growth, differentiation, cell death or survival in various cell types. It is a transcription factor downstream of several cytokines and plays a major role in the development of hypertrophy through the cell surface receptor gp130. [52].

1.3.2) Activation of STAT3

Certain cytokines and growth factors are necessary to direct signalling at a cellular level. STAT3 is a downstream signalling molecule of gp130 in cardiomyocytes, and it has been suggested that it is activated by interleukin (IL)-6-type cytokines such as IL-6, IL-11, leukaemia inhibitory factor, oncostatin M, ciliary neurotrophic factor, and cardiotrophin-like cytokine. These bind to a gp130 receptor on the plasma membrane, which in turn interacts with the janus kinase (JAK) protein thus commencing signal transduction from the cell surface [52], [58], [59], [60], [61]. Interestingly, cytokine interleukin 6 (IL6) activates serine phosphorylation of STAT3 independently of the ERK pathway [56].

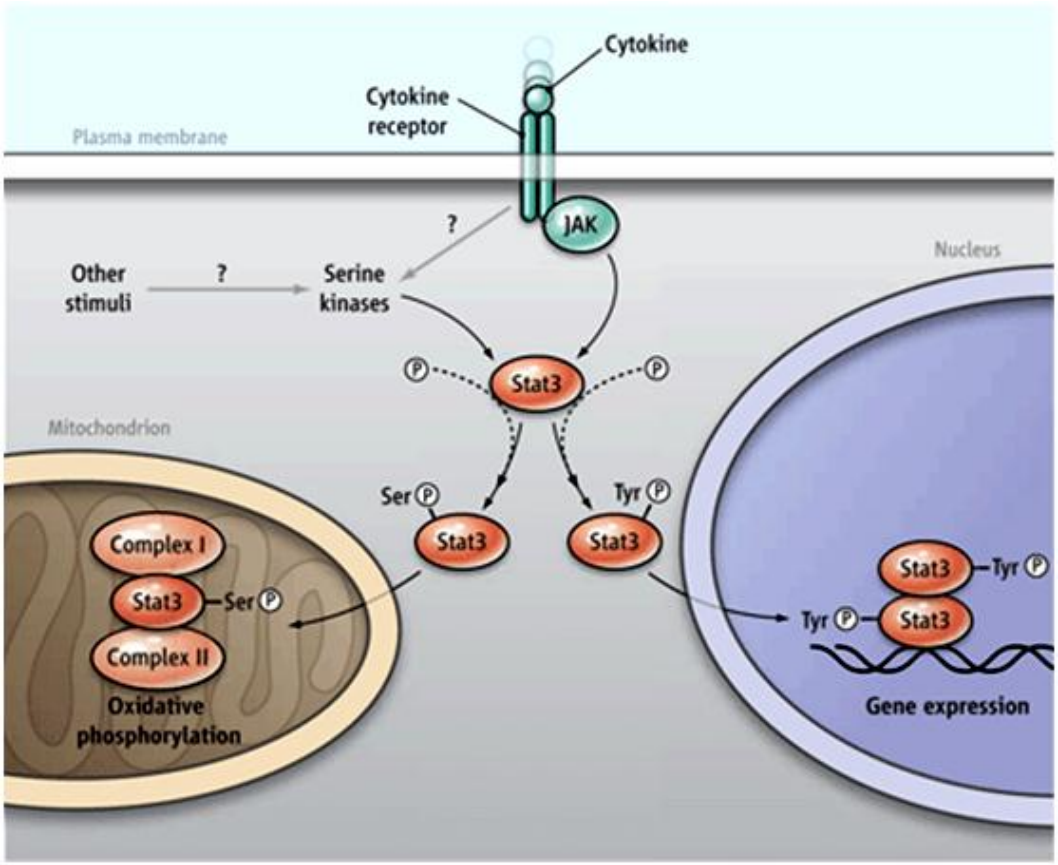

Figure 6: Activation of JAK by binding of a cytokine to the cell surface receptor causes recruitment of STAT3 and phosphorylation at a tyrosine residue (tyr705), after which dimerization occurs and STAT3 moves off to the nucleus to promote transcription. Phosphorylation of STAT3 at a serine residue (ser727) happens downstream of MAP kinase and ERK activity, though the exact mechanism is not clear. Once phosphorylated, STAT3 moves off to the mitochondrion where it is found to co-localize with complex I/ II of the electron transport chain, and where it is cardioprotective. [57].

Cytokines are key to many biochemical processes in the body. Leukaemia inhibitory factor (LIF), an IL-6 family member is a cytokine central to formation of the heart in the embryo which activates JAK/STAT signalling. It is also expressed in the adult heart under hemodynamic stress and it induces sarcomeric protein synthesis. Treatment of cardiac fibroblasts with LIF reduced matrix metalloprotease activity and collagen content, suggesting its involvement (along with STAT3) in remodelling of the extracellular matrix after myocardial injury [62]. In addition, granulocyte colony-stimulating factor (G-CSF) which prevents cardiac remodelling has been linked to STAT3,

supporting the idea that STAT3 is involved in cardiac re-modelling after myocardial infarction [61], [63].

1.3.3) STAT3 and the heart

Activation of STAT3 leads to anti-apoptotic and angiogenic activity in the heart, and it has been found to reduce fibrosis in the heart after events such as myocardial infarction and improve cardiac function when triggered by certain cytokines. Hence, a cardiac-specific ablation of STAT3 has shown a reversal of these anti-fibrotic effects, as well as resulting in ventricular enlargement. With an over-expression of activated STAT3, adverse cardiac re-modelling of the sort that may occur with heart failure is limited, reinforcing its cardioprotective effect [61].

Levels of both active and inactive STAT3 are not constant through the life span of an organism; it decreases with age in different organs and cell types. Reduction of STAT3 occurs in the aged rat brain [64] and in the myocardium of aged mice [65]. Cardiac-specific STAT3 deficient mice have shown development of heart failure with age, indicating the involvement of STAT3 in protection and maintenance of the heart tissue [66]. Activation of STAT3 is triggered by physiological stress, such as age [65], pregnancy [67] and pathophysiological stress, such as myocardial infarction [63] and heart failure [66]. Pathological stress may trigger signalling through mitogen-activated protein kinases (MAPKs) and pathways involving Protein Kinase C-epsilon (PKCε) [69], [70], [62].

1.3.4) Delineation of functions of STAT3

The functions of STAT3 have been identified mainly through rodent gene over-expression and deletion models. Transgenic mice with a cardiac-specific over-expression of constitutively active STAT3 produced smaller infracted areas (i.e. scars on the heart) after ischemia and reperfusion compared to non-transgenic mice [71], while a cardiomyocyte-specific deficiency of STAT3 produced larger infarcts after ischemia and reperfusion, confirming the cardioprotective role of STAT3. An increase in STAT3 levels reduces both apoptosis and necrosis after ischemia/reperfusion [72]. A conventional deletion of STAT3 leads to embryonic lethality, so studies involving the heart and STAT3 use the cre-lox system to restrict the deletion of STAT3 to cardiomyocytes. In cardiomyocytes, a constitutive deletion of STAT3 results in gross derangements such as decreased LV function, reduced capillary density, increased cardiac fibrosis and apoptosis, as well as dilated cardiomyopathy [73].

Cardiac-specific STAT3 over-expression models have also been used to determine the physiological role of STAT3 in transgenic mice. These mice showed development of myocardial hypertrophy at 12 weeks of age and an increase in expression of certain genes such as atrial natriuretic factor (ANF), β-myosin heavy chain (βMHC), and cardiotrophin 1 (CT-1) [52]. After a 10 day treatment with doxorubicin (Dox), these transgenic mice showed a far better survival rate compared to wildtype controls. Wildtype mice were found to have massive bilateral pleural effusion and ascites after death, suggesting they developed congestive heart failure [52]. These findings indicate that STAT3 contributes to hypertrophy, but also that it protects against cardiomyopathy by preserving expression of contractile genes and promoting protective factors in the heart.

Over-expression of STAT3 provided protection against cardiomyopathy and greatly improved survival by preventing heart failure with induced cardiotoxicity [52]. STAT3 plays an important role in heart failure and is key in transduction of gp130-induced protection and anti-apoptotic signal.

STAT3 overexpression amplifies mRNA expression of c-fos and atrial naturetic factor (ANF) via LIF, an observation which is attenuated with inhibition of STAT3 [74]. In the STAT3 overexpression model, inhibition of MAP kinase activity suppresses the mRNA expression of the factors mentioned. This is hypothesised to be as a result of cross-talk between JAK/STAT and MAP kinase signalling cascades, both of which contribute to upregulating transcription, as serine phosphorylation of STAT3 is induced by MAP kinase [75].

1.3.5) STAT3 and ischemic preconditioning

Preconditioning is a tool used to combat ischemia-reperfusion injury in the heart. Ischemic preconditioning (IPC) is a protective adaptation induced by short bursts of alternate ischemia / reperfusion – alternating bursts of reduced oxygen and blood flow prior to a prolonged ischemic incident in the heart, after which restoration of oxygenated blood flow occurs [76]. This has been shown to enhance resistance of the heart to damage and improve the outcome of ischemia-reperfusion (I/R) injury. These short bursts activate the protective signalling cascades which help to maintain the integrity and function of the tissue.

Pharmacological preconditioning using chemical agents such as isoflurane, diazoxide, TNFα or adenosine can also induce tolerance against injury in cardiomyocytes [77], [78], [48]. STAT3 is linked to pharmacological preconditioning, as STAT3 deficient cardiomyocytes do not respond to preconditioning agents to achieve protection as wildtype cardiomyocytes do. This carries through not just in an isolated cell system, but also in the intact heart, implicating STAT3 as a crucial molecule in preconditioning programs [53]. The involvement of STAT3 in preconditioning was first identified in a rat heart model where IPC increased levels of STAT3 phosphorylation, while treatment with a STAT3 inhibitor ablated the protection offered by the preconditioning stimulus and increased the infarct size in hearts exposed to ischemia [79].

1.3.6) STAT3 and ischemic postconditioning

Ischemic Postconditioning (IPostC) is another protective adaptation used to limit the damage caused by ischemia reperfusion by the application of short bursts of vascular occlusion (ischemia) at the onset of reperfusion [80]. STAT3 has also been implicated in the protection proffered by IPostC, as administration of a non-specific JAK inhibitor, AG490, at the start of reperfusion in the rat heart has been found to nullify the effect of both ischemic and pharmacological IPostC [81], [82]. IPostC is also lost in the hearts of aged mice, as well as STAT3 deficient mice [65]. The effects produced by STAT3 in IPC and IPostC are both rapid-onset, suggesting that STAT3 mediated cardioprotection involves translocation to the mitochondria and signal transduction there rather than the nucleus where it would regulate transcription of various genes, which would take time. The two different phosphorylation sites of STAT3 (tyrosine / serine phosphorylation) is linked to its translocation, with tyrosine phosphorylation (and dimerization) being associated with the nucleus

– thus transcriptive activity, and serine phosphorylation being associated with mitochondria – thus signal transduction and protein-protein interaction (see fig. 6) [83].

Loss of IPC protection has also been associated with reduced connexin 43 (Cx43) [84]. Cx43 is usually found in LV gap junctions and in the mitochondria of cardiomyocytes. Animal models with reduced cx43 show a loss in IPC-induced protection both in-situ and in isolated cardiomyocytes, even when stimulated with pharmacological preconditioning agents such as diazoxide [78], [85], [86]. With age, Cx43 levels decline, in much the same way as STAT3 [87]. In embryonic mouse stem cells, stimulation with LIF and bone morphogenic protein-2 show an increase in the amount of Cx43, and in the phosphorylation of STAT3 [88], while in astrocytes in mice increase in protein and mRNA levels of Cx43 by neural factors were found to be combined with the localization of STAT3 in the nucleus [89]. Treatment of these cells with the same nuclear factors in conjunction with a JAK/STAT3 pathway inhibitor (AG490) decreased levels of Cx43, illustrating the dependence of Cx43 on the JAK/STAT pathway and STAT3. Both of these are associated with the same outcomes, such as protection via IPC and diazoxide [90] and altered patterns of expression with age, indicating a link between their activities.

1.3.7) Sub-cellular activity of STAT3

STAT3 drives the activity of many proteins involved in anti-apoptotic responses, including Bcl-2, Bax and survivin. It also regulates the activity of anti-oxidants by upregulating manganese superoxide dismutase (MnSOD) which assists with the anti-oxidant effects that promote IPC and IPostC [53]. Among the genes upregulated by STAT3 is myocardial cyclooxygenase-2 (COX-2). Binding of activated STAT3 to DNA in the nucleus promotes transcription of COX-2 (as well as a number of other genes) which confers protection. Both tyrosine and serine phosphorylation are

required for the upregulation of COX-2 which is involved in preconditioning effects to reduce myocardial infarction. Additionally, various mitochondrial anti-apoptotic proteins [follicular B cell lymphomas xL (Bcl-xL) and myeloid cell leukemia-1 (Mcl-1)] are transcriptionally regulated by STAT1 and STAT3 [73]. Recruitment and activation of STAT3 is also important in inhibiting the death receptor pathway which is modulated by c-FLIPL and c-FLIPS [73].

1.3.8) STAT3, mitochondria and metabolism

STAT3 has anti-apoptotic effects with its involvement in mitochondria. It modifies the expression of Bcl-xL [91], an anti-apoptotic protein which is present in the mitochondrial membrane [92], [93] and inhibits opening of the mitochondrial permeability transition pore (mPTP) [87] in conjunction with inactivation of glycogen synthase kinase 3 β (GSK3 β) [94]. It also plays a role in modification of metabolism in mitochondria, which is consistent with its involvement in HF, as HF displays alteration in metabolism. STAT3 has been shown to play a part in regulation of carbohydrate metabolism, and deficiency of STAT3 may lead to disturbances in the metabolic processes associated with preconditioning [95], [96]. Hence, STAT3 has been found in cultured cells and primary heart and liver tissue to co-immunoprecipitate with complexes I and II involved in oxidative phosphorylation as part of the electron transport chain in the mitochondrial membrane [97]. In these tissue and cell systems, STAT3 deficient cells showed reduced complex I and II activities – an occurrence mimicked in cardiac-specific STAT3 knock-out mice, which further supports the idea that it plays a role in the heart and heart failure through metabolism. Phillips et al looked at the ratio of complex I/II to STAT3 in vivo in pigs and mice, and found it to be ~10^5, suggesting that the effect STAT3 has on mitochondrial function is indirect, despite co-localisation, as a direct protein-protein interaction between the two would yield a ratio of ~1 [98]. They

conclude that the effect STAT3 has on mitochondria should thus be through transcriptional regulation or as STAT3 being an upstream member of a signalling cascade.

D: Protein Kinase C epsilon (PKCε)

1.4.1) The Protein Kinase C family

The protein kinase C (PKC) family is comprised of 10 related serine/threonine kinases which are divided into 3 sub-families depending on their N-terminal domains and requirements for activation. PKCs play prominent roles in the regulation of growth and programmed cell death. There are the classical PKCs (α, βI, βII and γ) which require calcium and diacyl glycerol (DAG) to activate them , the atypical PKCs (including ζ and ι /λ) which require phosphatidylserine for activation, and the novel PKCs (ε, δ, θ and η), which require only DAG for activation [99], [100], [101]. The PKC chain has an N-terminal regulatory region containing an autoinhibitory pseudosubstrate domain (i.e. a domain which fits a specific substrate, preventing inhibition of the activity of the molecule), two elements which target the membrane, and a highly conserved catalytic domain on the C-terminal for ATP and substrate binding.

PKCs are thought to mediate a multitude of phosphorylation events in the myocardium, including those regulating cation transport, contractile force development, gene expression, metabolic processes, and cellular growth in the heart [102], [103].

1.4.2) The PKCε signalling cascade

There are a few known ways in which PKCε can be activated (see fig. 7) [100], [104]:

1) One of the means of activation employs signalling with molecules such as adenosine, catecholamines, angiotensin II, bradykinin, and endothelin [99]. These extracellular signalling molecules are released during ischemic events and bind to a G-protein-coupled receptor (GPCR) in the cell membrane, which then recruits a second intracellular subunit [105]. This complex begins a relay of messenger molecules starting with phospholipase-C at the cell membrane, which hydrolyses membrane phospholipids to generate diacyl glycerol (DAG). DAG moves from the membrane to the cytosol where it activates the PKCε cascade to promote its effects.

2) A second means of activation is by release of small amounts of reactive oxygen species (ROS) or nitric oxide (NO) from mitochondria which directly modify the regulatory domain of PKCε to its active form [106]. Elevated levels of ROS are known to be harmful to the cells, but small amounts are protective, especially as part of the initial phases of preconditioning [107]. This phenomenon is known as hormesis – a toxic agent acts has a stimulatory effect at a low dose, but an inhibitory effect at a high dose [108]. Aside from ROS, hormesis is a concept applicable to molecules such as TNFα in the heart which is also beneficial at low doses, but high levels have been implicated with pathogenesis [48], [109]. When PKCε is activated, it moves to the mitochondria where it causes further release of small amounts of ROS/NO, forming part of a positive feedback loop for transient self-activation to provide protection in cells [101]. This protection is lost in PKCε knockout mice. PKCε-induced IPC was lost in cardiomyocytes which have hydrogen peroxide removed [110], while treatment with NO selectively activates PKCε in cardiomyocytes [111], [112] producing an IPC-like effect, thus confirming the attribution of protection via ROS to PKCε. Furthermore, treatment with a PKCε activator increased levels of nitric oxide, while

treatment with a PKCε inhibitor decreased NO release in a dose-dependent manner [113]. Activation of PKCε through NO also promotes the binding of PKCε to the receptor for activated C-kinase (ψεRACK) assisting with its translocation and activation of its pro-survival pathways [106]. The release of NO activates soluble guanylyl cyclase, which synthesizes cyclic guanosine-3', 5'-monophosphate (cGMP), a secondary transduction messenger which leads to the activation of PKCε between the two mitochondrial membranes to open the mitochondrial ATP-sensitive K^+ channel (mitoK_{ATP}) on the inner mitochondrial membrane and close the mPTP on the outer mitochondrial membrane [114], [115].

3) A third means of activation is via renin–angiotensin system (RAS) signalling. Angiotensin II (AngII) type 1 receptor (AT_1) has been linked to the activity of PKCε, with downstream responses such as sarcolemmal Na^+–K^+ pump regulation mediated by PKCε [116], [117]. Chronic pre-treatment with AT_1 antagonists (ARB) protected the heart against myocardial infarction (MI), an effect which could not be further improved by IPC, but which was abolished by addition of the PKCε inhibitor, chelerythrine. Pre-treatment with ARB produced elevated levels of PKCε in the particulate fraction of mouse hearts [116]. Pre-treatment of hearts with angiotensin converting enzyme (ACE) inhibitors had the opposite effect – there was no protection afforded to hearts by IPC with ACE inhibitor treatment and the levels of PKCε were reduced [116]. Levels of PKCε and AngII were found to be simultaneously upregulated in LV hypertrophic myocardium of rats following induction of mechanical stretch with a Langendorf perfusion system. Pre-treatment with an AngII type 1 receptor blocker, valsartan, prevented PKCε activation with stretch-mediated stress [118]. The signal transduction pathway involving AT_1 and PKCε appears to be independent of

tyrosine-specific protein kinases and Ca^{2+} activity [119], but works via phospholipase C (PLC) and DAG for transduction of signals [120].

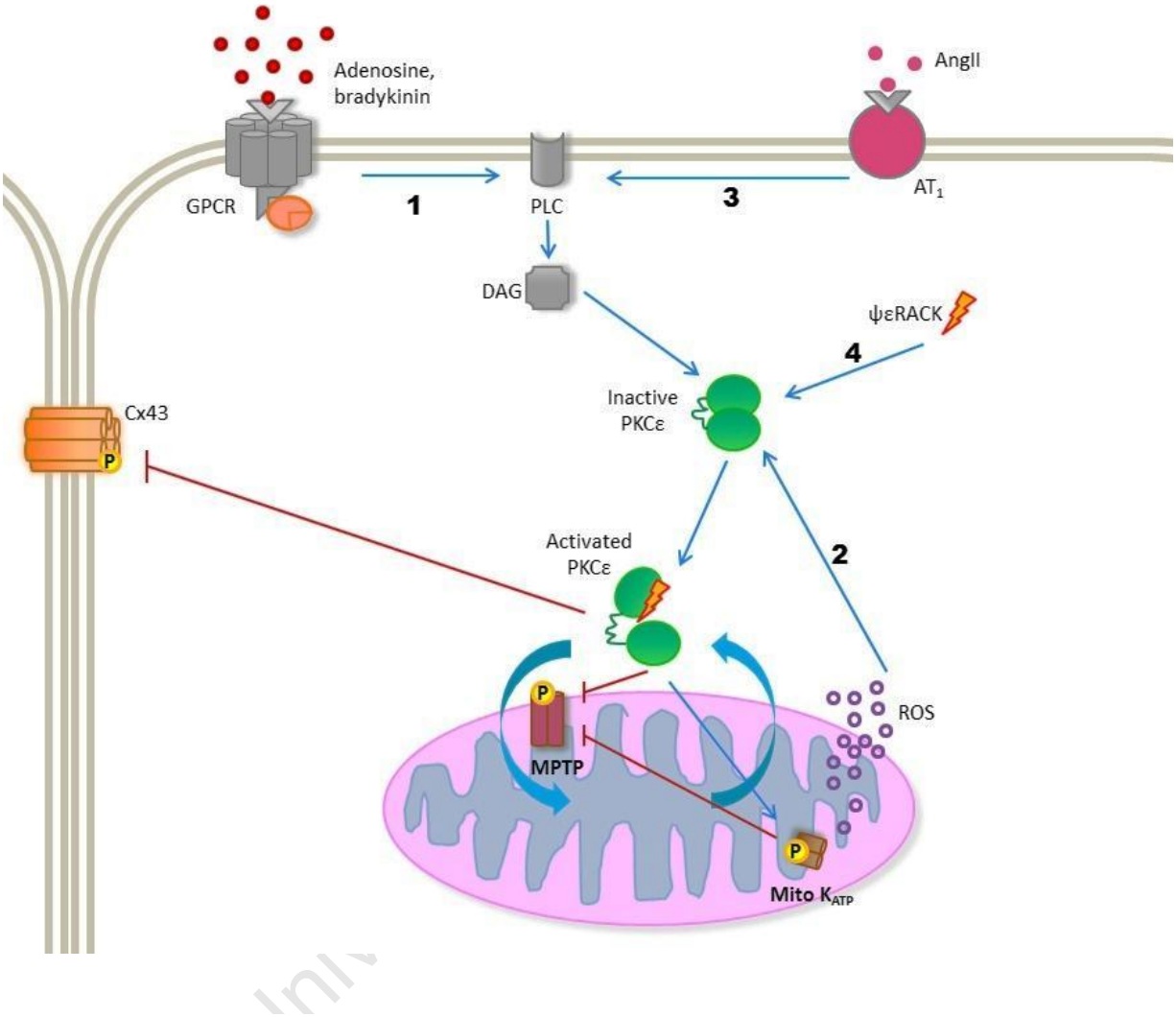

Figure 7: Activation of PKCε. (1) Cytokines and signalling factors bind to the G-protein coupled receptor at the cell surface, causing it to recruit a subunit which is modified and activates phospholipase-C (PLC). PLC then hydrolyses membrane lipids to produce diacylglycerol (DAG) which leads to phosphorylation and activation of PKCε. Once in the active conformation, PKCε moves to the mitochondria where it inhibits the mitochondrial permeability transition pore (mPTP), preventing the release of cytochrome C from the mitochondrial membrane and cell death. It also phosphorylates the mitochondrial potassium ATP channel, inhibits connexin 43 (Cx43) and promotes the release of low levels of reactive oxygen species (ROS) which further activate PKCε (2). Angiotensin II (AngII) binds to its receptor (AT_1), transducing a signal through PLC to activate PKCε. An alternate means of PKCε activation is by delivery of a ψεRACK peptide (4), which binds to the autoinhibitory pseudosubstrate domain, which prevents inhibition of the activity of PKCε.

4) A fourth known means of activation is by administration of a peptide promoting the binding of the receptor for activated C-kinase (ψεRACK) with PKCε. ψεRACK is an anchoring protein found in the cellular compartments close to where PKCε translocates once it is

activated to interact with its targets [106]. Binding of PKCε to this receptor places it nearby its substrates in the particulate fraction and mediates its downstream cardioprotective effects. Peptide activators promote the binding of PKCε to the ψεRACK, while peptide inhibitors compete for this binding site [104], [121].

Preconditioning mimetics that are used to activate PKCε mainly work through the signalling pathway involving the GPCR [104].

1.4.3) Downstream effectors of PKCε

PKCε is upregulated with several other cardioprotective genes including inducible nitric oxide synthase, cyclooxygenase-2, heme oxygenase-1, aldose reductase and MnSOD, acting downstream of transcription factors such as nuclear factor-κB (NFκB) and activator protein (AP)-1 [122], [123] [124], [125]. It resides in the cytosol at rest and is widely dispersed once activated, including to the region around the nucleus and sarcomeres [126], suggesting it is involved in a number of cellular events [100]. It triggers downstream transducers such as extracellular signal- regulated kinases (ERKs) p42 and p44 in the setting of ischemic/ hypoxic pre-conditioning, and inhibition of ERK attenuates the protection provided. Activation of PKCε using a ψεRACK activator also results in phosphorylation of ERK1/2, and PKCε has been co-localised with ERKs in the mitochondria [127], [128], [129], where this complex inactivates the pro-apoptotic protein BAD (Bcl-2-associated death promoter). This indicates the activity of PKCε may provide cardioprotection by blocking the action of pro-apoptotic proteins. Proteins relating to metabolism also show an altered expression with upregulation of PKCε, favouring an increase in glucose metabolism to decrease glucose levels in

blood [130], [131]. Glucose utilization by PKCε hearts relies on a GSK3β and hypoxia induced factor-1α (HIF-1α)-mediated mechanism, which has been shown to sustain cardiac function in mouse hearts in the setting of hypoxia [132].

A second route of transduction of the PKCε signal is through lymphocyte-specific protein tyrosine kinase (Lck), a tyrosine kinase that forms part of the sarcoma (Src) family. Pre-conditioning involving PKCε results in phosphorylation of Lck in cardiomyocytes and a knock-out model of the Lck gene loses the afforded protection with activation of PKCε. [133]. [104]. Ping et al have identified that PKCε has a direct effect on Lck by means of a proteomic approach. The two proteins have been found to form a complex in vivo in IPC. [133]. This complex does not form in Lck knockout mice and cardioprotection is lost.

PKCδ, another member of the PKC family acts antagonistically to PKCε in the heart. While PKCε over-expression leads to survival and proliferation, PKCδ slows proliferation, induces cell cycle arrest, and has the ability to enhance the differentiation of various undifferentiated cell lines [101], [134]. These two PKC isozymes have opposing and temporal roles in injury in the heart.

1.4.4) PKCε in ischemia / reperfusion and the heart

PKCε is a key-player in cardioprotection, and constitutive activation of PKCε has been shown to fully mimic IPC [112]. [135]. As previously described, IPC is a protective adaptation by which short bursts of ischemia and reperfusion are induced prior to an extended ischemic incident in the heart [100], [136]. The activity of PKCε in the heart is opposed by that of PKCδ, these two signalling messengers act antagonistically in the setting of I/R, the former to aid cell survival, and the latter

to promote cell death [104]. These two isoforms of PKC have opposing effects on the regulation of some of the same targets such as the adenosine transporters.

Improvement of cardiac function with IPC is accompanied by the activation and translocation of PKCε from the cytosolic to the membrane fraction of cells. This translocation of PKCε persists for a period of 30 min following activation, while translocation of other factors are short-lived [99]. Improvement in cardiac function is associated with activation of PKCε and includes improvement of the left ventricular developed pressure (LVDP) [113] – a measure of the strength of contraction of the heart muscle, which is decreased in individuals with heart failure [137]. The period of improvement coincides with that of the activation of PKCε.

The activity of PKCε is tightly regulated by highly specific binding of PKCε with a partner protein known at the Receptor for Activated C-Kinase (ψεRACK). The interaction of PKCε with the ψεRACK receptor leads to the activation of PKCε by phosphorylation of serine residue 727 on the protein chain, and triggers initiation of several cellular functional events [103], [101].

1.4.5) Functions of PKCε

Specific effects attributed to PKCε have been identified by using over-expression and inhibition models in animals and cell culture. A PKCε-specific antagonist peptide, εV1-2, used in rat neonatal and adult cardiomyocytes was one of the examples of PKCε activation used to confirm PKCε as the isoform responsible for IPC-induced protection [138], [100]. Moderate cardiac-specific over-expression of PKCε [133] and the addition of a PKCε-activating peptide [138] both result in the reduction of infarct size, confirm the beneficial action of PKCε in the setting of I/R in the heart.

These findings were supported by studies using PKCε-deficient mice which failed to reduce infarct size after induction of IPC [139], [104]. However, the degree of over-expression of PKCε affects the outcome of the heart in that a low to moderate over-expression level had no detrimental effects long-term, but a high overexpression model produces a different phenotype – the development of heart failure where the low- and moderate-overexpression had no such effect [133]. This indicates that differential expression / activity levels of PKCε display different cardiac phenotypes with low- and moderate- overexpression being favourable compared to a high-overexpression.

1.4.6) Sub-cellular activity of PKCε

PKCε, through its effectors, appears to alter the outcome of pro-apoptotic proteins in mitochondria. It also has effects in other sub-cellular locations such as gap junctions. Gap junctions found in the sarcolemmal space mediate electrical coupling in the heart enabling the direct connection of cytoplasm in adjacent cells. This connection is achieved by the assembly of a hexameric structure of connexin proteins, in particular connexin 43 (cx43), to form a semi-permeable channel between cells [140]. These channels are regulated by calcium ion concentration, pH, ATP levels and phosphorylation status141]. The channel is generally in a partially phosphorylated state, loss of phosphorylation occurs during ischemia and leads to high conductance between adjacent cells, possibly propagating ischemic injury [142]. PKCε directly phosphorylates cx43 in the human heart and in this way may decrease conduction between cells and decrease cardiac injury [143].

PKCε translocates to the mitochondria and sarcolemmal membrane and at both of these locations the ATP-sensitive K+ channel (K_{ATP} channel) is found [144], [145]. Stimulation of PKC by PMA (Phorbol 12-myristate 13-acetate) produces the cardioprotective effects attributed to

sarcolemmal K_{ATP} channels at the sarcolemma in rabbit ventricular myocytes [146]. Sarcoplasmic potassium gated-ATP channels are also involved in IPC as selective inhibition and/ or deletion of these channels abolishes IPC [147], [148] PKCε activation modulates binding of ATP to the sarc K_{ATP} channel by phosphorylating the channel. PKCε interacts directly with the K_{ATP} channel to produce its effects [149].The K_{ATP} channel opens as ATP levels fall [150]. Opening of the sarcolemmal channels by pharmacological agents or hypoxia may improve the viability of cells by decreasing the conductance between cells and shortening action potentials [151]. Activation of mitoK_{ATP} on the mitochondrial inner membrane by means of PMA or H_2O_2 prevents mPTP opening, an effect that is abolished when the PKCε-specific inhibitor εV1-2 is administered, suggesting that PKCε is the isoform responsible for keeping the mPTP closed [100], [104]. These experiments suggest that mitochondrial ATP channels are effectors of cardioprotection in IPC downstream of PKCε.

PKCε has also been shown to translocate to the nucleus, implying a possible role as a transcription factor or as part of a transcription complex [152], [145]. It increases the DNA-binding activity of AP-1 and NFκB in rabbit hearts through the activity of ERK [125]. Additionally, Xuan et al have shown that late preconditioning activates STAT1 and STAT3 via PKCε and ERK, suggesting that PKCε on its own, or as part of a complex with ERK leads to transcription of cardioprotective genes in the setting of late preconditioning [153], [104].

Along with the above, PKCε also has a direct effect on the production of reactive oxygen species in the mitochondria [113]. It increases NO release in a dose dependent manner when rat aortic cells are treated with a PKCε activator [106], [114]. NO, in turn, reactivates PKCε via soluble guanylyl cyclase and cGMP [114].

1.4.7) PKCε, mitochondria and metabolism

PKCε is found in cardiac mitochondria, and activation under stress further translocates PKCε to the mitochondria for it to be in reach of its targets. This movement appears to be dependent on ROS signalling, as the ROS scavenger *N*-acetyl-l-cysteine (NAC) prevented PKCε translocation to the mitochondria and prevents the closing of the mPTP (mitochondrial permeability transition pore) [154], thereby allowing cytochrome c to be released from the inner mitochondrial membrane, leading to apoptosis (see fig.7). Under normal conditions, the inner mitochondrial membrane is not permeable to ions and metabolites, however when an injury occurs in the heart, the mPTP opens, allowing passage of ions and metabolites through to the inner membrane. This uncouples oxidative phosphorylation and the mitochondria swells, the outer membrane tears and releases integral proteins such as cytochrome c. PKCε has been demonstrated to interact with the mPTP leading to phosphorylation of the mPTP and reduces the loss of cytochrome C [155], [156], [157].

Mitochondria are key to metabolism. They use substrates such as glucose and fatty acids to produce ATP. They are essential for survival of cardiac myocytes and provide the energy needed for the myocytes to contract and maintain the heartbeat. Under normoxic conditions in the heart, fatty acid oxidation produces most of the ATP stores, with glucose procuring the remainder to make up the full quantity of ATP [25], [28]. In I/R, glycolysis is decreased, lowering the pH of cells and resulting in stunted ATP levels which trigger cell death [158], [159]. Glycolysis is the preferred metabolic process in the failing heart [26] as it switches from the adult fatty acid oxidising programme to the foetal gene programme (preferentially using glucose) to protect itself and

continue beating [31]. Fatty acid oxidation uncouples mitochondrial respiration in the failing heart [22].

1.4.8) How do these effects of PKCε contribute to survival?

The mitochondria of aPKCε mice (overexpressing a moderate amount of PKCε) show greater resilience to oxidative stress damage compared to wildtype controls [157]. The protection proffered depends on the degree of activation, with modest activation of PKCε providing enhanced resistance to damage. The use of PKCε-knockout mice provides the greatest evidence for the implication of PKCε in protection of the heart against injury in I/R [156]. In part this is due to improved oxidative phosphorylation, which enhances cellular ATP capacity, fuelling resilience to damage through closing of the mPTP and opening of the mitoK_{ATP} channel in mitochondria [155], [114]. Sub-proteome analysis has revealed interactions between PKCε and several cellular proteins in mitochondria including those regulating oxidative phosphorylation, electron transfer, ion transport and the mPTP. PKCε appears to enhance the generation of ATP in response to I/R, thereby modulating the bioenergetic capacity of mitochondria to tolerate ischemic injury [157]. PKCε colocalizes directly with glycolytic enzymes like hexokinase 2, and citric acid cycle enzymes and is therefore directly able to affect metabolism [155].

PKCε is also responsible for a phenomenon known as Remote Preconditioning (RPC), where brief episodes of I/R in remote organs provides myocardial protection [160]. RPC significantly reduced infarct size, a protection which was abolished when the PKC inhibitor chelerythrine was

administered to hearts. RPC shifts the ratio of cytosolic to particulate PKCε indicating that PKCε is the isoform responsible for RPC-induced protection [161].

1.4.9) PKCε and cardiac remodelling

PKCε has also been reported to play a critical role in regulating the migration and adhesion of cardiac fibroblasts at the cellular level [162]. Migration of fibroblasts is promoted by AngII, and treatment with a specific PKC inhibitor calphostin blocks these processes [163]. This is shown in PKCε knockout mice which abolish these processes in myofibroblasts. PKCε forms a complex with β1-integrin to control the interaction between the cell and the extra-cellular matrix. These findings implicate PKCε as a role-player in cardiac remodelling, which are founding responses in the development of heart failure [121]. PKCε has been found to be significantly increased in the cytosolic and particulate fractions of failing rat hearts and PKCε over-expressing mice (with a high level of overexpression) have been shown to exhibit cardiac hypertrophy and diminished ventricular function [102].

Severe cardiac-specific expression of the ψεRACK peptide (i.e. PKCε-specific activator) also leads to development of concentric cardiac hypertrophy in mice [164], while mouse models with severe cardiac-specific overexpression of the PKCε inhibitor peptide εV1 developed lethal, dilated cardiomyopathy. In a salt-hypertensive rat model which usually develop fibrosis with age and continue to heart failure, sustained treatment with the εV1-2 PKCε inhibitor decreased the amount of fibrosis [165]. Sustained treatment with the inhibitor had a positive effect, but a mouse model of pressure-overload aortic banding together with a PKCε gene deletion show an increase in fibrosis in heart tissue [166], [121]. These observations support the idea of hormesis with respect to PKCε – a little is good, but too much is bad. These observations also suggest an association

between PKCε and heart failure, but the conflicting data make it unclear as to exactly how they relate. This particular link is still to be investigated in greater detail.

E: PKCε and STAT3 – linked pathways in heart failure?

In the context of the heart, STAT3 and PKCε both play a big role in protection and survival. STAT3 is noted for its role as a transcription factor, but also appears to be an upstream mediator in signal transduction in cardiac cell injury. In addition to transcription of pro-survival genes, it brings about cell responses in the setting of injury such as its inhibitory effect on the opening of the mPTP, its association with activity of anti-apoptotic proteins and colocalization with structures such as Cx43 channels which are involved in electrical transduction between adjacent cardiomyocytes. It is also involved in regulation of metabolism in situations of cell stress, as it associated with mitochondria – both by its translocation there when activated, as well as its colocalization with complex I/II of the electron transport chain. Transcending this level, STAT3 is also involved in the distribution of cells and structure of the heart, which is reflected in its involvement in heart failure.

PKCε is noted for the role it plays downstream of cell surface receptors, and its response to cell signalling molecules to transduce signals to processes promoting survival in cells. In response to injury, it closes the mPTP, prevents aberrant electrical signal transduction in adjacent cells by phosphorylating and inhibiting Cx43. It also closes the sarcolemmal K_{ATP} channels in cardiac and other cells when ATP levels drop. PKCε is well recognised for its involvement in heart metabolism under stress such as hypoxia, and its regulation of the glycolysis-fatty acid metabolic switch. It also has a marked effect at the level of the organ tissue as both severe over-expression, as well and complete inhibition produce fibrosis in tissues and HF-like structural symptoms.

The effects of STAT3 and PKCε are remarkably similar and seem to target the same organelles and cellular machinery. Neither of them has been directly associated with the other, but scrutinizing the evidence, it seems to indicate that they could work together to produce the cardioprotective effects consistent with each other in the heart, and particularly in the development of HF.

1.5) Hypothesis

We hypothesise that STAT3 and PKCε may act synergistically as part of separate cardioprotective pathways to target mitochondria of cardiomyocytes for cardioprotection.

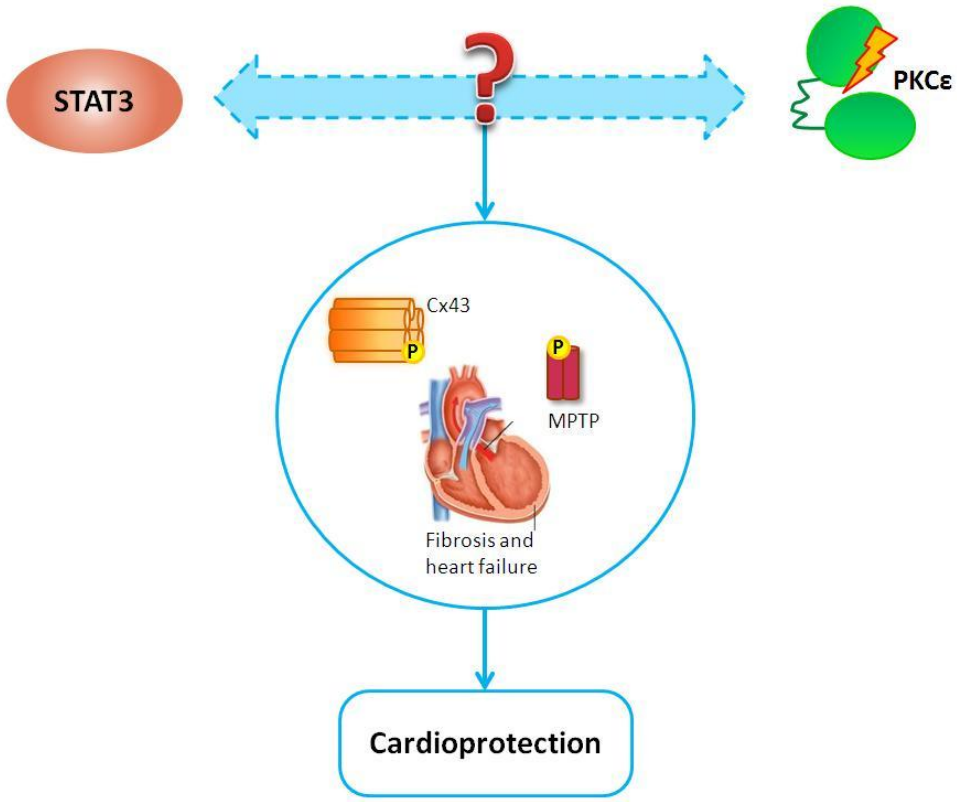

Figure 8: STAT3 and PKCε have consistent effects in cardioprotection, targeting the same organelles and systems. The activities of STAT3 and PKCε may be linked in the setting of cardioprotection. This project will investigate the possible link between the two pathways involving STAT3 and PKCε.

To answer our hypothesis we aim to:

- Delineate the interaction between the pathways involving STAT3 and PKCε by looking at the recovery of hearts:
    - From wildtype and cardiomyocytes STAT3 deficient mice treated with a PKCε activator
    - From wildtype and PKCε overexpressing mice treated with a STAT3 inhibitor
- Explore the development of heart failure in STAT3 deficient mouse hearts with age by means of histology staining.
- Conclusively determine whether signalling with STAT3 and PKCε are linked.

Knowledge of these signalling pathways would provide the information we need to develop better, more effective and efficient therapies for the treatment of heart failure, heart attacks and numerous other related conditions.

Both STAT3 and PKCε are known to be present in the mitochondrion. To explore the possible interactions of the pathways involving PKCε and STAT3 in cardioprotection, we used permeabilized heart fibres of BalbC mice pre-treated with a PKCε (ψεRACK) activator so as to mimic a PKCε-overexpressing mouse model, and fibres from an established STAT3 mouse model with a deletion in the STAT3 gene (STAT3 KO). Mitochondrial respiration and recovery after a simulated hypoxic incident were measured in permeabilized heart fibres of PKCε-activated (aPKCε) mice at baseline and with treatment of a STAT3 inhibitor to see whether this would abrogate the cardioprotection conferred by PKCε, thus implicating STAT3 as a downstream member of the PKCε cardioprotection

pathway. Conversely, heart fibres of STAT3 KO mice and littermate controls underwent the same procedure. Respiration and recovery were measured at baseline and with treatment of a PKCε activator to see whether this would have an advantageous effect on the recovery of hearts compromised for STAT3 and place PKCε downstream of STAT3. To further support the findings of this investigation, peptide levels for STAT3, PKCε and other key molecules will be evaluated in protein samples from these experiments (see fig.7).

Furthermore, to evaluate STAT3 and the effect it has on the development of heart failure, we used mice with a cardiomyocyte-specific deletion in the STAT3 gene. The mice were used between 9 and 10 months of age, their heart fibres permeabilized and their respiration measured using fatty acids as a substrate. Attenuated mitochondrial respiration in the presence of fatty acids only as a substrate is a sign of a failing heart, and inability to respire efficiently it would indicate that heart fibres have transitioned to the metabolic state of heart failure. Hearts will be harvested and prepared for histological staining to examine the compaction of the heart tissue and the amount of fibrosis in the heart. These findings were compared to previously established models of heart failure. Additionally, to see for colocalization of STAT3 and PKCε , we used conjugated fluorescent secondary antibodies for total PKCε and total STAT3 with fluorescence imaging to obtain the areas of colocalization in the genetically modified and wildtype mouse hearts.

In this project we investigated the possibility of a signalling interaction between PKCε and STAT3. The motivation for this project was an interesting finding in a mouse model with a cardiac-specific over-expression of PKCε in our lab – protein levels of p-serSTAT3 were found to be elevated in PKCε over-expressing hearts (2.33 A.U) compared to wildtype control hearts (1.25) (n=5, p>0.05, data not shown). These mouse hearts were found to be robustly cardioprotected

against both acute and chronic oxidant stress. This, together with the delineation of the cardioprotective SAFE pathway in their laboratory, led us to investigate the possibility that there may be cross-talk between STAT3 and PKCε, both signalling molecules contributing to the survival of the heart.

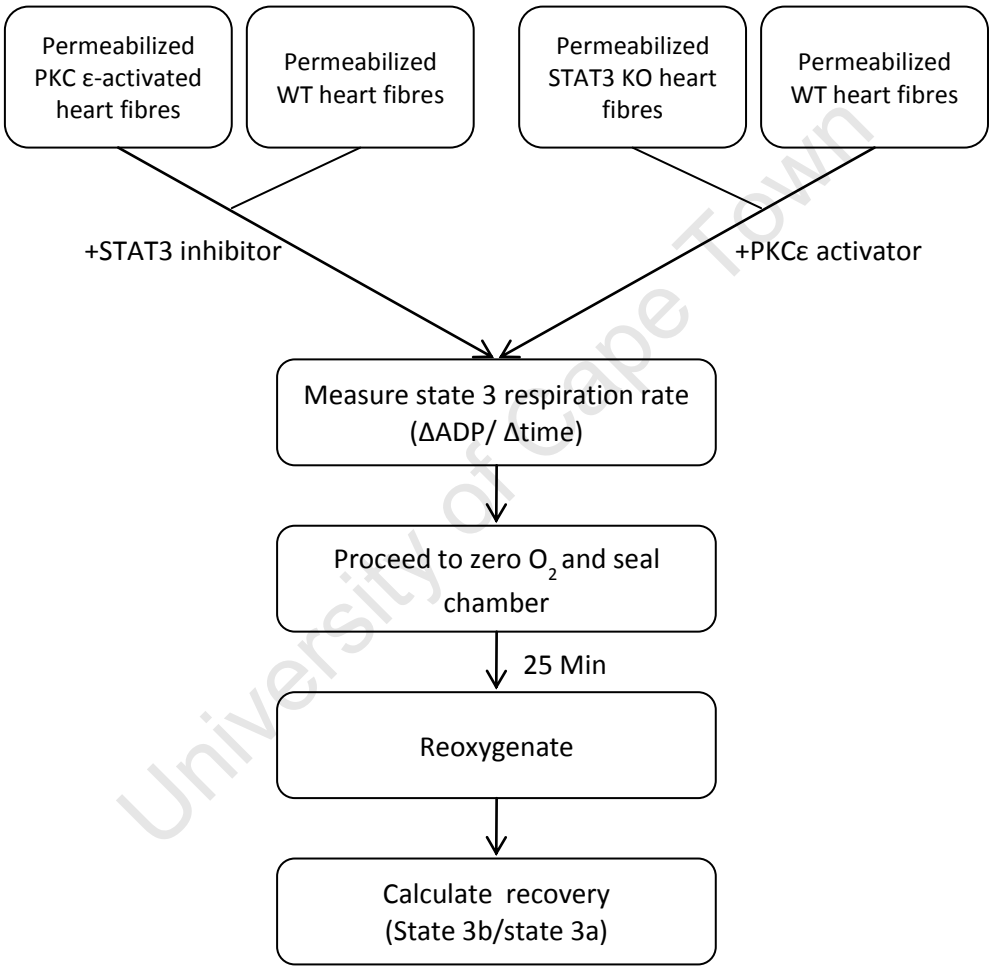

Figure 9: Schematic of the experiment to mimic ischemia-reperfusion in permeabilized heart fibres from PKCε-activated and STAT3 deficient hearts. By looking at how recovery in respiration is affected in PKCε-activated fibres with a STAT3 inhibitor and STAT3 deficient fibres with a PKCε activator, we would be able to determine whether the activities of STAT3 and PKCε are linked.

Materials and methods:

2.1) Animals

2.1.1) Cardiac-specific STAT3 knockout mouse model

Cardiac-specific STAT3-deficient mice (STAT3 KO) were created by crossing together mice heterozygous for an MLC2V-driven Cre-recombinase [167] with mice homozygous for flox-surrounded section of STAT3 [168]. Mice found to be homozygous for the deleted 1.4-kilobase fragment of STAT3 (containing exon 1, intron 1, exon 2 and part of intron 2) and MLC2V Cre-recombinase by means of PCR analysis [169], [170] were used as STAT3 KO, and mice found to lack Cre-recombinase by PCR analysis were used as wildtype littermate controls. BalbC inbred, albino laboratory mice were also used for experiments requiring PKCε overexpression and their wildtype, untreated controls.

2.1.2) Animal ethics

All mice (9 weeks – 10 months of age) were housed, and all experiments were conducted in accordance with the Guiding Principles in the Care and Use of Animals and National Institute of Health Guidelines (NIH publication No. 85-22, revised 1996) [171]. All procedures were also approved by the Faculty of Health Sciences Animal Ethics Committee of the University of Cape Town (project reference number: 011/025). Only male mice were employed for this study, as oestrogen levels vary through the reproductive cycle and, if used as part of this study, may cause inaccurate attribution of cardioprotective effects to treatment by drugs rather than to oestrogen levels.

2.2) Mitochondrial respiration studies

2.2.1) Permeabilization of heart fibres

Mice were anesthetized using sodium pentobarbitone (50mg/kg body mass, Bayer, SA; Bodene, trading as Intramed, Port Elizabeth, South Africa). Depth of anaesthesia was assessed by pedal reflex: once the pedal reflex had disappeared a sufficient degree of anaesthesia was obtained, the chest cavity was cut open and hearts were rapidly excised and arrested in ice-cold solution A (see appendix A). Excess connective tissue and right atria were removed using dissection scissors, and heart muscle tissue composed of the left and right ventricles, and the left atria was submerged in solution A and cut longitudinally into fine strips using a sharp blade. These strips were rinsed with solution A to remove excess blood and permeabilized for 20 minutes on ice using the detergent saponin (final concentration 50mg/ml in solution A). After permeabilizing, fibres were washed twice for 10 minutes with solution A on ice, unless otherwise specified, using the method of Boudina [172], [132]. The fibres were kept in solution A on ice before being assayed. This permeabilization procedure was performed as quickly as possible, keeping everything on ice to ensure that the heart fibres would be in optimal condition for the experiment. The entire procedure usually took less than 50 min and fibres were viable for up to 4 hours after extraction. Viability was checked during respiration experiments by looking at the respiratory control index – this is the ratio of the rate of respiration after the addition of ADP (state 3a) to the rate of respiration once the ADP has been consumed (state 4). A ratio of 3 or higher is considered to be indicative of viable mitochondria. This time period had also been determined from previous sets of experiments in the lab.

2.2.2) Determination of mitochondrial Respiration Coupling to measure fatty acid oxidation

Respiration studies were performed in a respirometer equipped with a Peltier temperature control unit [Oxytherm, Hansatech, Norfolk, UK]. The 3ml chamber contained 400µl of Solution B (See appendix A) at 25^{o}C. To ensure calibrations were stable, a baseline reading was taken before the addition of heart fibres. On addition of fibres, a second reading was taken to determine state 1 respiration. State 1 respiration is regarded as the endogenous respiration of the mitochondria. After approximately 1 min, 50µl of substrate (final concentration 20 µM palmitoyl carnitine, 2mM malate) was added, and state 2 respiration was measured. State 2 respiration shows the use of substrate (palmitoyl carnitine and malate) by mitochondria in the absence of ADP. State 2 respiration continued for approximately 1 min before the addition of 50 µl of ADP (final concentration 560µM) to the chamber to start state 3 respiration. During the conversion of ADP to ATP a large amount of oxygen is used, and the chamber was sealed during this time to obtain an accurate respiration rate. Respiration rates for this part of the study were normalised to dry weight of the heart fibres.

2.2.3) PKCε activation and STAT 3 inhibition

BalbC mice were injected with 1 unit (5µl) of 4mM of ψεRACK activator, intraperitoneally 10 minutes prior to anaesthesia, to mimic a PKCε over-expressing mouse model [173]. All permeabilization and running buffers for aPKCε (PKCε -activated) hearts contained 5µM of the ψεRACK activator (see fig. 10). Permeabilization of the heart fibres was done on ice, and subsequent rinsing of fibres was done at room temperature with STATTIC (STAT3 inhibitory compound) added to the buffer (final concentration 100µM) [Sigma, T3434, ST Louis MO]. STATTIC

is a small molecule shown to selectively inhibit the activation of the STAT3 transcription factor by blocking phosphorylation and dimerization events [174]. STATTIC attains maximal inhibition at 37°C [174], but the incubation of fibres at 37°C reduces the period for which fibres would be viable for experimental use. Thus fibres were rinsed at room temperature and then placed on ice until such time as they were added to the respiration chamber. Treatment with DMSO (Dimethyl Sulfoxide, 99.9%) was used as a vehicle control for STATTIC.

For the STAT3 deficient mouse model, the same treatment was done using only STATTIC as above, without the ψεRACK activator injection prior to anaesthetism.

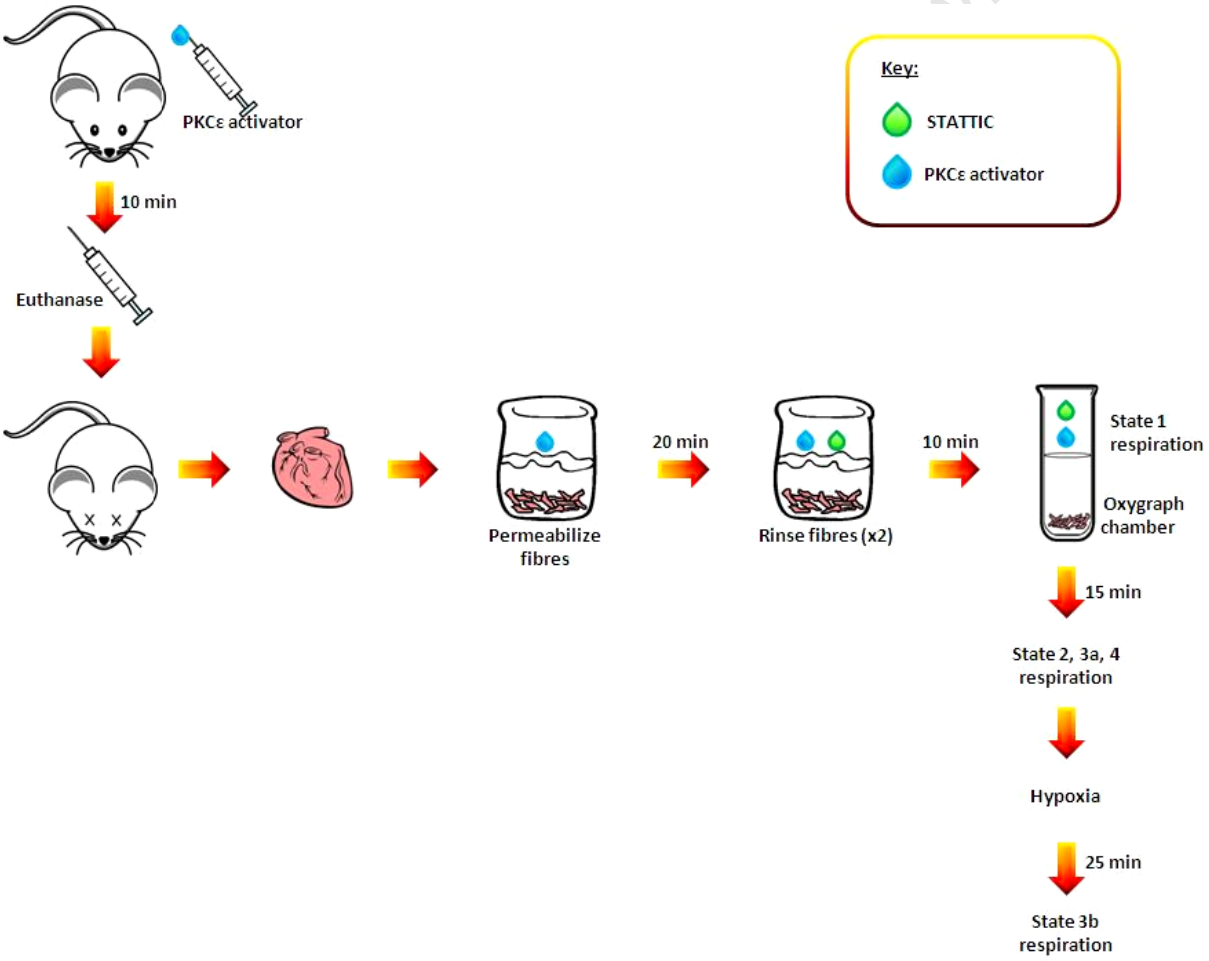

Figure 10: Schematic of the method to extract and permeabilize fibres to mimic a PKCε-activated mouse model. Mice will be injected with the ψεRACK activator prior to anaesthesia. Hearts were excised and cut into strips, before being permeabilized in a buffer containing the ψεRACK activator, and rinsed in a buffer containing both the ψεRACK activator and STATTIC. Fibres were incubated with both the ψεRACK activator and STATTIC for 15 minutes in the chamber before respiration studies were performed.

2.2.4) Determination of mitochondrial Respiration Coupling for PKCε-activated and STAT 3 deficient hearts

The 3ml respiration chamber contained 400µl of Solution B (See appendix A) at 30^{o}C with 1 µl of 100mM STATTIC (final concentration 200µM in chamber, after the addition of substrates) or DMSO as a control. Solution B also contained 32mM of the ψεRACK activator. A baseline reading was taken to ensure the stability of the calibration. On addition of fibres, a reading was taken for state 1 respiration. Fibres were left to stir in the chamber for 15 min prior to addition of substrates to allow time for the STATTIC treatment to achieve a 50 – 70% inhibition of STAT3 [174]. After 15 minutes in the chamber, 50µl of substrate (final concentration 5mM glutamate, 2mM malate) was added, and state 2 respiration was measured. State 2 respiration continued for approximately 1 minutes before 50 µl of ADP was added to the chamber (final concentration 560µM) and it was sealed to obtain state 3a respiration (i.e. the state 3 respiration before hypoxia). Once state 3a respiration had been measured, the fibres and buffer from the chamber were transferred to a petri dish and placed in a hypoxic chamber at 30^{o}C. Nitrogen gas was used to displace oxygen from the chamber to attain hypoxia. After 25 minutes of hypoxia, the samples were re-oxygenated by transferring the fibres to the respiration chamber containing 400 µl of fresh solution B with 50 µl of ADP and 50 µl of substrate (final concentration 5mM glutamate, 2mM malate). State 3 respiration was thus re-established. State 3 respiration prior to hypoxic insult is regarded as state 3a respiration, while post-hypoxic respiration is regarded as state 3b respiration. A percentage recovery was determined by the ratio of state 3a x 100/ state 3b for each treatment. Excess and assayed fibres were taken from each heart preparation, snap-frozen in liquid nitrogen and stored at -80^{o}C for western blotting. All measurements taken for this part of the study were normalised

to the protein content of fibres (see method below). This protocol was used for both aPKCε and STAT3 deficient hearts.

2.3. Western blot analysis

2.3.1) Protein extraction

Nuclear and cytosolic fractions were extracted for western blotting using the method of William and Ford [175]. Fibres were thawed and homogenised in 270 µl of solution C [see Appendix A] on ice using a polytron [Kinematica, Switzerland] at setting 4 for 2.5 seconds. The homogenate was transferred to an eppendorf tube and centrifuged at 10 000g for 5 minutes at 4^{o}C to pellet large debris and nuclei. The supernatant containing the cytosolic fraction was transferred to a clean eppendorf tube and the pellet was re-suspended in 150 µl of solution D and centrifuged at 15 000g for 30 minutes at 4^{o}C. The supernatant contained the nuclear fraction and was transferred to an eppendorf tube, and the pellet containing the cell debris was discarded.

2.3.2) ***Bradford protein determination***

Protein determination was done using a Bradford assay [176]. The Bradford reagent was diluted to a 1x working solution with distilled water. In an eppendorf, 5 µl of protein sample and 95 µl of distilled water were mixed, and 900 µl of the diluted Bradford reagent was added. After mixing, 200 µl of each sample was loaded onto a 99 well microplate for the absorbance to be measured. The components were protected from light as far as possible for the duration of the assay to prolong the stability of the working solution. BSA standards were added to separate wells and mixed, these served to construct a standard curve to determine the protein concentration. Protein extracts were added to separate wells (10 µl per well) and mixed. Absorbance was measured at

595nm using a microplate reader [GloMax, Promega, Fitchburg, WI 53711] and protein concentration was determined from the standard curve. All samples were assayed in duplicate.

2.3.3) Western blot procedure

Proteins were extracted as described above and diluted 1:1 on ice with Laemmli buffer (see appendix A) [177]. Western blots were run on a 7.5% sodium dodecyl sulphate-polyacrylamide gel electrophoresis gel. A lower separating gel (see appendix A) was prepared, poured, levelled with ethanol and left to set. Ethanol was removed using blotting paper before an upper stacking gel (see appendix A) was poured. Gels were set in glass plates and a plastic comb was inserted into the upper stacking gel formed lanes for the loading of samples, making sure there were no bubbles present. When set, gels were assembled in a running chamber, the inner chamber of which was filled with running buffer (see appendix A). Each lane was washed with running buffer before samples were loaded on to the gel. The first lane of each gel was loaded with 7µl of peqGOLD protein marker IV [Optima Scientific, 27-2110], and subsequent lanes were loaded with 100µg of protein samples (in buffer, see above), thawed on ice. Once samples were loaded, the outer chamber was filled with running buffer and samples were electrophoresed at 160V for 90 min, or until the gel front had reached the bottom of the gel. A transfer membrane was cut to size and soaked in fresh methanol for 5 min, in sterile distilled water for 2 minutes and in transfer buffer (see appendix A) for 15 min. The gels were then removed from the chamber and dissected to retain only the lower separating gel, which in turn was covered with a polyvinylidene difluoride (PVDF) membrane [Hybond, Amersham, UK] and sandwiched between blotting paper and sponge inside a transfer cassette. Care was taken to ensure that the membrane was on the side of the gel closer to the positive side of the transfer cassette, that there were no air bubbles between the membrane and gel, and that all elements of the sandwich were submerged in ice cold transfer

buffer prior to and during assembly. Cassettes were covered with ice cold transfer buffer and transferred at 0.2A for 2 hours, or 0.02A overnight. Membranes were removed and soaked in methanol for 30 sec before being dried completely. Once dried, membranes were labelled and washed vigorously with TBS-T (see appendix A) 3 times for 5 min. Membranes were blocked for 2 hours in 5% milk powder in TBS-T before being washed with TBS-T 3 times for 5 minutes each. Membranes were then exposed to a primary antibody (p-ser STAT3, p-tyr STAT3, total STAT3, total PKCε, total and phosphorylated AKT1 and total and phosphorylated Erk1/2 for PKCε-activated mice, STAT3-/- mice and their controls (all 1:10000 in TBS-T) [Santa Cruz Biotechnology, Santa Cruz CA] for 1hour at room temperature before being washed with TBS-T 3 times for 5minutesand being exposed to a secondary antibody for 1hour at room temperature. Membranes were washed again with TBS-T 3 times for 5 minutes each. Equal loading was verified with β-actin or Glyceraldehyde 3-phosphate dehydrogenase (GAPDH) (1:10000 in TBS-T). GAPDH was used as a loading control for the membranes which were probed for proteins with approximately the same size as β-actin. Membranes were then treated with enhanced chemiluminescent (ECL) Western Blotting Detection Reagents [Amersham, UK], and images were captured over 5 minute periods and superimposed by means of a GeneGnome HR [Syngene Bioimaging, UK]. Image densitometry analysis was used to quantify luminescence using computerized software package [UVI Soft, UVI Band, UVI Tech, Cambridge, UK and Image –J]. Image densitometry results for each protein of interest were normalised by ratio to the loading control before statistical analyses were performed.

2.4. Histology

2.4.1) Histological fixing of hearts

Mice were anesthetized by intraperitoneal injection of sodium pentobarbitone (50mg/kg body mass) [Bayer, SA; Bodene, trading as Intramed, Port Elizabeth, South Africa]. Once a sufficient degree of anaesthesia had been obtained, the chest was cut open and 0.1ml of saturated potassium chloride (KCl) solution was injected into the left ventricular chamber to arrest the hearts in diastole. The heart was excised and excess connective tissue was removed before flushing with solution A (see appendix A) to eliminate all blood. The heart was then submerged in paraformaldehyde for 1 – 2 days to set before slicing. When set, the atrium was trimmed off the heart and the remainder of the heart was sliced into three transverse sections from the apex to the basal part of the left ventricle by means of a cryostat at 10µm thickness with an interval of approximately 300 µm between each section. All sections were mounted on glass slides for staining and quantitative analysis. [178]

2.4.2) De-waxing of paraffin-embedded tissue sections

Paraffin sections were de-waxed and hydrated. This was done by submerging the slides with tissue sections on them in xylene twice, for five minutes each time. These were then hydrated by dipping slides 10 times in two changes of 95% ethanol, followed by 70% ethanol, then distilled water, tapping off excess liquid between changing of solutions. Slides were stored in phosphate buffered saline (PBS) until staining was performed.

2.4.3) Sirius Red collagen staining

Slides were removes from PBS and tapped dry before being submerged in picro-sirius red solution (1g Sirius red F3B per litre saturated aqueous solution of picric acid) for an hour. Sections were washed twice in acidified water (5ml acetic acid per litre water) and drained before dehydrating in

3 changes of 100% ethanol. Sections were then cleared in xylene and mounted in a resinous medium for analysis.

2.4.4) Examination of histological sections

Picro-sirius stained histological sections were examined with a Nikon Eclipse 90i microscope using a 4x objective. Images were captured with the use of NIS-Elements Basic Research software [Nikon Instech Co. Ltd, Japan]. ImageJ 1.34 software was used to measure fibrotic areas [178].

The amount of fibrosis for each heart was determined using a scale from 0 to 10, with a score of 0 having no visible signs of fibrosis, and 10 having complete tissue fibrosis with Sirius Red staining for collagen. Assessment of the tissue was done blinded, with no knowledge of the identity of the sections during the investigation.

2.4.5) Fluorescence staining

Slides were removes from PBS and tapped dry before being incubated with 100µl of 5% donkey serum [Invitrogen Life Technologies Corporation, Paisley, UK] for 20 minutes at room temperature. The serum was drained and 100 µl of primary antibody (1:100 in PBS for total STAT3 and total PKCε) was distributed over sections and incubated for 90 minutes at room temperature. A PBS control was included to evaluate secondary antibody binding. Sections were then carefully rinsed with 100 µl of PBS before 100 µl of secondary antibody (1:200 in PBS), FITC-conjugated anti-rabbit antibody [Jackson ImmunoResearch Laboratories, Inc. PA, USA] or Alexa Fluor-568 conjugated anti-goat antibody [Invitrogen Life Technologies Corporation, Paisley, UK] was added and incubated for 30 minutes at room temperature. Thereafter, 100 µl of Hoechst (final concentration 50µg/ml PBS) [Invitrogen Life Technologies Corporation, Paisley, UK] was added and incubated for

15 minutes at room temperature. Sections were washed with 100 µl of PBS thrice before mounting with a fluorescent mounting medium [Dako Cytomation, Denmark], and sealed. For this protocol, care was taken to ensure minimal light exposure during the preparation of slides and antibody solutions. Slides were wrapped and stored at -20^{o}C until examination.

2.4.6) Fluorescence Imaging

Image acquisition was performed on an Olympus Cell R system attached to an IX 81 inverted fluorescence microscope equipped with an F-view-II cooled CCD camera [Soft Imaging Systems GmbH, Germany]. Using a Xenon-Arc burner [Olympus BioSystems GmbH, Germany] as light source, images were acquired using the 360 nm, 472 nm or 572 nm excitation filter. Emission was collected using a UBG triple-bandpass emission filter cube [Chroma Technology Corporation, VT, USA]. Z-stack image frames were acquired by using a step width of 0.4 µM, utilizing an Olympus Plan Apo N 60x/1.4 Oil objective and the Cell R imaging software [Olympus BioSystems, GmbH, Germany]. Images were processed, background-subtracted and projected as maximum intensity projection. Signal co-localization was performed using the Cell R software.

2.5. Chemicals

Unless specified, all chemicals were obtained from Sigma-Aldrich Inc., and all antibodies from Santa Cruz Biotechnologies.

2.6. Statistical analysis

Results are expressed as means ± SEM. Significance ($p < 0.05$) was determined for continuous variables by using the Student's 2-way t-test with Welch correction, and one-way Anova and Tukey's post-test.

Results:

3.1 PKCε -STAT3 interaction in PKCε -activated heart fibres

3.1.1) The effect of STAT3 inhibition on respiration in PKCε -activated heart fibres subjected to hypoxia

Respiration parameters were measured in isolated heart fibres subjected to 25 minutes of hypoxia. Wildtype (WT) hearts treated with DMSO served as the comparative control for the recovery in respiration of heart fibres after hypoxia. These fibres showed a recovery of (1.00±0.02 A.U) (see fig. 11). When treated with the STAT3 inhibitor, STATTIC, recovery decreased very slightly to (0.94±0.02), with no significant difference compared to the control ($p>0.05$). PKCε -activated (aPKCε) fibres treated with DMSO showed a recovery of (0.94±0.08), with no significant difference compared to the control ($p>0.05$). aPKCε fibres treated with the inhibitor STATTIC showed a recovery of (0.99±0.07), which was not significantly different from the WT control, nor from the aPKCε DMSO control ($p>0.05$) (n=6 per group).

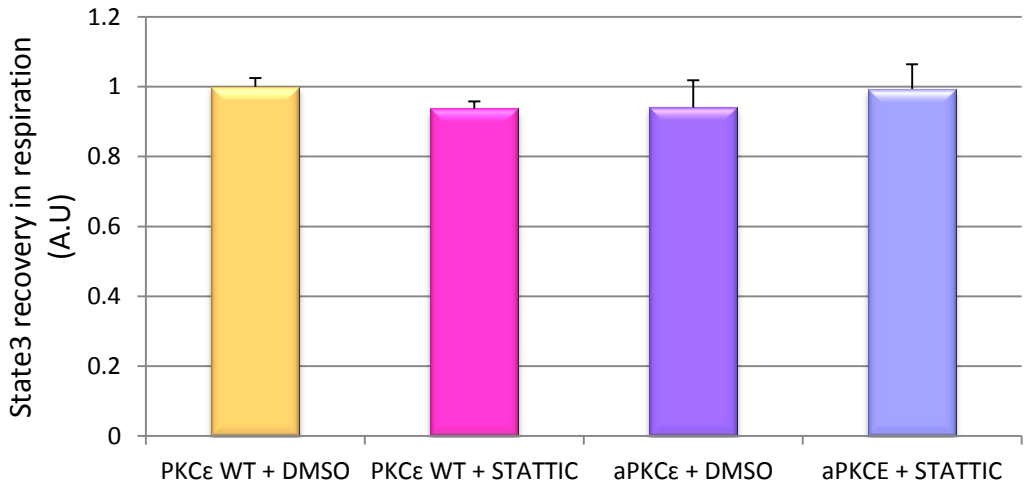

Figure 11: Normalised values for recovery of state3 respiration after hypoxia in PKCε-activated (aPKCε) and wildtype (PKCε WT) mouse heart fibres. Percentage recovery is measured by comparing the post-hypoxic respiration rate (state 3a) to the baseline, pre-hypoxic respiration rate (state 3b). There were no significant differences found in state 3 percentage recovery of respiration within or between STATTIC and DMSO treatment groups for aPKCε and WT mouse heart fibres. (n=6 per group, $p>0.05$).

3.1.2) The effect of STAT3 inhibition on protein levels in PKCε-activated fibres subjected to hypoxia

3.1.2.1) Levels of total STAT3, phosphorylated STAT3 and PKCε in aPKCε heart fibres

Western blots were performed on STAT3 WT and STAT3 KO heart fibres after completion of hypoxia and respiration studies, to evaluate the levels of the phosphorylated STAT3 present (p-tyr STAT3, p-ser STAT3 and total STAT3), as well as levels of total PKCε in the treated samples. Banding patters appeared to be consistent between groups (see fig. 12).

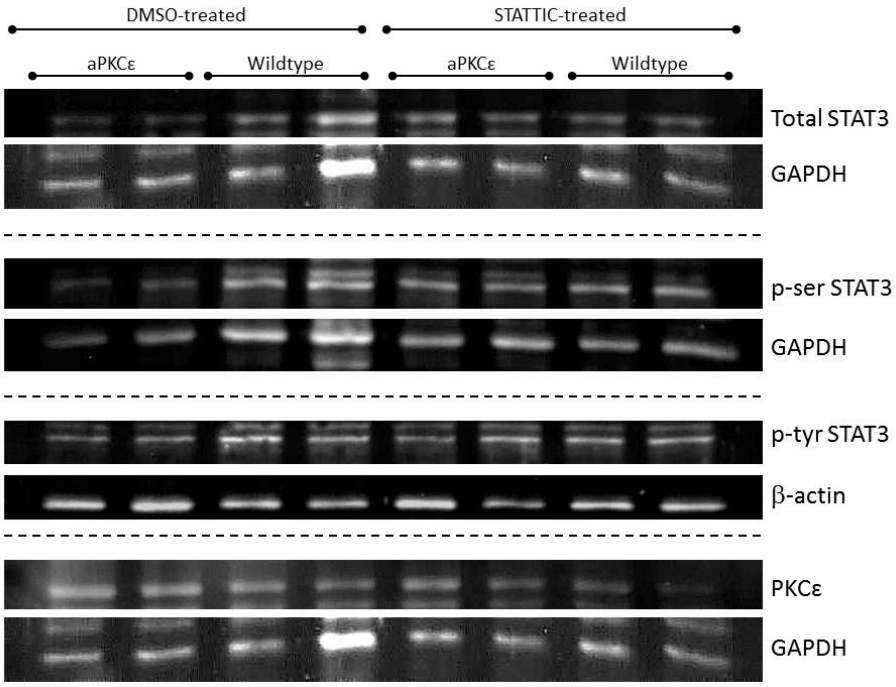

Figure 12: Banding patterns obtained from western blots for total STAT3, p-ser STAT3, p-tyr STAT3, total PKCε for DMSO-treated (vehicle control) and STATTIC-treated aPKCε and WT hearts after hypoxia. GAPDH and β-actin bands served as loading controls. Banding patterns appear to be consistent for all groups for each probe of interest (n=4 per group, $p>0.05$).

After analysis and correction for loading, levels for the total STAT3 in the WT DMSO control were 0.62±0.08 A.U. STATTIC-treated WT showed no significant difference in levels (0.61±0.06)

compared to the control group (p>0.05) (see fig. 13). There was also no significant difference in total STAT3 in the DMSO control-treated aPKCε group (0.70±0.08) compared to the WT control, nor the STATTIC-treated aPKCε group (0.72±0.02) when compare to the WT control or the aPKCε DMSO control-treated groups (p>0.05, n=4 per group)

Levels for the p-ser STAT3 in the WT DMSO control were 0.85±0.05 A.U. STATTIC-treated WT showed no significant difference in levels of p-ser STAT3 (0.73±0.07) compared to the control group (p>0.05) (see fig. 13). There was also no significant difference in p-ser STAT3 in the DMSO control-treated aPKCε group (0.74±0.11) compared to the WT control, nor the STATTIC-treated aPKCε group (0.85±0.09) when compare to the WT control or the aPKCε DMSO control-treated groups (p>0.05, n=4 per group).

Levels for the p-tyr STAT3 in the WT DMSO control were 0.67±0.04 A.U. STATTIC-treated WT showed no significant difference in levels of p-tyr STAT3 (0.78±0.05) compared to the control group (p>0.05) (see fig. 13). There was also no significant difference in p-tyr STAT3 in the DMSO control-treated aPKCε group (0.67±0.11) compared to the WT control, nor the STATTIC-treated aPKCε group (0.82±0.23) when compare to the WT control or the aPKCε DMSO control-treated groups (p>0.05, n=4 per group).

Levels for total PKCε in the WT DMSO control were 0.60±0.05 A.U. STATTIC-treated WT showed no significant difference in levels of total PKCε (0.59±0.05) compared to the control group (p>0.05) (see fig. 13). Total PKCε in the control-treated aPKCε group (0.79±0.03) was significantly elevated compared to the WT control and to the STATTIC-treated WT group (p<0.05). The STATTIC-treated aPKCε group (0.68±0.01) showed no significant difference when compare to the WT control or the aPKCε DMSO control-treated groups (p>0.05, n=4 per group).

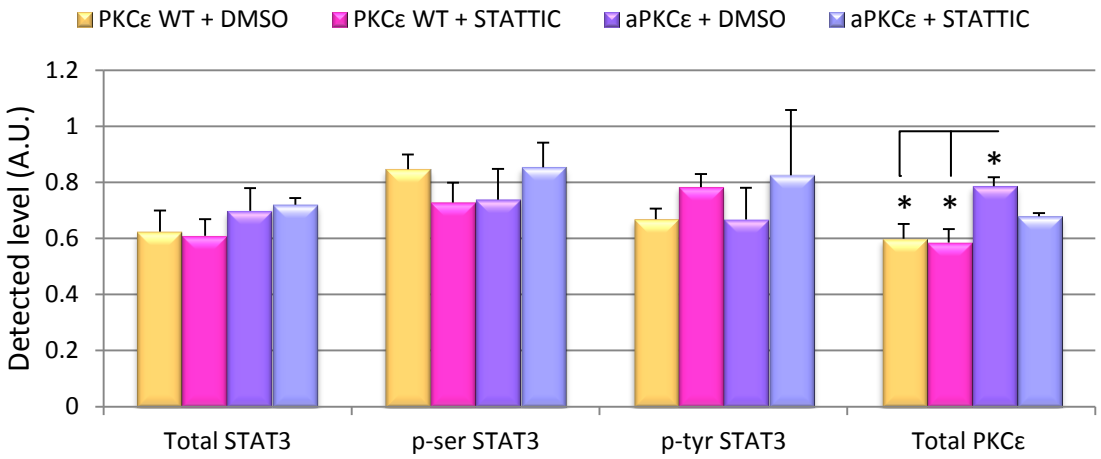

Figure 13: Western blot detected levels of total STAT3, p-ser STAT3, p-tyr STAT3 and total PKCε, corrected for loading in aPKCε and WT hearts treated with DMSO control, or STATTIC. No significant differences were found for levels of total STAT3, p-ser STAT3 or p-tyr STAT between treatment groups (n=4 per group, $p>0.05$). In the set detecting levels of total PKCε, the aPKCε group treated with DMSO control was significantly elevated compared to the DMSO- and STATTIC-treated PKCε WT groups (*$p<0.05$).

Levels of the two phosphorylated isoforms of STAT3 (p-ser STAT3 and p-tyr STAT3) were compared to total STAT3 to determine their levels of activation (see fig. 14). Levels of activation of p-ser STAT3 in the control group were found to be 1.42±0.19 A.U. There were no significant differences found in the level of p-ser STAT3 activation between STATTIC-treated WT (1.20±0.06), control-treated aPKCε (1.16±0.32), STATTIC-treated aPKCε (1.19±0.14) and the WT control ($p>0.05$), nor were there any differences between the two treated aPKCε groups ($p>0.05$).

Levels of activation of p-tyr STAT3 in the control group were found to be 1.12±0.16 A.U. There were no significant differences found in the level of p-tyr STAT3 activation between STATTIC-treated WT (1.35±0.23), control-treated aPKCε (1.02±0.23), STATTIC-treated aPKCε (1.15±0.33) and the WT control ($p>0.05$), nor were there any differences between the control- and STATTIC-treated aPKCε groups ($p>0.05$, n=4 per group). There were also no significant differences in the levels of activated p-ser STAT3 and p-tyr STAT3 within each group ($p>0.05$).

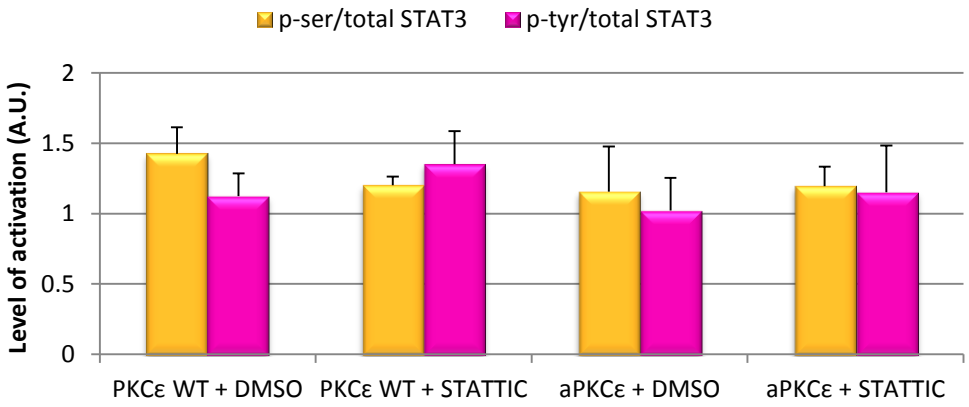

Figure 14: Levels of activation of p-ser STAT3 and p-tyr STAT3 when compared to total STAT3 in PKCε WT and aPKCε heart fibres after hypoxia. Levels of activation of p-ser STAT3 (p-ser/total STAT3) and p-tyr STAT3 (p-tyr/total) were consistent within each group, as well as between WT and aPKCε treatment groups (n=4 per group, p>0.0.5)

3.1.2.2) Levels of activation of ERK and AKT in aPKCε heart fibres

Activation levels were determined for ERK1/2 (MAP42/44) and AKT1, both downstream effectors of PKCε, using bands detected by western blotting (see fig. 15). Activation levels were determined by taking the ratio of phosphorylated to total ERK1/2 and AKT1 from western blots for total ERK (t-ERK), phosphorylated-ERK (p-ERK), total AKT1 (t-AKT1) and phosphorylated AKT1 (p-AKT1) after correction for loading. No significant differences were found for the activation levels of ERK1/2 between the control-treated WT (0.56±0.48 A.U.) and STATTIC-treated WT (0.50±0.06) groups (see fig. 16). No significant differences were found on comparison of the control-treated aPKCε group (0.64±0.05) to the WT control group, nor the STATTIC-treated aPKCε group (0.81±0.14). The STATTIC-treated aPKCε group showed no significant difference to the WT control groups (p>0.05, n=4 per group).

Activation levels of AKT1 in the control-treated WT group were 0.48 ±0.05 A.U. STATTIC-treated WT levels (0.39 ±0.07) showed no significant difference when compared to control-treated WT group. No significant differences were found for levels of AKT1 between control-treated aPKCε

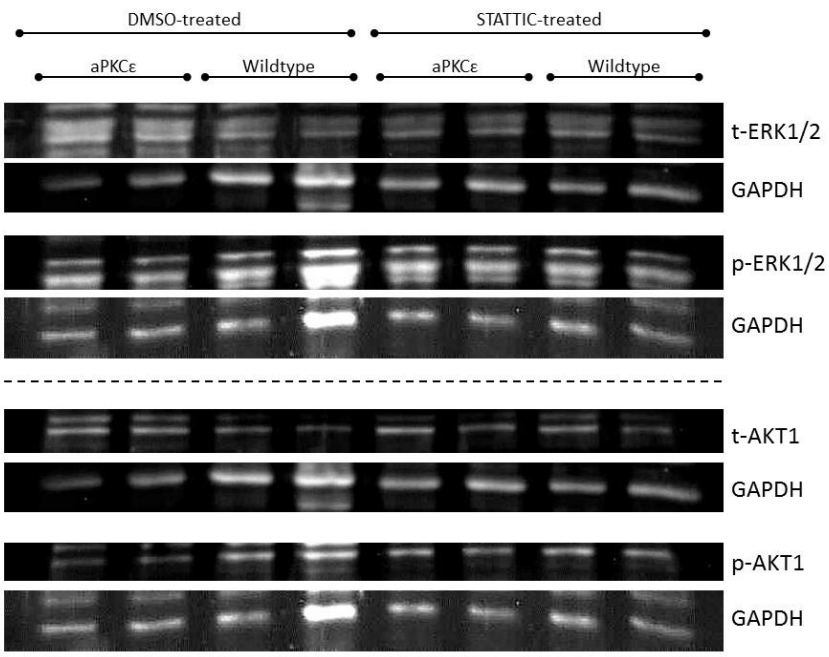

Figure 15: Banding patterns obtained from western blots for total ERk1/2 (t-ERK1/2) and its phosphorylated/activated isoform (p-ERK1/2) as well as total AKT1 (t-AKT1) and its phosphorylated / activated isoform (p-AKT1) together with their loading controls. Banding patterns appear to be consistent for both isoforms of ERK1/2 and AKT1/2 for all four groups.

(0.45 ±0.05) and WT control, nor between STATTIC-treated aPKCε (0.51 ±0.04) and WT control groups. There were no significant differences between the two aPKCε treatment groups ($p>0.05$, $n=4$ per group). There is a trend toward an increase of activated ERK1/2 in the PKCε -activated groups, but no significant differences in levels of activation over all.

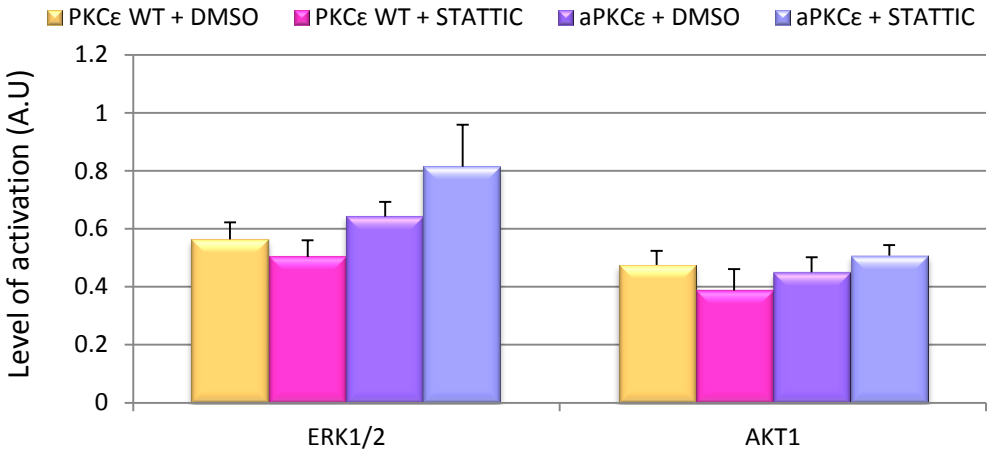

Figure 16: Activation levels of ERK1/2 and AKT1 determined using western blots. Activation levels were determined by comparison of phosphorylated to total levels of ERK1/2 and AKT1 after correction for loading. No significant differences were found for activation levels of ERK1/2 or AKT1 within or between groups ($n=4$ per group, $p>0.05$)

3.2 PKCε -STAT3 interaction in STAT3 KO heart fibres

3.2.1) The effect of PKCε activation on respiration in STAT3 deficient mouse heart fibres subjected to hypoxia

STAT3 wildtype (STAT3 WT) untreated heart fibres served as the comparative control for the recovery in respiration of heart fibres after hypoxia. These fibres showed a recovery of 1.00±0.19 A.U. (see fig. 17). When treated with the PKCε activator, ψεRACK, recovery was 0.85±0.28, with no significant difference compared to the control ($p>0.05$). STAT3 deficient (STAT3 KO) untreated fibres showed a recovery of 0.56±0.23, with no significant difference compared to the control ($p>0.05$). STAT3 KO fibres treated with the ψεRACK activator showed a mildly improved recovery of 1.16±0.35, but was not significantly different from the STAT3 WT control, nor from the untreated STAT3 KO group ($p>0.05$) ($n=4$ for STAT3 KO, $n=8$ for STAT3 WT).

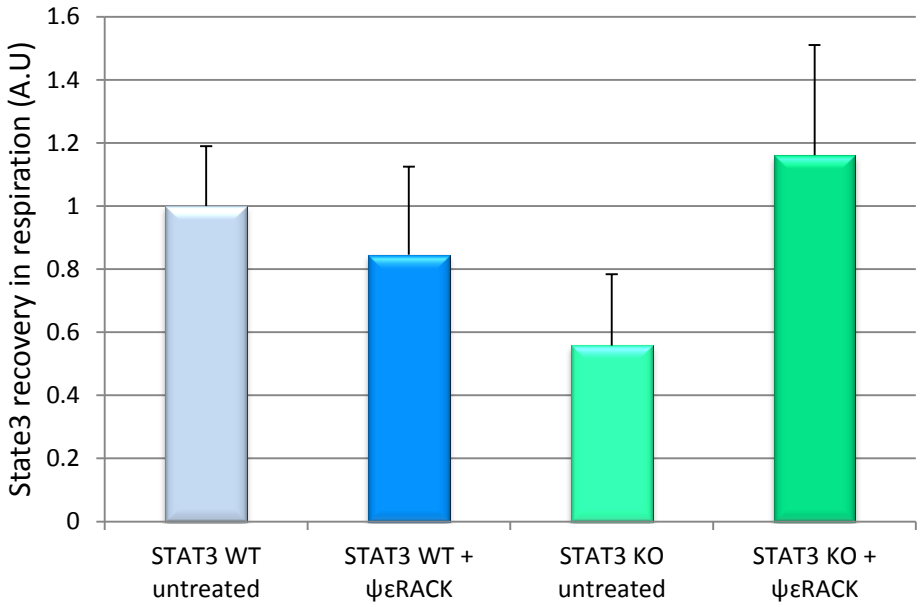

Figure 17: Percentage recovery of state3 respiration after hypoxia in STAT3 KO (n=4) and STAT3 WT (n=8) mouse heart fibres. There were no significant differences found in state 3 percentage recovery of respiration within or between ψεRACK-treated and control groups for STAT3 KO and WT mouse heart fibres ($p>0.05$).

3.2.2) The effect of PKCε activation on protein levels in STAT3 deficient fibres subjected to hypoxia

3.2.2.1) Levels of total STAT3, phosphorylated STAT3 and PKCε in STAT3 KO heart fibres

Western blots were performed on STAT3 WT and STAT3 KO heart fibres after completion of hypoxia and respiration studies, to evaluate the levels of the phosphorylated STAT3 present (p-tyr STAT3, p-ser STAT3 and total STAT3), as well as levels of total PKCε in the treated samples. Banding patters appeared to be consistent between groups (see fig. 18).

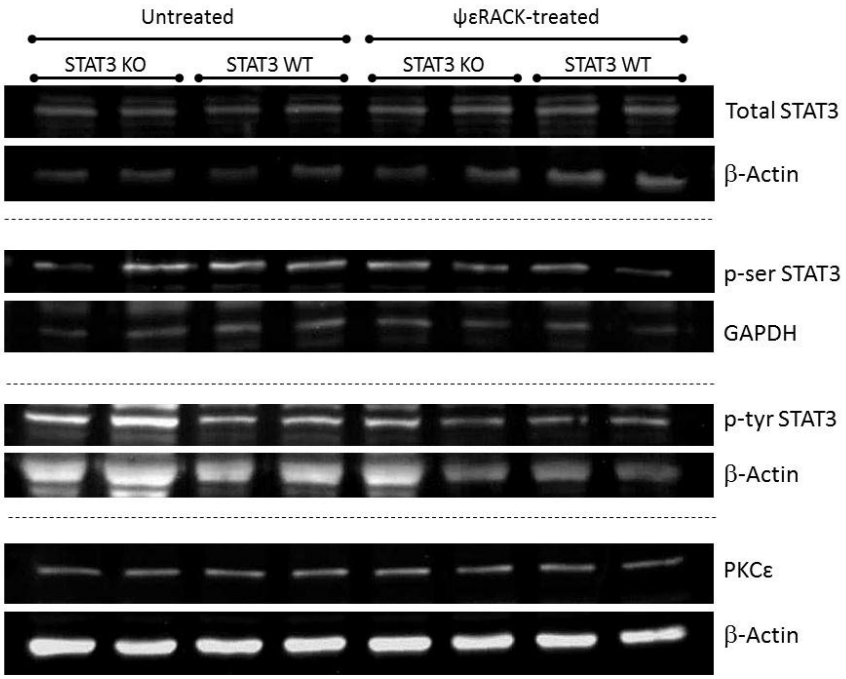

Figure 18: Banding patterns obtained from western blots for total STAT3, p-ser STAT3, p-tyr STAT3, total PKCε for untreated and ψεRACK-treated STAT3 KO and STAT3 WT hearts after hypoxia. GAPDH and β-actin bands served as loading controls. Banding patterns appear to be consistent for all groups for each probe of interest.

After analysis and correction for loading, levels for total STAT3 in the STAT3 WT control were 0.53±0.06 A.U. ψεRACK-treated WT showed no significant difference in levels (0.54±0.06) compared to the control group ($p>0.05$) (see fig. 19). There was also no significant difference in

total STAT3 in the untreated STAT3 KO group (0.76±0.06) compared to the STAT3 WT control, nor the ψεRACK-treated STAT3 KO group (0.59±0.06) when compared to the STAT3 WT control or the STAT3 KO untreated groups (p>0.05, n=4 for STAT3 KO, n=8 for STAT3 WT).

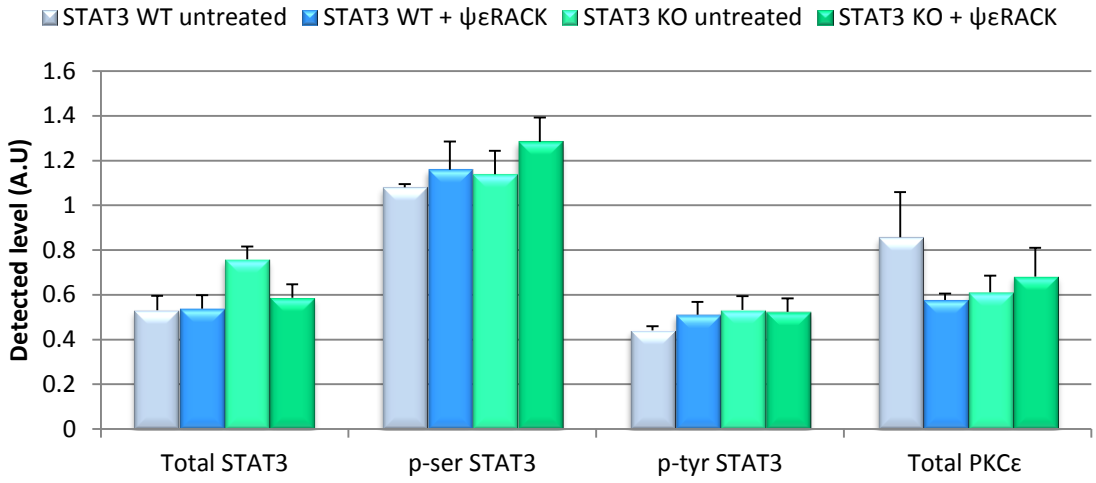

Figure 19: Detected levels of total STAT3, p-ser STAT3, p-tyr STAT3 and total PKCε from western blots, corrected for loading in STAT3 KO and STAT3 WT hearts. No significant differences were found in corrected levels between treatment groups for each probe of interest (n=4 per treatment group, p>0.05).

Levels for p-ser STAT3 in the STAT3 WT control were 1.08±0.02 A.U. ψεRACK-treated WT showed no significant difference in levels (1.16±0.13) compared to the control group (p>0.05) (see fig. 19). There was also no significant difference in p-ser STAT3 in the untreated STAT3 KO group (1.14±0.11) compared to the STAT3 WT control, nor the ψεRACK-treated STAT3 KO group (1.28±0.11) when compared to the STAT3 WT control or the STAT3 KO untreated groups (p>0.05, n=4 for STAT3 KO, n=8 for STAT3 WT).

Levels for p-tyr STAT3 in the STAT3 WT control were 0.44±0.02 A.U. ψεRACK-treated WT showed no significant difference in levels (0.51±0.06) compared to the control group (p>0.05) (see fig. 19). There was also no significant difference in p-tyr STAT3 in the untreated STAT3 KO group (0.53±0.06) compared to the STAT3 WT control, nor the ψεRACK-treated STAT3 KO group

(0.52±0.06) when compared to the STAT3 WT control or the STAT3 KO untreated groups (p>0.05, n=4 for STAT3 KO, n=8 for STAT3 WT).

Levels for total PKCε in the STAT3 WT control were 0.86±0.20 A.U. ψεRACK-treated WT showed no significant difference in total PKCε levels (0.58±0.03) compared to the control group (p>0.05) (see fig. 19). There was also no significant difference in total PKCε in the untreated STAT3 KO group (0.61±0.07) compared to the STAT3 WT control, nor the ψεRACK-treated STAT3 KO group (0.68±0.13) when compared to the STAT3 WT control or the STAT3 KO untreated groups (p>0.05, n=4 for STAT3 KO, n=8 for STAT3 WT).

Levels of the two phosphorylated isoforms of STAT3 (p-ser STAT3 and p-tyr STAT3) were compared to total STAT3 to determine their levels of activation (see fig. 20). Levels of activation of p-ser STAT3 in the control group were found to be 2.14±0.30 A.U. There were no significant differences found in the level of p-ser STAT3 activation between ψεRACK -treated STAT3 WT (2.18±0.19), control-treated STAT3 KO (1.51±0.14), ψεRACK -treated STAT3 KO (2.22±0.20) and the WT control (p>0.05), nor were there any differences between the two treated aPKCε groups (p>0.05).

Levels of activation of p-tyr STAT3 in the control group were found to be 0.88±0.14 A.U. There were no significant differences found in the level of p-tyr STAT3 activation between ψεRACK-treated STAT3 WT (0.99±0.15), control-treated STAT3 KO (0.71±0.09), ψεRACK -treated STAT3 KO (0.93±0.16) and the WT control (p>0.05), nor were there any differences between the untreated and ψεRACK -treated STAT3 KO groups (p>0.05, n=4 per group). There were also no significant differences in the levels of activated p-ser STAT3 and p-tyr STAT3 within each group (p>0.05, n=4 per group). The level of activation of p-ser STAT3 was greater in all groups compared to the levels of activation of p-tyr STAT3.

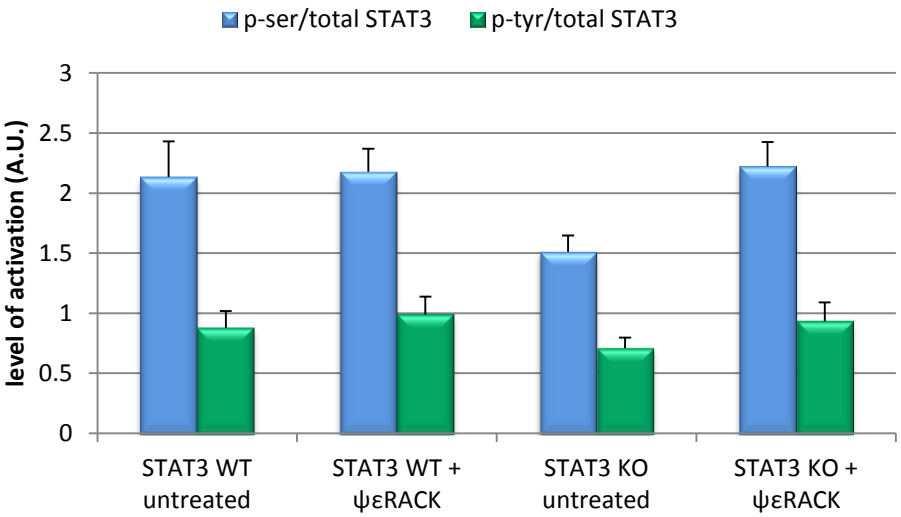

Figure 20: Levels of activation of p-ser STAT3 and p-tyr STAT3 in STAT3 WT and STAT3 KO heart fibres after hypoxia. Levels of activation of p-ser STAT3 (p-ser/total STAT3) were decreased in the untreated STAT3 KO group compared to the untreated STAT3 WT control. Activation of p-tyr STAT3 (p-tyr/total) was consistent between treatment groups, but markedly lowered in each group compared to the level of activation of p-ser STAT3 (n=4 per group, p>0.05).

3.2.2.2) Levels of activation of ERK and AKT in STAT3 KO heart fibres

Activation levels were determined for ERK1/2 (MAP42/44) and AKT1, both downstream effectors of PKCε, using bands detected by western blotting (see fig. 21).

Activation levels were determined by taking the ratio of phosphorylated to total ERK1/2 and AKT1 from western blots for total ERK (t-ERK), phosphorylated-ERK (p-ERK), total AKT1 (t-AKT1) and phosphorylated AKT1 (p-AKT1) after correction for loading. No significant differences were found for the activation levels of ERK1/2 between the untreated STAT3 WT control (1.90±0.44 A.U.) and ψεRACK -treated STAT3 WT (1.21±0.12) groups (see fig. 22). No significant differences were found on comparison of the untreated STAT3 KO group (1.52±0.31) to the STAT3 WT control group, nor on comparison of the ψεRACK-treated STAT3 KO group (1.19±0.15) to the control group. The ψεRACK -treated STAT3 KO group showed no significant difference to the untreated STAT3 KO group (p>0.05, n=4 per group).

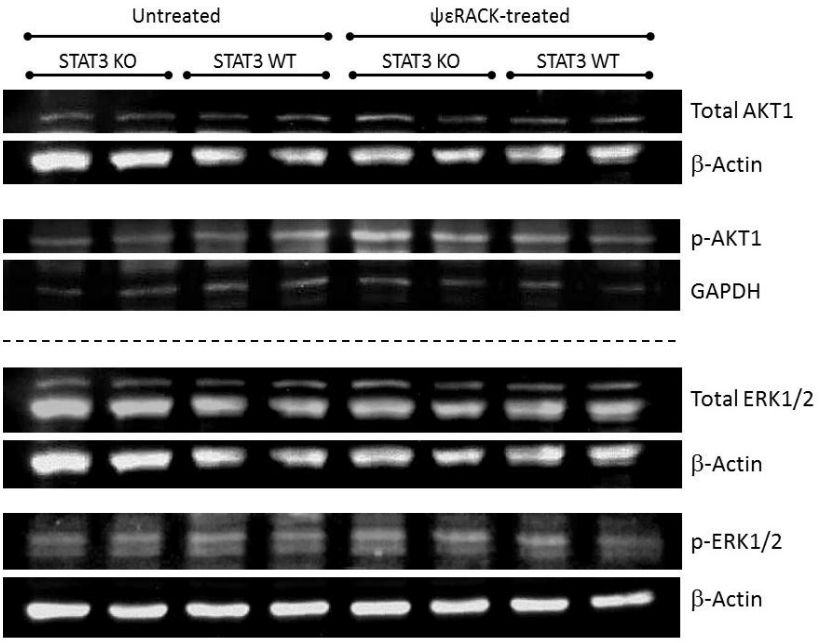

Figure 21: Western blot detected bands for total ERK1/2, phosphorylated ERK1/2, total AKT1 & phosphorylated AKT1 in DMSO (vehicle control) & STATTIC-treated groups for aPKCε and WT hearts. Banding patterns appear to be consistent between groups. GAPDH served as loading controls.

No significant differences were found for the activation levels of AKT1 between the untreated STAT3 WT control (3.18±0.18 A.U.) and ψεRACK -treated STAT3 WT (2.29±0.20) groups (see fig. 22). No significant differences were found for levels of activation of AKT1 on comparison of the untreated STAT3 KO group (2.28±0.46) to the STAT3 WT control group, nor on comparison of the ψεRACK-treated STAT3 KO group (2.72±0.24) to the control group. The ψεRACK -treated STAT3 KO group showed no significant difference to the untreated STAT3 KO group ($p>0.05$, $n=4$ per group).

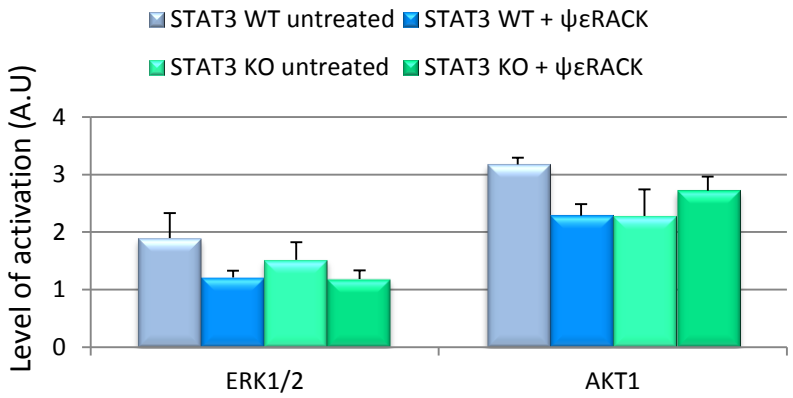

Figure 22: Activation levels of ERK1/2 and AKT1 for STAT3 KO and STAT3 WT hearts with and without ψεRACK treatment. Activation levels were determined using results from western blot analysis after correction for loading. No significant differences were found for activation levels of ERK1/2 or AKT1 within or between STAT3 KO and STAT3 WT groups (n=4 per group, p>0.05).

3.3 Studies in aged STAT3 KO hearts

3.3.1) Fatty acid oxidation in aged STAT3 KO hearts

Aged STAT3 KO heart fibres showed no significant difference in mitochondrial respiration rate (4.60±1.30 ng O_2/min/mg protein) compared to STAT3 WT fibres (6.40±1.91) with glutamate as a substrate (p>0.05) (fig. 21). Switching to fatty acids (FA) as a substrate, there were no significant differences in mitochondrial respiration between STAT3 KO (3.34±1.12) and WT (1.72±0.18) mitochondria (p>0.05, n=4 for all groups). This indicates a similar metabolic profile in both groups. A failing heart would have impaired metabolism with a fatty acid substrate compared to glutamate, as the failing heart preferentially favours the use of glucose over FA, as glucose requires less oxygen to break down, and oxygen is limited in the failing heart. These similar metabolic profiles indicate that the STAT3 KO hearts are not in the metabolic state of a failing heart, although from the graph (see fig. 23), there appears to be a trend toward failing metabolism in STAT3 KO hearts with an FA substrate.

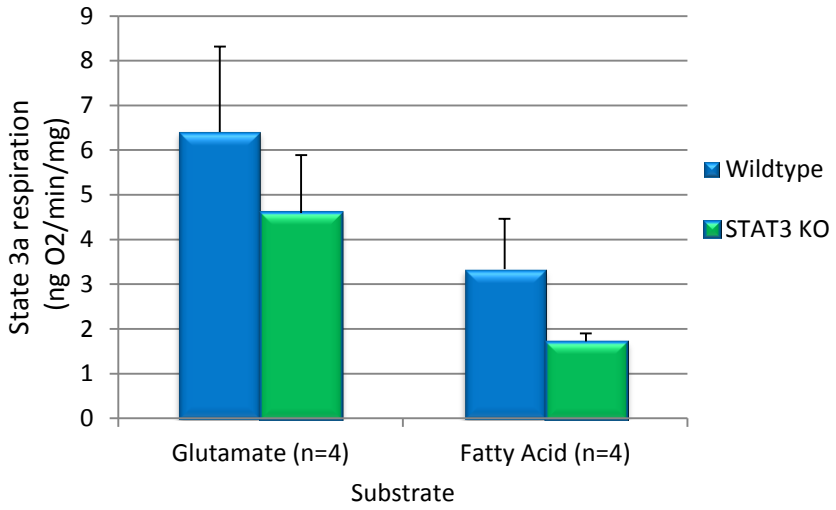

Figure 23: Respiration with a fatty acid substrate (FA oxidation) in aged STAT3 KO and WT heart fibres compared to respiration with a control substrate (glutamate). WT and KO hearts showed no significant difference with glutamate as a substrate. There were no significant differences in FA oxidation within or between groups, although there appears to be a trend to a lower respiration rate with fatty acid substrate in the STAT3 KO group compared to the wildtype fatty acid group and the glutamate group (n=4 per group, $p>0.05$). This indicates similar metabolic profiles in WT and KO groups.

3.3.2) Histology staining for fibrosis in aged STAT3 KO hearts

Histology staining with picro-sirius red showed minimal collagen deposition in STAT3 KO hearts (0.83±0.20%, n=6), similar to WT hearts (0.57±0.10%, n=4, $p> 0.05$) (fig. 24). This indicates that both groups have minimal fibrosis, with no significant difference in the amount of fibrosis between the two groups. This shows that STAT3 KO hearts display a similar phenotype to STAT3 WT hearts, with minimal fibrosis. This is atypical of heart failure phenotype.

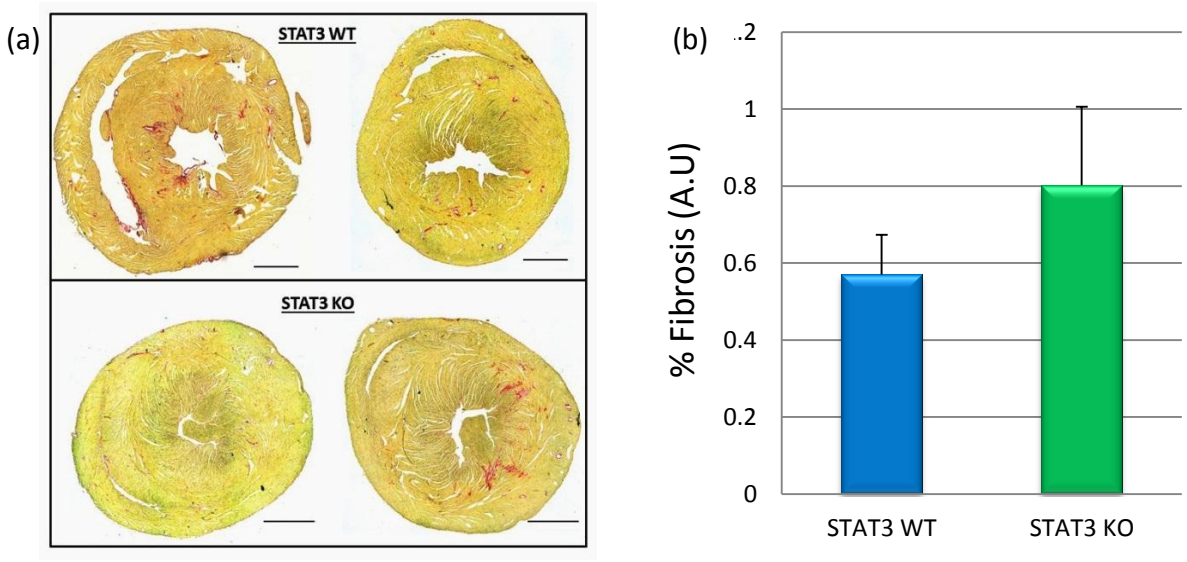

Figure 24: (a) Aged STAT3 KO and WT hearts stained with picro-sirius red were used to look at the development of fibrosis with age. Scale bar = 1000µm (b) Wildtype hearts showed 0.57±0.104% fibrosis compared to 0.83±0.203% in KO hearts. There was no significant difference between the percentage fibrosis in the two groups ($p>0.05$)

3.3.3) Fluorescence microscopy imaging for colocalization of STAT3 and PKCε in aged STAT3 KO hearts

Fluorescence microscopy imaging was used to determine whether PKCε and STAT3 would colocalize in aged STAT3 hearts. Images of the endocardium and epicardium were captured at 10 x magnification for aged STAT3 WT and STAT3 KO hearts (see fig. 23). This was done to determine whether there was a difference in localization between the two regions for

(a)

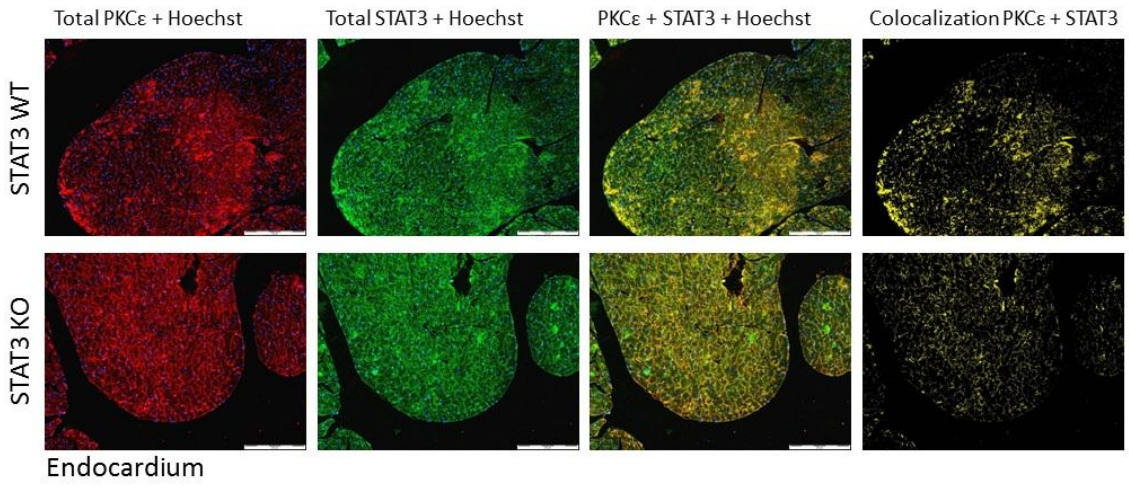

(b)

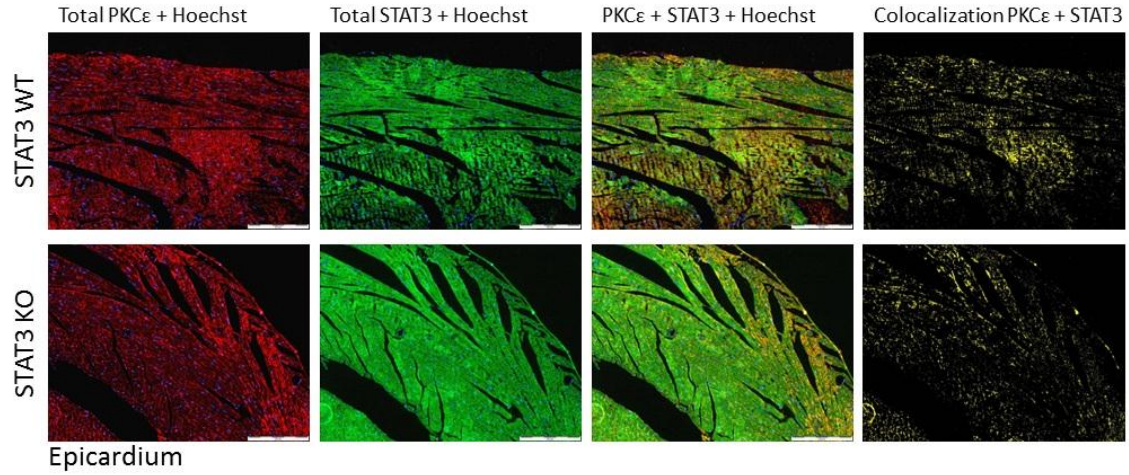

(c)

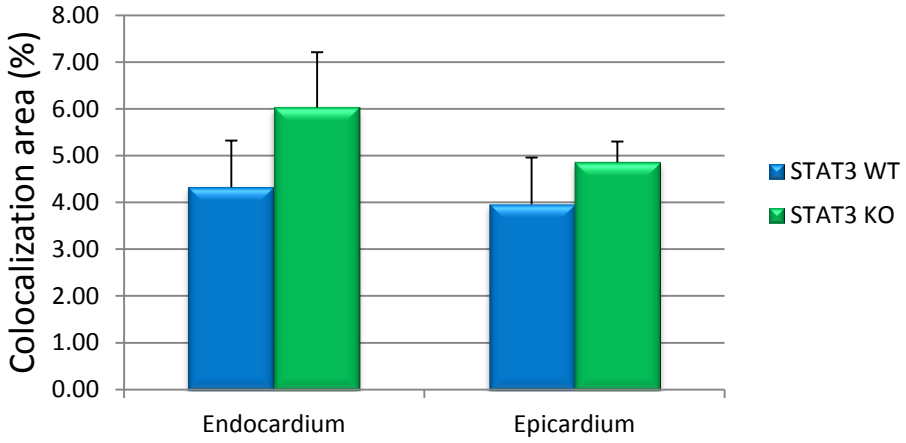

Figure 25: (a) 10x magnification of the endocardium of aged STAT3 WT and KO hearts stained for total PKCε (red) and total STAT3 (green). An overlay of red and green images showed sites of colocalization in the tissue. Background noise was removed to determine the area of colocalization of PKCε and STAT3. The same was done for the epicardium (b) to determine whether there was a difference in localization between the two regions. Localization was found to be similar in both regions (c), there were no significant differences detected between groups for the endocardium and epicardium for either the STAT3 WT or the STAT3 KO group.(Scale bar = 1000 µm).

further analysis. No significant difference was found in the area of colocalization for the STAT3 WT group between the endocardium (4.33±1.14%) and epicardium (3.96±0.78%) ($p>0.05$), nor for the STAT3 KO group between the endocardium (6.03±1.18%) and epicardium (4.86±0.44%) ($p>0.05$, n=4 per group). No significant differences were found for colocalization between the STAT3 WT and STAT3 KO groups for both the endocardium and epicardium ($p>0.05$).

Images of the cross sections and longitudinal sections were captured at 60 x magnification using oil immersion for aged STAT3 WT and STAT3 KO hearts (see fig. 24). This was done to determine whether there was a difference in patterning of colocalization between the two sections and to identify possible cellular locations thereof. Final images and percentage area of colocalization were composed of information gathered from z-stacking of the tissue. No significant difference was found in the area of colocalization for the cross sections in the STAT3 WT group (3.77±0.81%) compared to the STAT3 KO group (5.02±1.65%) ($p>0.05$). No significant difference was found in the area of colocalization for the longitudinal sections in the STAT3 WT group (3.10±0.31%) compared to the STAT3 KO group (3.20±0.86%) ($p>0.05$). No significant differences were detected for colocalization between cross sections and longitudinal sections within or between groups ($p>0.05$, n=4 per group). Prominent areas of colocalization were found to be in the intercalated discs (also known as the sarcolemma) in cross sections of hearts.

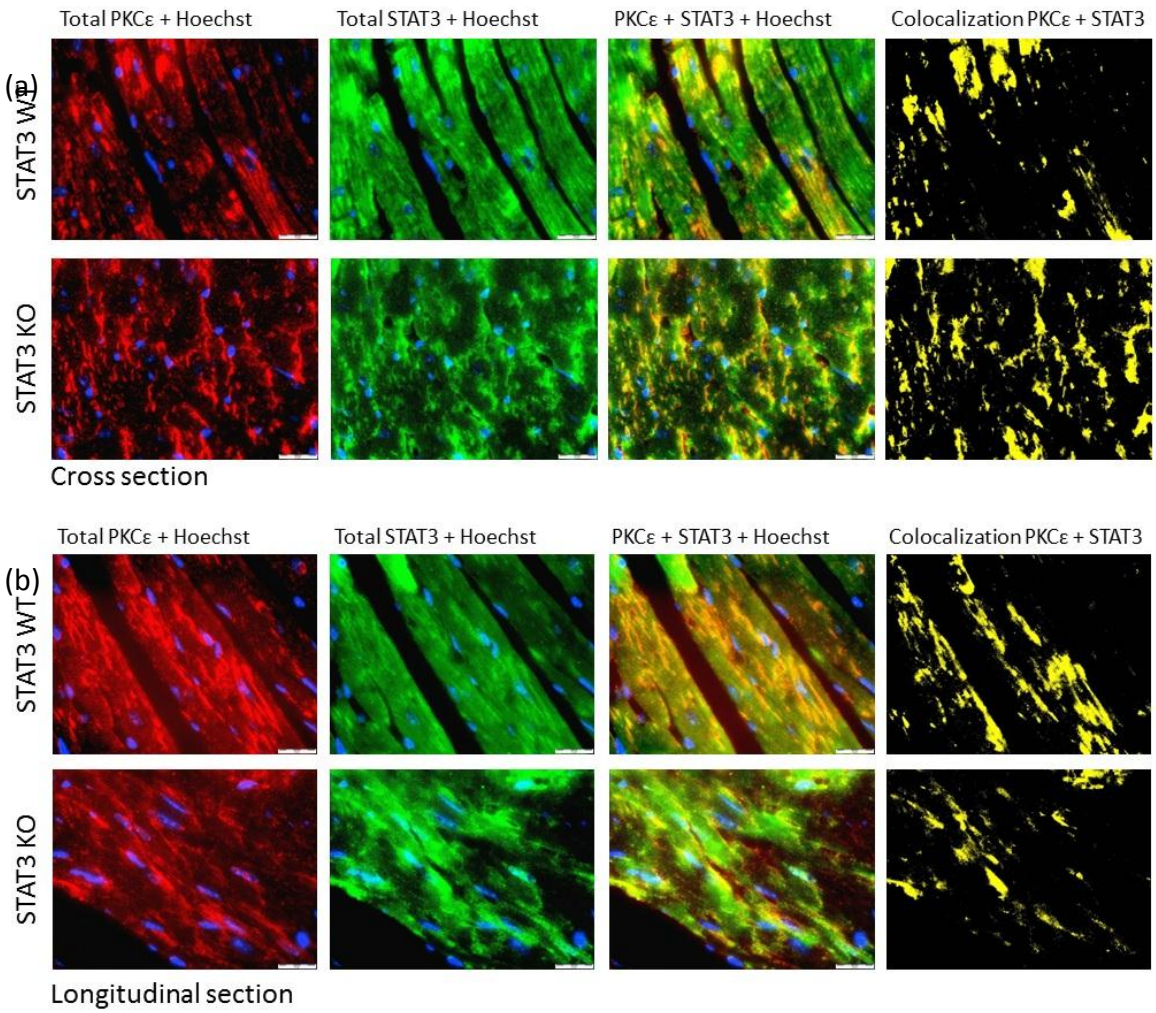

Figure 26: (a) 60x magnification of a cross section of aged STAT3 WT and KO hearts stained for total PKCε (red) and total STAT3 (green). An overlay of red and green images showed sites of colocalization in the tissue. Background noise was removed to determine the area of colocalization of PKCε and STAT3. The same was done for longitudinal sections (b) to observe differences in patterning of colocalization between the two. Localization was found to be similar in both regions (c), there were no significant differences detected between areas of cross section and longitudinal section for either the STAT3 WT or the STAT3 KO group.(Scale bar = 100 µm).

3.4. Summary of results

3.4.1) aPKCε heart fibres with STAT3 inhibition:

- No significant differences were found in recovery of respiration between WT and aPKCε heart fibres treated with DMSO (control) or STATTIC.
- Western blots show no significant differences in total STAT3, p-ser STAT3 or p-tyr STAT3 in WT and aPKCε control and STATTIC-treated groups.
- Control-treated aPKCε group showed a significant increase in PKCε levels compared to WT groups, but no significant increase compared to STATTIC-treated aPKCε group.
- No significant differences were found in levels of activated p-ser and p-tyr STAT3 within or between WT and aPKCε groups.
- No significant differences were found for activation levels of AKT1 or ERK1/2 within of between WT and aPKCε groups, although there was a trend toward an increase in the levels of activated ERK1/2 in the aPKCε groups.

3.4.2) STAT3 KO heart fibres with PKCε activation:

- No significant differences were found in recovery of respiration between STAT3 WT and STAT3 KO heart fibres when untreated or treated with a ψεRACK activator
- Western blots show no significant differences in total STAT3, p-ser STAT3, p-tyr STAT3 or total PKCε in STAT3 WT and STAT3 KO control and ψεRACK -treated groups
- No significant differences were found in levels of activated p-ser and p-tyr STAT3 within or between WT and aPKCε groups. However, levels of activated p-ser STAT3 were higher in than p-try STAT3 in all groups.

- No significant differences were found for activation levels of AKT1 or ERK1/2 within of between STAT3 WT and STAT3 KO untreated and ψεRACK-treated groups.

3.4.3) Markers for heart failure in aged STAT3 KO hearts:

- STAT3 KO and STAT3 WT hearts showed no significant differences in state 3a respiration with glutamate as a substrate, or with a fatty acid substrate.
- There was no significant difference in the amount of fibrosis in STAT3 WT and STAT3 KO hearts.
- There was no significant difference in the percentage area of colocalization between the epicardium and endocardium in STAT3 WT and STAT3 KO hearts at 10 x magnification.
- There was no significant difference in the percentage area of colocalization between cross-sections and longitudinal sections in STAT3 WT and STAT3 KO hearts at 60 x magnification.
- Colocalization in cross sections of both STAT3 WT and STAT3 KO hearts shows a strong signal in the sarcolemma between cardiomyocytes.

Discussion:

Given the limitations of animal experiments in this current study, we could not categorically verify the interactions of PKCε and STAT3.

4.1) PKCε -activated mouse experiments.

Originally, a strain of mice with a genetic modification for moderate cardiac-specific over-expression of PKCε were investigated for cardioprotection in a setting of acute and chronic oxidant stress, the rationale being that, as activated PKCε translocates to the mitochondrion at the site of the mitoK_{ATP} channel, overexpression could prove to be cardioprotective in a setting of ischemia.. Respiration studies with these mice had already been established in our laboratory, with PKCε over-expressing mice showing a significantly improved recovery in respiration after acute anoxia when compared to their wildtype controls, and required 45 minutes of anoxia in order to trigger the PKCε cardioprotective cascade and show improved recovery of respiration. In the initial stages of this study we had used these PKCε over-expressing mice and their wildtype littermate controls, but found the patterns in respiration between the two groups to be inconsistent with previous findings– both wildtype and aPKCε mitochondria/permeabilized fibres exhibited the same response to the hypoxic (anoxic) challenge . We then started investigating the genotype, given the altered phenotype. On analysis of protein levels for PKCε between the two groups, we found there were no differences in the levels of PKCε between the wildtype and PKCε over-expressing groups despite the presence of the genetic markers which indicated one set should be over-expressing PKCε and the other should not. On further investigation, we found that there had been incorrect breeding for a long period of time by the external breeding facility to which our animal breeding is outsourced. The transgenic males were being mated with BalbC

females instead of wildtype littermates, effectively back-breeding the strain and weakening the PKCε overexpression. As a result, the PKCε over-expression was lost, despite presence of the appropriate genetic markers. As we had spent moths delineating the cause of the problems with the experimentation, time was of the essence and we had to devise a way to create a viable PKCε over-expressing model in short space of time. We employed the use of a proven, highly-specific PKCε -activator (ψεRACK) to mimic this model (see chapters 1&2) [173]. As our experiments were being performed on the more physiological permeabilized freer method and not on isolated mitochondria, we used a period of 25 minutes of hypoxia, as the heart fibres failed to recover at all after 45 minutes of hypoxia. Further, a 25 minute hypoxic insult has previously been shown to be sufficient to detect changes in respiration.

In our experiments, activation of PKCε by means of the ψεRACK activator proved successful, as PKCε levels were elevated in the control-treated PKCε group compared to the WT group with analysis of protein levels.

In the PKCε-activated mouse model, treatment with the STAT3-specific inhibitor, STATTIC, did not attenuate recovery in respiration after a hypoxic insult [174]. This suggests that the effects produced by PKCε do not require signalling through STAT3. Recovery in respiration was also uninhibited in the WT groups, indicating that the hypoxic insult may have been ineffective, or it may not have been long enough.

Activation of PKCε by means of the ψεRACK peptide produced no changes in levels of any of the isoforms of STAT3. This suggests that an activation of PKCε has no effect on the activation or expression of STAT3. This further confirms the above – in this setting, PKCε does not require STAT3 to produce its beneficial effects, as external activation of PKCε does not change the amount of

STAT3 in fibres. The elevation of PKCε in the activated group was marked, but could have been greater – a larger dose of the ψεRACK activator, or perhaps a longer, chronic treatment with the activator could produce a more marked effect with clearer data, particularly for the STATTIC-treated aPKCε group which showed no significant elevation (or depression) in the amount of PKCε present compared to all of the other groups. A larger sample number would also be beneficial in clarifying these data.

There were no significant differences detected in the PKCε activated group for the level of activation of ERK1/2 or AKT1, both of which are downstream targets of PKCε [127], [128], [180], [181]. However, there appears to be a trend toward an increase in activation levels of ERK1/2 in the aPKCε groups. A greater sample number would also be beneficial in clearly discerning whether this trend of ERK1/2 activation with PKCε activation is one of significance.

4.2) STAT3 inhibition

Activation of PKCε had no effect on the recovery in respiration for STAT3 KO or WT heart fibres. This further confirms the findings with the PKCε -activated mouse experiments – in this setting PKCε does not function upstream of STAT3.

We were surprised to find that STAT3 KO and WT heart fibres did not demonstrate a marked difference in levels of any of the isoforms of STAT3 with protein analysis, indicating that this knock out model is not truly performing as the originally established STAT3 knock out model. Genotyping of mice prior to commencement of experiments in this project indicated that the mice we considered to be WT did not have the cre components present which would drive splicing of the STAT3 gene, while the KO model had both cre and lox components present which should have produced the STAT3 KO model. However, the protein analysis performed on the STAT3 KO mouse

heart samples showed no depression in the levels of STAT3. This is not consistent with the original STAT3 KO model in which protein analysis showed a marked reduction in levels of STAT3 in the STAT3 KO hearts compared to STAT3 WT hearts.

There are no changes in STAT3, indicating that the STAT3 KO model did not behave as expected, most likely due to a an error with the breeding.

4.3) STAT3 with age

Evaluation of the amount of fibrosis in STAT3 KO hearts compared to STAT3 WT hearts showed that there was no difference in the amount of fibrosis between the two groups, both of which had very low levels. Fibrosis is a marker for failing hearts, and absence of this in these STAT3 KO hearts shows that these hearts have not reached the state of heart failure. Other models using STAT3 KO mice have shown development of moderate fibrosis with age [66], or with postpartum cardiomyopathy (i.e. heart failure in the late stages of pregnancy and the early post-natal period) [179]. Our model does not prove consistent with these models of heart failure, as STAT3 KO hearts do not develop fibrosis when compared to STAT3 WT hearts as would be expected, reinforcing the hypothesis of a breeding issue.

The respiration profiles in STAT3 KO and STAT3 WT hearts showed no difference both with glutamate as a substrate, and with fatty acids as a substrate. Failing hearts should display inhibited respiration with a fatty acid substrate when compared to normal hearts, as heart failure favours the use of glucose over fatty acids. The respiration in STAT3 KO hearts does not appear to be impaired by the administration of a fatty acid substrate when compared to the STAT3 WT hearts, which indicates that the STAT3 KO hearts have not reached the metabolic state of a failing heart.

This, together with the findings for development of fibrosis in STAT3 KO and STAT3 WT hearts, indicates that our STAT3 KO model has not developed heart failure with age.

In addition, colocalization for total PKCε and total STAT3 in aged STAT3 KO and STAT3 WT hearts showed a strong signal for total STAT3 in both STAT3 KO and STAT3 WT hearts. Colocalization areas for both STAT3 WT and STAT3 KO hearts showed similar levels. This confirms that the hearts considered to be STAT3 KO hearts did not have a diminished level of STAT3, as they displayed total STAT3 levels, and colocalization areas which were consistent and comparable to STAT3 WT hearts. Genotyping of these animals prior to experiments indicated that the mice we used and considered to be STAT3 KO had the expected genotype of STAT3 KO mice with both the cre and lox components present, and mice considered to be STAT3 WT had the expected genotype of STAT3 WT mice with no cre component present. The phenotype observed is not consistent with the genotype for these STAT3 KO mice. Unfortunately, we were not able to confirm the genotyping of these mice after experiments as we did not keep tail-cuts once mice were sacrificed.

Considering our findings with the STAT3 KO mice for both the hypoxia studies, as well as the analysis of heart failure with age studies, we speculate that there has been an error in either the breeding, or genotyping of these mice, both processes of which are overseen by external sources.

An interesting observation with the fluorescence imaging is that PKCε and STAT3 colocalize in the sarcolemma. This could mean that they have the same target (e.g. connexin 43) in the area they are located (see chapter 1) [84].

4.4) Limitations of this study:

One of the limitations of this study may have been the method and duration of hypoxia employed with heart fibres. Previous respiration studies used anoxia with heart fibres in the chamber

connected to a Clarke-type electrode for a period of 45 minutes. We measured respiration in the chamber of the Clarke-electrode and found that we could not sustain anoxia for more than 10- 15 minutes. As a result, we transferred fibres to a hypoxic chamber as an oxidant stress, and back to the Clarke electrode chamber to assess the post-hypoxic recovery of respiration. This method proved not to be as effective as desired for either group.

Optimal respiration in permeabilized heart fibres is usually measured at 25^{O}C. However, the use of STATTIC requires a temperature of 37^{O}C to achieve maximal inhibition of STAT3 [174]. We compromised the temperature of experiments involving STATTIC and kept it at 30^{O}C to attain 50-70% inhibition of STAT3, as trial runs at higher temperatures produced no viable fibres for respiration.

The greatest limitations of this project were the availability of animals, and the incorrect breeding and genotyping of animals. Larger samples sizes would have been a great benefit in reducing errors and clearly indicating statistical significance. However, bottle-necking events in the breeding facilities left a small number available for use. Furthermore, given the genotyping results, we suspect a problem with the breeding in the STAT 3 knock-out mice as well, possibly similar to that discovered for the PKCε over-expressing mice. The accuracy of the genotyping is highly questionable, as in the aged mice alone, none of the STAT3 KO hearts showed a lack of STAT3 with fluorescence imaging as would have been expected. The probability of all of these mice having been incorrectly genotyped is 6.25% (when considering genotyping as an independent event), and this favours the possibility of incorrect breeding being carried out by the external animal-breeding unit.

A further limitation of this study was the use of an activator to mimic the original PKCε over-expressing model rather than the original genetically modified cardiac-specific PKCε over-expressing model. The effects produced by the activator were not as marked when compared to the original findings in the PKCε over-expressing mouse model. This model, as outlined earlier in the discussion, was no longer viable, as incorrect breeding had diluted the gene of interest, and it could no longer be used for this project.

4.5) The way forward:

Considering the genetic inaccuracies discovered in these mouse models, the way forward to determine the possible interaction between PKCε and STAT3 would be to use accurate, verified, functional STAT3 KO and PKCε over-expressing models, with highly-specific, appropriate activators and inhibitors. A longer period of hypoxia to produce differences in recovery of respiration would be a step forward, or a period of exposure of the whole mouse to hypobaric hypoxia , in our in-house designed and built hypobaric hypoxic chamber which has proven suitable to elicit the cardioprotective cascade in the at least the PKCε mice and their littermate controls. This was our original intention, but due to the limitations and animal availability as outlined we had to revert to a different model.

A second possible approach would be long-term delivery of the STAT3 inhibitor or PKCε activator by means of osmotic pumps placed subcutaneously under the skin between the shoulder blades. This technique has also been used previously in the lab for the investigation of the effects of chronic beta-adrenergic stimulation. This method could also have produced a knock-out or over-expression model without the hassle of genotyping. Subject to hypoxia with the appropriate

inhibitors and activators, this would in theory produce a model similar to the genetically modified one.

Another alternative approach could be the use of a cardiomyocyte cell-culture model with the long-term use of inhibitory RNAs for STAT3 and PKCε.

4.6) Conclusion:

In conclusion, given the above limitations, our study does not allow us to conclude a possible interaction between PKCε and STAT3. PKCε has an involvement in metabolic signalling and is likely to produce its pro-survival effects by altering activity of proteins involved in metabolism, such as GSK3β, AMPK and FoxO1. It is also possible that PKCε and STAT3 are part of independent pathways that can be triggered by the same extra-cellular signalling molecules (and possibly intra-cellular ROS), each as an alternative to the other.

References:

1. http://www.who.int/mediacentre/factsheets/fs317/en/index.html, WHO 2011, accessed 22 December 2011
2. http://apps.who.int/ghodata/, WHO 2008, accessed 22 December 2011
3. http://www.sciencedaily.com/releases/2011/07/110708124546.htm, 8 July 2011, accessed 22 December 2011
4. Steyn, K and Fourie, JM. The heart and stroke foundation South Africa: Heart disease in South Africa, media document. 2007. http://www.heartfoundation.co.za/sites/default/files/Heart Disease in SA MRC Report.pdf, accessed 03 January 2013
5. Leeder, S, Raymond, S, Greenberg, H, Liu, H and Esson, K. A Race Against Time: The Challenge of Cardiovascular Disease in Developing Countries. New York, NY: Trustees of Columbia University; 2004
6. Hausenloy, DJ, Tsang, A and Yellon, DM. The Reperfusion Injury Salvage Kinase Pathway: A Common Target for Both Ischemic Preconditioning and Postconditioning. Trends in Cardiovascular Medicine. 2005. 15(2): p.69–75
7. Stanley, WC, Recchia, FA and Lopaschuk, GD. Myocardial Substrate Metabolism in the Normal and Failing Heart. Physiol Rev. 2005. 85: p.1093–1129 |doi:10.1152/physrev.00006.2004
8. Cowie, MR, Mosterd, A, Wood, DA, Deckers, JW, Poole-Wilson, PA, Sutton, GC and Grobbee, DE. The epidemiology of heart failure. European Heart Journal. 1997. 18: p.208 – 225
9. Ventura-Clapier, R., Garnier, A. and Veksler, V. Energy metabolism in heart failure. J Physiol. 555(1): p.1 – 13
10. Cohn, JN. The Management of Chronic Heart Failure. N Engl J Med. 1996. 335: p.490-498
11. Palaniyandi, SS, Sun, L, Ferreira, JCB and Mochly-Rosen, D. Protein kinase C in heart failure: a therapeutic target? Cardiovasc. Res. 2009. 82: p229–239. doi:10.1093/cvr/cvp001
12. Mudd, JO and Kass, DA. Tackling heart failure in the twenty-first century. Nature. 2008. 451(21): p.919 – 928 |doi:10.1038/nature06798
13. http://www.drugs.com/health-guide/heart-failure.html, Copyright © 2000-2013 Drugs.com. Accessed 25/01/2013
14. Perez, JM, Rathz, DA, Petrashevskaya, NN, Hahn, SH, Wagoner, LE, Schwartz, A, Dorn II, GW and Liggett, SB. β1-adrenergic receptor polymorphisms confer differential function and predisposition to heart failure. Nat. Med. 2003. 9: p.1300 – 1305
15. Sharov, VG, Sabbah, HN, Shimoyama, H, Goussev, AV, Lesch, M, and Goldstein, S. Evidence of cardiocyte apoptosis in myocardium of dogs with chronic heart failure. Am J Pathol. 1996. 148(1): p.141–149
16. Narula, J, Haider, N, Virmani, R, DiSalvo, TG, Kolodgie, FD, Hajjar, RJ, Schmidt, U, Semigran, MJ, Dec, GW and Khaw, BA. Apoptosis in Myocytes in End-Stage Heart Failure. N Engl J Med. 1996. 335: p.1182-1189. |doi: 10.1056/NEJM199610173351603
17. Wyllie AH. Glucocorticoid-induced thymocyte apoptosis is associated with endogenous endonuclease activation. Nature. 1980. 284: p.555–556
18. Klionsky, DJ and Ohsumi, Y. Vacuolar import of proteins and organelles from the cytoplasm. Annu. Rev. Cell. Dev. Biol. 1999. 15: p.1 – 32

19. Rubinsztein, DC, DiFiglia, M, Heintz, N, Nixon, RA, Qin, ZH, Ravikumar, B, Stefanis, L and Tolkovsky, A. Autophagy and Its Possible Roles in Nervous System Diseases, Damage and Repair. Autophagy. 2005. 1(1): p.11-22
20. Kuma, A, Hatano, M, Matsul, M, Yamamoto, A, Nakaya, H, Yoshimori, T, Ohsumi, Y, Tokuhisa, T and Mizushima, N. The role of autophagy during the early neonatal starvation period. Nature. 2004. 432: p.1032-1036 | doi:10.1038/nature03029
21. Nakai, A, Yamaguchi, O, Takeda, T, Higuchi, Y, Hikoso, S, Taniike, M, Omiya, S, Mizote, I, Matsumura, Y, Asahi, M, Nishida, K, Hori, M, Mizushima, N and Otsu, K. The role of autophagy in cardiomyocytes in the basal state and in response to hemodynamic stress. Nat. Med. 2007. 13: p.619–624
22. Sack MN, Rader TA, Park S, Bastin J, McCune SA, Kelly DP. Fatty acid oxidation enzyme gene expression is downregulated in the failing heart. Circulation. 1996. 94: p.2837–2842 |doi: 10.1161/01.CIR.94.11.2837
23. Wallhaus, TR, Taylor, M, DeGrado, TR, Russel, DC, Stanko, P, Nickles, RJ and Stone, SK. Myocardial Free Fatty Acid and Glucose Use After Carvedilol Treatment in Patients With Congestive Heart Failure. Circulation. 2001. 103: p.2441-2446 |doi: 10.1161/01.CIR.103.20.2441
24. Saavedra, WF, Paolocci, N, St John, ME, Skaf, MW, Stewart, GC, Xie, JS, Harrison, RW, Zeichner, J, Mudrick, D, Marban, E, Kass, DA and Hare, JM. Imbalance Between Xanthine Oxidase and Nitric Oxide Synthase Signalling Pathways Underlies Mechanoenergetic Uncoupling in the Failing Heart. Circ. Res. 2002. 90: p.297-304. doi: 10.1161/hh0302.104531
25. Wisneski, JA, Gertz, EW, Neese, RA and Mayr, M. Myocardial metabolism of free fatty acids. Studies with 14C-labeled substrates in humans. J. Clin. Invest. 79: 359–366, 1987
26. Lei, B, Lionetti, V, Young, ME, Chandler, MP, Agostino, C, Kang, E, Altarejos, M, Matsuo, K, Hintze, TH, Stanley, WC and Recchia, FA. Paradoxical downregulation of the glucose oxidation pathway despite enhanced flux in severe heart failure. J Mol Cell Cardiol 36: 567–576, 2004
27. Mootha, VK, Arai, AE and Balaban, RS. Maximum oxidative phosphorylation capacity of the mammalian heart. AJP – Heart. 1997. 272(2): p.H769-H775
28. Gertz, EW, Wisneski, JA, Stanley, WC and Neese, RA. Myocardial substrate utilization during exercise in humans. Dual carbonlabeled carbohydrate isotope experiments. J. Clin. Invest. 1988. 82: p.2017-2025
29. Fillmore, N and Lopaschuk, GD. Targeting mitochondrial oxidative metabolism as an approach to treat heart failure. Biochim. Biophys. Acta. 2012. |http://dx.doi.org/10.1016/j.bbamcr.2012.08.014 [Epub ahead of print]
30. Dzeja, PP, Pucar, D, Redfield, MM, Burnett, JC, Terzic A. Reduced activity of enzymes coupling ATP-generating with ATP-consuming processes in the failing myocardium. Mol Cell Biochem. 1999. 201(1-2): p.33-40
31. Razeghi, P, Young, ME, Alcorn, JL, Moravec, CS, Frazier, OH and Taegtmeyer, H. Metabolic Gene Expression in Fetal and Failing Human Heart. Circulation. 2001. 104: p.2923-2931
32. Zelis, R, Delea, CS, Coleman, HN and Mason, DT. Arterial Sodium Content in Experimental Congestive Heart Failure. Circulation. 1970. 41: p.213-216
33. Donaldson, C, Palmer, BM, Zile, M, Maughan, DW, Ikonomidis, JS, Granzier, H, Meyer, M, VanBuren, P and LeWinter, MM. Myosin Cross-Bridge Dynamics in Patients With Hypertension and Concentric Left Ventricular Remodelling. Circ. Heart Fail. 2012. 5: p.803-811

34. Hasenfuss, G, Mulierli, LA, Blanchard, EM, Holubarsch, C, Leavitt, BJ, Ittleman, F and Alpert, NR. Energetics of isometric force development in control and volume-overload human myocardium. Comparison with animal species. Circ. Res. 1991. 68: p.836 – 546 | doi: 10.1161/01.RES.68.3.836
35. VanBuren, P, Harris, DE, Alpert, NR and Warshaw, DM. Cardiac V_1 And V_3 Myosins Differ in Their Hydrolytic and Mechanical Activities In Vitro. Circ. Res. 1995. 77: p.439 – 444 | doi: 10.1161/01.RES.77.2.439
36. Rafiee, P, Shi, Y, Kong, X, Pritchard Jr, KA, Tweddell, JS, Litwin, SB, Mussatto, K, Jaquiss, RD, Su, J and Baker, JE. Activation of Protein Kinases in Chronically Hypoxic Infant Human and Rabbit Hearts. Circulation. 2002. 106: p.239-245
37. Dzau, VJ, Colucci, WS, Hollenberg, NK and Williams, GH. Relation of the renin-angiotensin-aldosterone system to clinical state in congestive heart failure. Circulation. 1981. 63: p.645-651 |doi: 10.1161/01.CIR.63.3.645
38. Izumiya, Y, Shiojima, I, Sato, K, Sawyer, DB, Colucci, WS and Walsh, K. Vascular Endothelial Growth Factor Blockade Promotes the Transition From Compensatory Cardiac Hypertrophy to Failure in Response to Pressure Overload. Hypertension. 2006. 47: p.887-893 | doi:10.1161/01.HYP.0000215207.54689.31
39. Doughty, RN, Whalley, GA, Gamble, G, MacMahon, S and Sharpe, N. Left Ventricular Remodeling With Carvedilol in Patients With Congestive Heart Failure Due to Ischemic Heart Disease. J. Am. Coll. Cardiol. 1997. 29(5): p.1060-1066 |doi:10.1016/S0735-1097(97)00012-0
40. Testa, M, Yeh, M, Lee, P, Fanelli, R, Loperfido, F, Berman, JW and LeJemtel, TH. Circulating Levels of Cytokines and Their Endogenous Modulators in Patients With Mild to Severe Congestive Heart Failure Due to Coronary Artery Disease or Hypertension. J Am Coll Cardiol. 1996. 28(4): p.964-971. |doi:10.1016/S0735-1097(96)00268-9
41. Tsutamoto, T, Wada, A, Maeda, K, Mabuchi, N, Hayashi, M, Tsutsui, T, Ohnishi, M, Sawaki, M, Fujii, M, Matsumoto, T and Kinoshita, M. Angiotensin II type 1 receptor antagonist decreases plasma levels of tumor necrosis factor alpha, interleukin-6 and soluble adhesion molecules in patients with chronic heart failure. J Am Coll Cardiol. 2000. 35(3): p.714-721. doi:10.1016/S0735-1097(99)00594-X
42. Koller-Strametz, J, Pacher, R, Frey, B, Kos, T, Woloszczuk, W and Stanek, B. Circulating tumor necrosis factor-alpha levels in chronic heart failure: relation to its soluble receptor II, interleukin-6 and neurohumoral variables. J. Heart Lung Transplant. 1998. 17(4): p.356-362
43. Hirota, H, Izumi, M, Hamaguchi, T, Sugiyama, S, Murakami, E, Kunisada, K, Fujio, Y, Oshima, Y, Nakaoka, Y, Yamauchi-Takihara, K. Circulating interleukin-6 family cytokines and their receptors in patients with congestive heart failure. Heart Vessels. 2004. 19:237–24
44. Kaur, K, Sharma, AK and Singal, PK. Significance of changes in TNF-α and IL-10 levels in the progression of heart failure subsequent to myocardial infarction. AJP – Heart. 2006. 291(1): p.H106-H113
45. Stumpf, C, Lehner, C, Yilmaz, A, Daniel, WG and Garlichs, CD. Decrease of serum levels of the anti-inflammatory cytokine interleukin-10 in patients with advanced chronic heart failure. Clin. Sci. 2003. 105: p.45–50
46. Aukrust, P, Ueland, T, Lien, E, Bendtzen, K, Müller, F, Andreassen, AK, Nordøy, I, Aass, H, Espevik, T, Simonsen, S, Frøland, SS and Gullestad, L. Cytokine Network in Congestive Heart Failure Secondary to Ischemic or Idiopathic Dilated Cardiomyopathy. Am J Cardiol. 1999. 83: p.376–382

47. Lecour, S. Multiple protective pathways against reperfusion injury: A SAFE path without Aktion? J. Mol. Cell. Cardiol. 2009. 46: p.607–609
48. Lecour, S, Suleman, N, Deuchar, GA, Somers, S, Lacerda, L, Husamen, B and Opie, LH. Pharmacological preconditioning with tumor necrosis factor-alpha activates signal transducer and activator of transcription-3 at reperfusion without involving classic prosurvival kinases (Akt and extracellular signal-regulated kinase). Circulation. 2005. 112: p.3911–3918
49. Hausenloy, DJ and Yellon, DM. New directions for protecting the heart against ischaemia–reperfusion injury: targeting the Reperfusion Injury Salvage Kinase (RISK)-pathway. Cardiovasc. Res. 2004. 61(3): p.448-460 |doi:10.1016/j.cardiores.2003.09.024
50. Taub, R. Hepatoprotection via the IL-6/Stat3 pathway. J. Clin. Invest. 2003. 112(7): p.978–980 |doi:10.1172/JCI19974
51. Chen, CL, Loy, A, Cen, L, Chane, C, Hsieh, FC, Cheng, G, Wu, B Qualman, SJ, Kunisada, K, Yamauchi-Takihara, K and Lin, J. Signal transducer and activator of transcription 3 is involved in cell growth and survival of human rhabdomyosarcoma and osteosarcoma cells. BMC Cancer. 2007. 7: p.111 |doi:10.1186/1471-2407-7-111
52. Kunisada, K, Negoro, S, Tone, E, Funamoto, M, Osugi, T, Yamadat, S, Okabet, M, Kishimoto, T and Yamauchi-Takihara, K Signal transducer and activator of transcription 3 in the heart transduces not only a hypertrophic signal but a protective signal against doxorubicin-induced cardiomyopathy. Proc. Nat. Acad. Sci. USA. 2000. 97(1): p.315-319
53. Smith, RM, Suleman, N, Lacerda, L, Opie, LH, Akira, S, Chien, KR and Sack, MN. Genetic depletion of cardiac myocyte STAT-3 abolishes classical preconditioning. Cardiovasc. Res. 2004. 63: p.611 – 616 |doi:10.1016/j.cardiores.2004.06.019
54. Qin, HR, Kim, HJ, Kim, JY, Hurt, EM, Klarmann, GJ, Kawasaki, BT, Serrat, MAD and Farrar, WL. Activation of Signal Transducer and Activator of Transcription 3 through a Phosphomimetic Serine 727 Promotes Prostate Tumorigenesis Independent of Tyrosine 705 Phosphorylation. Cancer Res. 2008. 6(19)8: p.7736 – 7741
55. Samavati, L, Rastoqi, R, Du, W, Huttemann, M, Fite, A and Franchi, L. STAT3 tyrosine phosphorylation is critical for interleukin 1 beta and interleukin-6 production in response to lipopolysaccharide and live bacteria. Mol. Immunol. 2009, 46(8–9): p.1867–1877
56. Chung, J, Uchida, E, Grammer, TC and Blenis, J. STAT3 serine phosphorylation by ERK-dependent and -independent pathways negatively modulates its tyrosine phosphorylation. Mol. Cell. Biol. 1997. 17(11): p.6508-6516
57. Myers Jr, MG. Moonlighting in Mitochondria. Science. 2009. 323: p.723-724 | DOI: 10.1126/science.1169660
58. Yamauchi-Takihara, K, Ihara, Y, Ogata, A, Yoshizaki, K, Azuma, J, and Kishimoto, T. Hypoxic stress induces cardiac myocyte-derived interleukin-6. Circulation. 1995. 91: p.1520−1524
59. Kukielka, GL, Smith, CW, Manning, AM, Youker, KA, Michael, LH and Entman, ML.. Induction of interleukin-6 synthesis in the myocardium — potential role in postreperfusion inflammatory injury. Circulation. 1995. 92: p.1866−1875
60. Chandrasekar, B, Mitchell, DH, Colston, JT and Freeman, GL. Regulation of CCAAT/enhancer binding protein, interleukin-6, interleukin-6 receptor and gp130 expression during myocardial ischemia/reperfusion. Circulation. 1999. 99: p.427−433
61. Obana, M, Maeda, M, Takeda, K, Hayama, A, Mohri, T, Yamashita, T, Nakaoka, Y, Komuro, I, Takeda, K, Matsumiya, G, Azuma, J and Fujio, Y. Therapeutic Activation of Signal Transducer and Activator of

Transcription 3 by Interleukin-11 Ameliorates Cardiac Fibrosis After Myocardial Infarction. Circulation. 2010. 121: p.684-691. DOI: 10.1161/CIRCULATIONAHA.109.893677

62. Boengler, K, Hilfiker-Kleiner, D, Drexler, H, Heusch, G and Schulz, R. The myocardial JAK/STAT pathway: From protection to failure. Pharmacol. Therapeut. 2008. 120: p.172–185
63. Harada, M, Qin, Y, Takano, H, Minamino, T, Zou, Y, Toko, H, Ohtsuka, M, Matsuura, K, Sano, M, Nishi, J, Iwanaqa, K, Akazawa, H, Kunieda, T, Zhu, W, Hasegawa, H, Kunisada, K, Naqai, T, Nakaya, H, Yamauchi-Takihara, K and Komuro, I. G-CSF prevents cardiac remodeling after myocardial infarction by activating the Jak-Stat pathway in cardiomyocytes. Nat. Med.2005. 11: p.305 - 311 |doi:10.1038/nm1199
64. De-Fraja, C, Conti, L, Govini, S, Battaini, F and Cattaneo, E. STAT signalling in the mature and aging brain. Int. J. Dev. Neurosci. 2000. 18(4–5): p.439–446
65. Boengler, K, Buechert, A, Heinen, Y, Roeskes, C, Hilfiker-Kleiner, D, Heusch, and Schulz, R. Cardioprotection by Ischemic Postconditioning Is Lost in Aged and STAT3-Deficient Mice. Circ. Res. 2008. 102: p.131-135 | doi: 10.1161/CIRCRESAHA.107.164699
66. Jacoby, JJ, Kalinowski, A, Liu, MG, Zhang, SSM, Gao, Q, Chai, GX, Ji, L, Iwamoto, Y, Li, E, Schneider, M, Russek, KS and Fu, XY. Cardiomyocyte-restricted knockout of STAT3 results in higher sensitivity to inflammation, cardiac fibrosis and heart failure—with advanced age. Proc Natl Acad Sci USA. 2005. 100: p12929−12934
67. Cataldo L, Chen, NY, Yuan, Q, Li, W, Ramamoorthy, P, Wagner, TE, Sticca, RP and Chen, WY. Inhibition of oncogene STAT3 phosphorylation by a prolactin antagonist, hPRL-G129R, in T-47D human breast cancer cells. Int. J. Oncol. 2000. 17(6):1179–1185
68. Negoro, S, Kunisada, K, Tone, E, Funamoto, M, Oh, H, Kishimoto, T and Yamauchi-Takihara, K. Activation of JAK/STAT pathway transduces cytoprotective signal in rat acute myocardial infarction. Cardiovasc. Res. 2000. 47 (4): p.797-805 |doi: 10.1016/S0008-6363(00)00138-3
69. Liao, D, Georgakopoulos, D, Kovacs, A, Zheng, M, Lerner, D, Pu, H, Saffitz, J, Chien, K, Xiao, RP, Kass, DA and Wang, Y. The in vivo role of p38 MAP kinases in cardiac remodeling and restrictive cardiomyopathy. Proc Natl Acad Sci USA. 2001. 98: p.12,283–12,288
70. Lemke, LE, Bloem, LJ, Fouts, R, Esterman, M, Sandusky, G and Vlahos, CJ. Decreased p38 MAPK activity in end-stage failing human myocardium: P38 MAPK alpha is the predominant isoform expressed in human heart. J. Mol. Cell Cardiol, 33 (2001), pp.1527–1540
71. Oshima, Y, Fujio, Y, Nakanishi, T, Itoh, N, Yamamoto, Y, Negoro, S, Tanaka, K, Kishimoto, T, Kawase, I and Azuma, J. STAT3 mediates cardioprotection against ischemia/ reperfusion injury through metallothionein induction in the heart. Cardiovasc. Res. 2005. 65: p.428−435
72. Hilfiker-Kleiner, D, Hilfiker, A, Fuchs, M, Kaminski, K, Schaefer, A, Schieffer, B, Hillmer, A, Schmiedl, A, Ding, Z, Podewski, E, Poli, V, Schneider, MD, Schulz, R, Park, JK, Wollert, KC and Drexler, H. Signal transducer and activator of transcription 3 is required for myocardial capillary growth, control of interstitial matrix deposition and heart protection from ischemic injury. Circ. Res. 2004. 95: p187−195
73. Bolli, R, Stein, AB, Guo, Y, Wang, OL, Rokosh, G, Dawn, B, Molkentin, JD, Sanganalmath, SK, Zhu, Y and Xuan, YT. A murine model of inducible, cardiac-specific deletion of STAT3: Its use to determine the role of STAT3 in the upregulation of cardioprotective proteins by ischemic preconditioning. J. Mol. Cell. Cardiol. 2011. 50: p589–597
74. Zhang, X, Blenis, J, Li, HC, Schindler, C and Chen-Kiang, S. Requirement of serine phosphorylation for formation of STAT promoter complexes. Science. 1995. 267: p.1990– 1994

75. Yamauchi-Takihara, K and Kishimoto, T. A Novel Role for STAT3 in Cardiac Remodeling. Trends Cardiovas. Med. 2000. 10(7): p.298–303
76. Murry, CE, Richard, VJ, Reimer, KA and Jennings, RB. Ischemic preconditioning slows energy metabolism and delays ultrastructural damage during a sustained ischemic episode. Circ. Res. 1990. 66: p.913-931 |doi: 10.1161/01.RES.66.4.913
77. Wakeno-Takahashi, M, Otani, H, Nakao, S, Uchiyama, Y, Imamura, H and Shingu, K. Adenosine and a Nitric Oxide Donor Enhances Cardioprotection by Preconditioning with Isoflurane through Mitochondrial Adenosine Triphosphate-sensitive K+ Channel-dependent and -independent Mechanisms. Anesthesiology. 2004. 100(3): p.515 – 524
78. Heinzel, FR, Luo, Y, Li, X, Boengler, K, Buechert, A, Carcia-Dorado, D, Di Lisa, F, Schulz, R and Heusch, G et al. Impairment of Diazoxide-Induced Formation of Reactive Oxygen Species and Loss of Cardioprotection in Connexin 43 Deficient Mice. Circ. Res. 2005. 97: p.583-586
79. Hattori, R, Maulik, N, Otani, H, Zhu, L, Cordis, G, Engelman, RM, Siddiqui, MA and Das, DK. Role of STAT3 in ischemic preconditioning. J. Mol. Cell. Cardiol. 2001. 33: p.1929–1936
80. Zhao, ZQ, Corvera, JS, Halkos, ME, Kerendi, F, Wang, NP, Guyton, RA and Vinten-Johansen, J. Inhibition of myocardial injury by ischemic post-conditioning during reperfusion: comparison with ischemic preconditioning. Am. J. Physiol. Heart Circ. Physiol. 2003. 285: p.H579–H588
81. Lacerda, L, Somers, S, Opie, LH and Lecour, S. Ischaemic postconditioning protects against reperfusion injury via the SAFE pathway. Cardiovasc. Res. 2009. 84(2): p.201 – 208 |doi: 10.1093/cvr/cvp274
82. Somers, SJ, Frias, M, Lacerda, L, Opie, LH and Lecour, S. Interplay between SAFE and RISK pathways in sphingosine-1-phosphate-induced cardioprotection. Cardiovasc. Drug Ther. 2012. 26(3): p.227 – 237 |doi: 10.1007/s10557-012-6376-2
83. Gough, DJ, Corlett, A, Schlessinger, K, Wegrzyn, J, Larner, AC and Levy, DE. Mitochondrial Stat3 Supports Ras-Dependent Oncogenic Transformation. Science. 2009. 324(5935): p.1713–1716
84. Boengler, K, Konietzka, I, Buechert, A, Heinen, Y, Garcia-Dorado, D, Heusch, G and Schulz, R. Loss of cardioprotection with IPC in aged mouse hearts is associated with reduced gap junctional and mitochondrial levels of connexin 43. AJP – Heart. 2007. 292(4): p.H1764-H1769
85. Li, X, Heinzel, FR, Boengler, K, Schulz, R and Heusch, G. Role of connexin 43 in ischemic preconditioning does not involve intercellular communication through gap junctions. J. Mol. Cell. Cardiol. 2004. 36(1): p.161–163
86. Schwanke, U, Konietzka, I, Duschin, A, Xiaokui, L, Schulz, R and Heusch, G. No ischemic preconditioning in heterozygous connexin43-deficient mice. AJP – Heart. 2002. 283(4): p.H1740-H1742
87. Boengler, K, Hilfiker-Kleiner, D, Heusch, G and Schulz, R. Inhibition of permeability transition pore opening by mitochondrial STAT3 and its role in myocardial ischemia/reperfusion. Basic Res. Cardiol. 2010. 105(6): p.771-785
88. Rajasingh, J, Bord, E, Hamada, H, Lambers, E, Qin, G, Losordo, DW and Kishore, R. STAT3-Dependent Mouse Embryonic Stem Cell Differentiation Into Cardiomyocytes. Analysis of Molecular Signaling and Therapeutic Efficacy of Cardiomyocyte Precommitted mES Transplantation in a Mouse Model of Myocardial Infarction. Circ. Res. 2007. 101: p.910 – 918
89. Ozog, MA, Bernier, SM, Bates, DC, Chatterjee, B, Lo, CW and Naus, CC. The Complex of Ciliary Neurotrophic Factor-Ciliary Neurotrophic Factor Receptor α Up-Regulates Connexin43 and

Intercellular Coupling in Astrocytes via the Janus Tyrosine Kinase/Signal Transducer and Activator of Transcription Pathway. Mol. Biol. Cell. 2004. 15(11): p.4761 – 4774

90. Hsieh, YJ, Wakiyama, H, Levitsky, S and McCully, JD. Cardioplegia and Diazoxide Modulate STAT3 Activation and DNA Binding. Ann. Thorac. Surg. 2007. 84(4):p.1272–1278
91. Pacher, P and Hajnóczky, G. Propagation of the apoptotic signal by mitochondrial waves. EMBO J. 2001. 20: p.4107 – 4121 |doi:10.1093/emboj/20.15.4107
92. Zhang, X, Zhang, J, Wei, H and Tian, Z. STAT3-decoy oligodeoxynucleotide inhibits the growth of human lung cancer via down-regulating its target genes. Oncol. Rep. 2007. 17: p.1377−1382
93. Lin, Q, Lai, R, Chirieac, LR, Li, C, Thomazy, VA, Grammatikakis, I, Rassidakis, GZ, Zhang, W, Fujio, Y, Kunisida, K, Hamilton, SR and Amin, HM. Constitutive activation of JAK3/STAT3 in colon carcinoma tumors and cell lines — inhibition of JAK3/STAT3 signaling induces apoptosis and cell cycle arrest of colon carcinoma cells. Am. J. Pathol. 2005. 167: p.969−980
94. Juhaszova, M Zorov, DB, Kim, SH, Pepe, S, Fu, Q, Fishbein, KW, Ziman, BD, Wang, S, Ytrhus, K, Antos, CL, Olson, EN and Sollot, SJ. Glycogen synthase kinase-3β mediates convergence of protection signaling to inhibit the mitochondrial permeability transition pore. J. Clin. Invest. 2004. 113(11): p.1535–1549 |doi:10.1172/JCI19906
95. Inoue, H, Ogawa, W, Ozaki, M, Haga, S, Matsumoto, M, Furukawa, K, Hashimoto, N, Kido, Y, Mori, T, Sakaue, H, Teshigawara, K, Jin, S, Iguchi, H, Hiramatshu, R, LeRoith, D, Takeda, K, Akira, S and Kasug, M. Role of STAT-3 in regulation of hepatic gluconeogenic genes and carbohydrate metabolism in vivo. Nat. Med. 2004. 2: p.168–174
96. Opie, LH and Sack, MN. Metabolic plasticity and the promotion of cardiac protection in ischemia and ischemic preconditioning. J. Mol. Cell. Cardiol. 2002. 34: p.1077 – 1089
97. Wegrzyn, J, Potla, R, Chwae, YJ, Sepuri, NBV, Zhang, Q, Koeck, T, Derecka, M, Szczepanek, K, Szelag, M, Gornicka, A, Moh, A, Moghaddas, S, Chen, Q, Bobbili, S, Cichy, J, Dulak, J, Baker, DP, Wolfman, A, Stuehr, D, Hassam, MO, Fu, XY, Avadhani, N, Drake, JI, Fawcett, P, Lesnefsky, EJ and larner, AC. Function of Mitochondrial Stat3 in Cellular Respiration. Science. 2009. 323: p.793- 797 |DOI: 10.1126/science.1164551
98. Phillips, D, Reilley, MJ, Aponte, AM, Wang, G, Boja, E, Gucek, M and Balaban, RS. Stoichiometry of STAT3 and Mitochondrial Proteins. Implications for the regulation of oxidative phosphorylation by protein-protein interactions. J. Biol, Chem. 2010. 285(31): p.23532–23536
99. Kawamura, S, Yoshida, KI, Miura, T, Mizukami, Y and Matsuzaki, M. Ischemic preconditioning translocates PKC-δ and -ε, which mediate functional protection in isolated rat heart. Am J Physiol Heart Circ Physiol. 1998. 275:p226-2271
100. Budas, GR, Churchill, EN and Mochly-Rosen, D. Cardioprotective mechanisms of PKC isozyme-selective activators and inhibitors in the treatment of ischemia-reperfusion injury. Pharmacol. Res. 2007. 55: p523–536
101. Steinberg, SF. Distinctive activation mechanisms and functions for protein kinase Cδ. Biochem. J. 2004. 384: p449–459
102. Jingwei, W, Liu, X, Sentex, E, Takeda, N and Dhalla, NS. Increased expression of protein kinase C isoforms in heart failure due to myocardial infarction. Am. J. Physiol. Heart Circ. Physiol. 2003. 284: p.2277–2287
103. Poole, AW, Pula, G, Hers, I, Crosby, D and Jones, ML. PKC-interacting proteins: from function to pharmacology. Trends Pharmacol. Sci. 2004. 25(10): p 528 – 535

104. Inagaki, K, Churchill, E and Mochly-Rosen, D. Epsilon protein kinase C as a potential therapeutic target for the ischemic heart. Cardiovasc. Res. 2006. 70: p 222 – 230
105. Zvi, N. Signaling by G-protein-coupled receptor (GPCR): Studies on the GnRH receptor. Front. Neuroendocrin. 2009. 30(1): p.10–29
106. Balafanova, Z, Bolli, R, Zhang, J, Zheng, Y, Pass, JM, Bhatnagar, A, Tang, XL, Wang, O, Cardwell, E and Ping, P. Nitric Oxide (NO) Induces Nitration of Protein Kinase Cε (PKCε), Facilitating PKCε Translocation via Enhanced PKCε-RACK2 Interactions. J. Biol. Chem. 277(17): p.15021–15027, 2002
107. Baines, CP, Goto M and Downey JM. Oxygen radicals released during ischemic preconditioning contribute to cardioprotection in the rabbit myocardium. J Mol Cell Cardiol. 1997. 29: p.207– 216
108. Calabrese, EJ and Baldwin, LA. Hormesis: The Dose-Response Revolution. Annu. Rev. Pharmacol. Toxicol. 2003. 43:p.175–97
109. Belosjorow, S, Schulz, R, Dorge, H, Schade, FU and Heusch, G. Endotoxin and ischemic preconditioning: TNF-alpha concentration and myocardial infarct development in rabbits. Am. J. Physiol. 1999. 277: p.H2470-H2475
110. Zhang, HY., McPherson, BC., Liu, H, Baman, TS., Rock, P and Yao, Z. H_2O_2 opens mitochondrial K(ATP) channels and inhibits GABA receptors via protein kinase C-epsilon in cardiomyocytes. Am J Physiol Heart Circ Physiol. 2002. 282: p.1395– 1403
111. Ping, P, Takano, H, Zhang, J, Tang, XL, Qiu, Y, Li, RC, Banjeree, S, Dawn, B, Balafanova, Z and Bolli, R. Isoform selective activation of protein kinase C by nitric oxide in the heart of conscious rabbits: a signalling mechanism for both nitric oxide-induced and ischemia-induced preconditioning. Circ. Res. 1999. 8: p.587– 604
112. Balafanova, Z, Bolli, R, Zhang, J, Zheng, Y, Pass, JM, Bhatnagar, A, Tang, XL, Ouli, W, Cardwell, E and Ping, P. Nitric Oxide (NO) Induces Nitration of Protein Kinase Cε (PKCε), Facilitating PKCε Translocation via Enhanced PKCε-RACK2 Interactions. J. Biol. Chem. 2002. 277(17): p.15021-15027
113. Teng, JC, Kay, H, Chen, Q, Adams, JS, Grilli, C, Guglielmello, G, Zambrano, C, Krass, S, Bell, A and Young, LH. Mechanisms related to the cardioprotective effects of protein kinase C epsilon (PKCε) peptide activator or inhibitor in rat ischemia/reperfusion injury. Naunyn-Schmiedeberg's Arch Pharmacol. 2008. 378: p.1–15
114. Costa, ADT, Pierre, SV, Cohen, MV, Downey, JM and Garlid, KD. cGMP signalling in pre- and post-conditioning: the role of mitochondria. Cardiovasc. Res. 2008. 77(2): p.344 – 352 |.doi: 10.1093/cvr/cvm050
115. Quinlan, CL, Costa, AD, Costa, Cl, Pierre, SV, Dos Santos, P and Garlid, KD. Conditioning the heart induces formation of signalosomes that interact with mitochondria to open mitoK_{ATP} channels. AJP – Heart. 2008. 295(3): p.H953-H961
116. Lange, SA, Wolf, B, Schober, K, Wunderlich, C, Marquetant, R, Weinbrenner, C and Strasser, RH. Chronic Angiotensin II Receptor Blockade Induces Cardioprotection During Ischemia by Increased PKC-ε Expression in the Mouse Heart. J. Cardiovasc. Pharmacol. 2007. 49: p.46–55
117. Buhagiar, KA, Hansen, PS, Bewick, NL and Rasmussen, HH. Protein kinase C-epsilon contributes to regulation of the sarcolemmal Na(+)–K(+) pump. Am. J. Physiol. Cell Physiol. 2001. 281: p.C1059–C1063
118. Inagaki, K, Iwanaga, Y, Sarai, N, Onozawa, Y, Takenaka, H, Mochly-Rosen, D and Kihara, Y. Tissue Angiotensin II During Progression of Ventricular Hypertrophy to Heart Failure in Hypertensive Rats: Differential Effects on PKCε and PKCβ. J. Mol. Cell. Cardiol. 2002. 34: p.1377–1385

119. Malhotra, A, Kang, BP, Cheung, S, Opawumi, D and Meggs, LG. Angiotensin II Promotes Glucose-Induced Activation of Cardiac Protein Kinase C Isozymes and Phosphorylation of Troponin I. Diabetes. 2001. 50(8): p.1918 – 1926
120. Griendling, KK, Delafontaine, P, Rittenhouse, SE, Gimbrone, MA and Alexander, RW. Correlation of receptor sequestration with sustained diacylglycerol accumulation in angiotensin II-stimulated cultured vascular smooth muscle cells. J. Biol. Chem. 1987. 262: p.14555 – 14562
121. Palaniyandi, SS, Sun, L, Ferreira, JCB and Mochly-Rosen, D. Protein kinase C in heart failure: a therapeutic target? Cardiovasc. Res. 2009. 82: p229 – 239. doi:10.1093/cvr/cvp001
122. Stein, AB, Tang, XL, Guo, Y, Xuan, YT, Dawn, B and Bolli, R. Delayed adaptation of the heart to stress: late preconditioning. Stroke. 2004. 35: p.2676 – 26799
123. Gupta, S, Purcell, NH, Lin, A and Sen, S . Activation of nuclear factor kappaβ is necessary for myotrophin-induced cardiac hypertrophy. J Cell Biol. 2002. 159: p.1019 – 1028
124. Huang, WC, Chen, JJ and Chen, CC. c-Src-dependent tyrosine phosphorylation of ικκbeta is involved in tumor necrosis factor-alpha induced intercellular adhesion molecule-1 expression. J. Biol. Chem. 2003. 278: p.9944 – 9952
125. Li, RC, Ping, P, Zhang, J, Wead, WB, Cao, X, Gao, J, Zheng, Y, Huang, S, Han, J and Bolli, R. PKCεpsilon modulates NF-kappaβ and AP-1 via mitogen-activated protein kinases in adult rabbit cardiomyocytes. Am. J. Physiol. Heart Circ. Physiol. 2000. 279: p.H1679– 1689
126. Disatnik, MH, Buraggi, G and Mochly-Rosen, D. Localization of protein kinase C isozymes in cardiac myocytes. Exp. Cell Res. 1994. 210: p.287–297
127. Heidkamp, MC, Bayer, Al, Martin, JL and Samarel, AM. Differential activation of mitogen-activated protein kinase cascades and apoptosis by protein kinase C epsilon and delta in neonatal rat ventricular myocytes. Circ. Res. 2001. 89(10): p.882-890
128. Ping, P, Zhang, J, Cao, X, Li, RCX, Kong, D, Tang, XL, Qiu, Y, Manchikalapudi, S, Auchampach, JA, Black, RG and Bolli, R. PKC-dependent activation of p44/p42 MAPKs during myocardial ischemia-reperfusion in conscious rabbits. AJP – Heart. 1999. 276(5): p.H1468-H1481
129. Baines, CP, Zhang, J, Wang, GW, Zheng, YT, Xiu, JX, Cardwell, EM, Bolli, R and Ping, P. Mitochondrial PKCε and MAPK Form Signaling Modules in the Murine Heart Enhanced Mitochondrial PKCε-MAPK Interactions and Differential MAPK Activation in PKCε-Induced Cardioprotection. Circ. Res. 2002. 90: p.390 – 397
130. Edmondson, RD, Vondriska, TM, Bieder,an, KJ, Zhang, J, Jones, RC, Zheng, Y, Allen, DL, Xiu, JX, Cardwell, EM, Pisano, MR and Ping, P. Protein Kinase C ε Signaling Complexes Include Metabolism- and Transcription/Translation-related Proteins. Mol. Cell. Proteomics. 2002. 1: p.421-433
131. Mayr, M, Liem, D, Zhang, J, Li, X, Avliyakulov, NK, Yang, JI, Young, G, Vondriska, TM, Ladroue, C, Madhu, B, Griffiths, JR, Gomes, A, Xu, Q and Ping, P. Proteomic and metabolomic analysis of cardioprotection: Interplay between protein kinase C epsilon and delta in regulating glucose metabolism of murine hearts. J. Mol. Cell. Cardiol. 2009. 46(2): p.268 – 277
132. McCarthy, J, Lochner, A, Opie, LH, Sack, MN and Essop, MF. PKCε promotes cardiac mitochondrial and metabolic adaptation to chronic hypobaric hypoxia by GSK3β inhibition. J. Cell. Physiol. 2011. 226:p.2457–2468
133. Ping, P, Song, C, Zhang, J, Guo, Y, Cao, X, Li, RCX, Wu, W, Vondriska, TM, Pass, JM, Tang, XL, Piercer, WM and Bolli, R. Formation of protein kinase C(epsilon)-Lck signaling modules confers cardioprotection. J. Clin. Invest, 2002. 109(4): p.499-507

134. Murriel, CL and Mochly-Rosen, D. Opposing roles of δ and εPKC in cardiac ischemia and reperfusion: targeting the apoptotic machinery. Arch. Biochem. Biophy. 2003. 420(2): p.246–254
135. Murry CE, Jennings RB and Reimer KA. Preconditioning with ischemia: a delay of lethal cell injury in ischemic myocardium. Circulation. 1986. 74: p.1124– 36
136. Suleman, N, Somers, S, Smith, R, Opie, LH and Lecour, S. Dual activation of STAT-3 and Akt is required during the trigger phase of ischaemic preconditioning. Cardiovasc. Res. 2008. 79: p.127–133
137. Herman, MV, Heinle, RA, Klein, MD and Gorlin, R. Localized Disorders in Myocardial Contraction — Asynergy and Its Role in Congestive Heart Failure. N Engl J Med. 1967. 277: p.222 – 232
138. Dorn, GW 2nd, Souroujon, MC, Liron, T, Chen, CH, Gray, MO, Zhou, HZ, Csukai, M, Wu, G, Lorenz, JN and Mochly-Rosen, D. Sustained in vivo cardiac protection by a rationally designed peptide that causes epsilon protein kinase C translocation. Proc. Natl. Acad. Sci. USA 1999. 96(22): p.12798 – 12803
139. Saurin, AT, Pennington, DJ, Raat, NJ, Latchman, DS, Owen, MJ and Marber, MS. Targeted disruption of the protein kinase C epsilon gene abolishes the infarct size reduction that follows ischaemic preconditioning of isolated buffer-perfused mouse hearts. Cardiovasc. Res. 2002. 55: 672 – 680
140. Bowling, N, Huang, XD, Sandusky, GE, Fouts, RL, Mintze, K, Esterman, M, Allen, PD, Maddi, R, McCall, E and Vlahos, CJ. Protein kinase C-alpha and -epsilon modulate connexin- 43 phosphorylation in human heart. .J Mol. Cell. Cardiol. 2001. 33(4): p.789–798
141. Bao, X, Altenberg, GA and Reuss, L. Mechanism of regulation of the gap junction protein connexin 43 by protein kinase C-mediated phosphorylation. Am. J. Physiol. Cell. Physiol.2004. 286: p.C647–C654
142. Beardslee, MA, Lerner, DL, Tadros, PN, Laing, JG, Beyer, EC, Yamada, KA, Kleber, AG, Schuessler, RB and Saffitz, JE. Dephosphorylation and Intracellular Redistribution of Ventricular Connexin43 During Electrical Uncoupling Induced by Ischemia. Circ. Res. 2000. 87: p.656 – 662 |doi: 10.1161/01.RES.87.8.656
143. Doble, BW, Ping, P and Kardami, E. The ε Subtype of Protein Kinase C Is Required for Cardiomyocyte Connexin-43 Phosphorylation. Circ. Res. 2000. 86: p.293 – 301 |doi: 10.1161/01.RES.86.3.293
144. Fryer, RM, Wang, Y, Hsu, AK and Gross, GJ. Essential activation of PKC delta in opioid-initiated cardioprotection. Am. J. Physiol. Heart Circ. Physiol. 2001. 280: p.H1346– 53
145. Zhang J, Bolli R, Lalli J, Tang XL, Li RCX, Zheng Y, et al. Ischemic preconditioning and phorbol ester redistribute protein kinase C epsilon to the nucleus, sarcolemmal membranes and mitochondria in rabbit myocardium. Circulation. 1999. 100(Suppl I):I-325
146. Liang, BT. Protein kinase C-mediated preconditioning of cardiac myocytes: role of adenosine receptor and KATP channel. Am J Physiol. 1997. 273: p.H847– 53
147. Gross GJ, Auchampach JA. Blockade of ATP-sensitive potassium channels prevents myocardial preconditioning in dogs. Circ. Res 1992:70(2):223–33
148. Suzuki M, Sasaki N, Miki T,Sakamoto, N, Ohmoto-Sekine, Y, Tamagawa, M, Seino, S, Marban, E and Nakaya, H. Role of sarcolemmal K(ATP) channels in cardioprotection against ischemia/reperfusion injury in mice. J. Clin. Invest 2002:109(4):509–16
149. Gustafsson, AB, and Gottlieb, RA. Heart mitochondria: gates of life and death. Cardiovasc. Res. 2007.77(2): p334 – 343. doi:10.1093/cvr/cvm005
150. Noma, A. ATP-regulated K+ channels in cardiac muscle. Nature. 1983. 305: p.147 – 148

151. Cole, WC, McPherson, CD and Sontag, D. ATP-regulated K+ channels protect the myocardium against ischemia/reperfusion damage. Circ. Res. 1991. 69: p.571 – 581
152. Mitchell MB, Meng X, Ao L, Brown JM, Harken AH, Banerjee A. Preconditioning of isolated rat heart is mediated by protein kinase C. Circ. Res 1995. 76: p.73– 81
153. Xuan YT, Guo Y, Zhu Y, Wang OL, Rokosh G, Messing RO, et al. Role of the protein kinase C-epsilon-Raf-1-MEK-1/2-p44/42 MAPK signaling cascade in the activation of signal transducers and activators of transcription 1 and 3 and induction of cyclooxygenase-2 after ischemic preconditioning. Circulation. 2005:112:1971– 8
154. Yao, YT, Li, LH, Chen, L, Wang, WP, Li, LB and Gao, CQ. Sevoflurane postconditioning protects isolated rat hearts against ischemia-reperfusion injury: the role of radical oxygen species, extracellular signal-related kinases 1/2 and mitochondrial permeability transition pore. Mol. Biol. Rep. 2010. 37(5): p.2439 – 2446
155. Baines, CP, Song, CX, Zheng, YT, Wang, GW, Zhang, J, Wang, OL, Guo, Y, Bolli, R, Cardwell, EM and Ping, PP. Protein kinase C ϵ interacts with and inhibits the permeability transition pore in cardiac mitochondria. Circ. Res. 2003:92:873– 80
156. Clarke, SJ, Khaliulin, I, Das, M, Parker, JE, Heesom, KJ and Halestrap, AP. Inhibition of Mitochondrial Permeability Transition Pore Opening by Ischemic Preconditioning Is Probably Mediated by Reduction of Oxidative Stress Rather Than Mitochondrial Protein Phosphorylation. Circ. Res. 2008. 102: p1082-1090. DOI: 10.1161/CIRCRESAHA.107.167072
157. McCarthy, J, McLeod, CJ, Minners, J, Essop, MF, Ping, PP and Sack, MN. PKCε activation augments cardiac mitochondrial respiratory post-anoxic reserve—a putative mechanism in PKCε cardioprotection. J. Mol. Cell. Cardiol. 2005. 38(4): p.607 – 700
158. Finegan, BA, Lopaschuk, GD, Gandhi, M and Clanachan, AS. Inhibition of glycolysis and enhanced mechanical function of working rat hearts as a result of adenosine A_1 receptor stimulation during reperfusion following ischaemia. Brit. J. Pharmacol. 1996. 118(2): p.355–363
159. Gores, GJ, Nieminen, AL, Wray, BE, Herman, B and Lemasters, JJ. Intracellular pH during "chemical hypoxia" in cultured rat hepatocytesprotection by intracellular acidosis against the onset of cell death. J. Clin. Invest. 1989. 83: p.386–396
160. Wolfrum, S, Neinstedt, J, Heidbreder, M, Schneider, K, Dominiak, P and Dendorfer, A. Calcitonin gene related peptide mediates cardioprotection by remote preconditioning. Regul. Peptides. 2005. 127(1-3): p.217 – 224
161. Wolfrum, S, Schneider, K, Heidbreder, M, Neinstedt, J, Dominiak, P and Dendorfer, A. Remote preconditioning protects the heart by activating myocardial PKCε-isoform. Cardiovasc. Res. 2002. 55: p.583 – 589
162. Braun, MU and Mochly-Rosen D. Opposing effects of delta- and zeta-protein kinase C isozymes on cardiac fibroblast proliferation: use of isozyme selective inhibitors. J. Mol. Cell. Cardiol 2003: 35:895–903
163. Stawowy, P, Margeta, C, Blaschke, F, Lindschau, C, Spencer-Hansch, C, Leitges, M, Biaginig, G, Fleck, E and Graf, K. Protein kinase C epsilon mediates angiotensin II-induced activation of β_1-integrins in cardiac fibroblasts. Cardiovasc. Res. 2005. 67(1): p.50 – 59 |doi:10.1016/j.cardiores.2005.03.002
164. Mochly-Rosen, D, Wu, G, Hahn, H, Osinska, H, Liron, T, Lorenz, JN, Yatani, A, Robbins, J and Dorn, GW 2nd. Cardiotrophic effects of protein kinase C epsilon: analysis by in vivo modulation of PKCεpsilon translocation. Circ. Res. 2000. 86: p.1173 – 1179

165. Inagaki, K, Koyanagi, T, Berry, NC, Sun, L and Mochly-Rosen, D. Pharmacological inhibition of epsilon-protein kinase C attenuates cardiac fibrosis and dysfunction in hypertension-induced heart failure. Hypertension. 2008. 51: p.1565–1569
166. Klein, G, Schaefer, A, Hilfiker-Kleiner, D, Opperman, D, Shukla, P, Quint, A, Podewski, E, Hilfiker, A, Schrder, F, Leitges, M and Drexler, H. Increased collagen deposition and diastolic dysfunction but preserved myocardial hypertrophy after pressure overload in mice lacking PKCεpsilon. Circ. Res. 2005. 96: p.748 – 755
167. Depre, C, Shipley, GL, Chen, W, Han, Q, Doenst, T, Moore, ML, Stepkowski, S, Davies, PJA and Taegtmeyer, H. Unloaded heart in vivo replicates fetal gene expression of cardiac hypertrophy. Nat Med. 1998. 4(11): p.1269 – 1275
168. Takeda, K, Kaisho, T, Yoshida, N, Takeda, J, Kishimoto, T and Akira, S. STAT3 activation is responsible for IL-6-dependent T cell proliferation through preventing apoptosis: generation and characterization of T cell-specific STAT3-deficient mice. J. Immunol. 1998. 161: p.4652 – 4660
169. Suleman, N. The role of Signal Transducer and Activator of Transcription 3 (STAT3) in ischemic and pharmacological preconditioning. Thesis presented for the Degree of Doctor of Philosophy (Medicine), University of Cape Town. August 2006. p.55 – 59
170. Aznar, S, Valeron, PF, del Rincon, SV, Perez, LF, Perona, R and Lacal, JC. Simultaneous Tyrosine and Serine Phosphorylation of STAT3 Transcription Factor Is Involved in Rho A GTPase Oncogenic Transformation. Mol. Biol. Cell. 2001. 12: p.3282 – 3294
171. Sumeray, MS, Rees, DD, Yellon, DM. Infarct size and nitric oxide synthase in murine myocardium. J. Mol. Cell. Cardiol. 2000. 32: p.35– 42
172. Boudina, S, Sena, S, O'Neill, BT, Tathireddy, P, Young, ME and Abel, D. Reduced mitochondrial oxidative capacity and increased mitochondrial uncoupling impair myocardial energetics in obesity. Circulation. 2005. 112: p.2686 - 2695 |doi: 10.1161/CIRCULATIONAHA.105.554360
173. Inagaki, K, Begley, R, Ikeno, F and Mochly-Rosen, D. Cardioprotection by e-Protein Kinase C Activation From Ischemia: Continuous Delivery and Antiarrhythmic Effect of an e-Protein Kinase C-Activating Peptide. Circulation. 2005. 111: p.44 – 50
174. Schust, J, Sperl, B, Hollis, A, Mayer, TU and Berg, T. Stattic: A Small-Molecule Inhibitor of STAT3 Activation and Dimerization. Chembiol. 2006. 13: p.1235 – 1242 |DOI 10.1016/j.chembiol.2006.09.018
175. Williams, SD and Ford, DA. Calcium-independent phospholipase A(2) mediates CREB phosphorylation and c-fos expression during ischemia. Am J Physiol Heart Circ Physiol. 2001. 281(1): p.168 – 176
176. Bradford, MM. A rapid and sensitive method for the quantification of microgram quantities of protein utilizing the principle of protein-dye binding. Analytical Biochemistry. 1976. 72: p.248 – 254
177. U.K Laemmli. Cleavage of Structural Proteins during the Assembly of the Head of Bacteriophage T4. Nature. 227: 680-685. 1970
178. Takagawa, J, Zhang, Y, Wong, ML, Sievers, RE, Kapasi, NK, Wang, Y, Yeghiazarians, Y, Lee, RJ, Grossman, W and Springer, ML. Myocardial infarct size measurement in the mouse chronic infarction model: comparison of area- and length-based approaches. J Appl Physiol. 2007. 102: p.2104 – 2111 |doi:10.1152/japplphysiol.00033.2007
179. Hilfiker-Kleiner, D, Kaminski, K, Podewski, E, Bonda, T, Schaefer, A, Sliwa, K, Forster, O, Quint, A, Landmesser, U, Doerries, C, Luchtefeld, M, Poli, V, Schneider, MD, Balligand, JL, Desjardins, F, Ansari, Aftab, Struman, I, Nguyen, NQN, Zschemisch, NH, Klein, G, Heusch, G,

Schulz, R, Hilfiker, A and Drexler, H. A Cathepsin D-Cleaved 16 kDa Form of Prolactin Mediates Postpartum Cardiomyopathy. Cell. 2007. 128(3): p.589–600

180. Lu, D, Huang, J and Basu, A. Protein kinase Cepsilon activates protein kinase B/Akt via DNA-PK to protect against tumor necrosis factor-alpha-induced cell death. J. Biol. Chem. 2006. 281(32): p.22799-22807

181. Greco, S, Storelli, C and Marsigliante, S. Protein kinase C (PKC)-delta/epsilon mediate the PKC/Akt-dependent phosphorylation of extracellular signal-regulated kinase 1 and 2 in MCF-7 cells simulated by bradykinin. J. Endocrinol. 2006. 188(1):79-89

Budget Estimate:

Item	Quantity	Cost (R)	Total Cost (R)
Chemicals:			
EDTA	500g	730	730
KCl	500g	390	390
Sucrose	500g	370	370
Tris HCl	500g	1300	1300
KH_2PO_4	500g	370	370
Heparin	2ml	25	25
Euthanaze	25ml	250	250
Glutamic acid	100g	330	330
Malic acid	25g	220	220
ADP	1g	650	650
AG490	5mg	800	800
PMA	1mg	1000	1000
peqGOLD protein marker IV	1 vial	1100	1100
Transfer membrane	10sheets	1300	1300
Blotting paper	100	270	270
Methanol	100	220	220
Milk powder	100g	10	10
Primary antibodies	6	1560	9660
Secondary antibodies	2	420	840
ECL western blotting reagents	1	1800	1800
Na_2CO_3	500g	500	500
$CuCO_4.5H_2O$	25g	230	230
K_2-tartarate	100g	130	130
SDS	25g	250	250
NaOH	500g	310	310
Folin-Ciocalteu's phenol reagent	100ml	240	240
B-mercaptoethanol	100ml	200	200
Glycerol	100ml	370	370
Acrylamide	100g	250	250
Ammonium persulphate	25g	220	220
TEMED	25ml	200	200
Glycine	50g	330	330
NaCl	250g	230	230
Tween-20	25ml	120	120
Equipment:			
Forceps	2	120	240
Needles	100	450	450
Dissecting scissors	2	150	150

Petri dish	500	980	380
Dounce glass homogenizer	1	9 000	9000
Plastic packets	1 pack	5	5
Paper towel	1 pack	10	10
Cotton buds	1 pack	10	10
Gloves	1 pack	350	350
Eppendorfs	200	950	950
Test tubes	1000	1 050	1050
1mL disposable cuvettes	2 boxes	950	1900
10mL disposable pipettes	200	1100	1100
Pasteur pipettes	200	160	160
Micropipette tips	-	-	800
Glassware	-	1500	1500
Animals:			
BalbC mice	48	36	432
STAT-3 deficient mice	8	36	432
Wild type STAT-3 mice	8	36	432
Total:			44 566

Appendix A

Solution A
7.23mM K_2EGTA
2.77mM CaK_2EGTA
6.56mM $MgCl_2.6H_2O$
20mM Imidazole
0.5mM DTT
20mM Taurine
53.3mM K-MES
3mM KH_2PO_4
pH to 7.1 for use
Add 5.3mM ATP and 15mM PCR before use

Solution B
7.23mM K_2EGTA
2.77mM CaK_2EGTA
1.38mM $MgCl_2.6H_2O$
20mM Imidazole
0.5mM DTT
20mM Taurine
100mM K-MES
3mM KH_2PO_4
pH to 7.1 for use
Add 2mg BSA per mL

Solution C
20mM Hepes, pH 7.9
2.5mM $MgCl_2$
100uM EDTA
20mM β-glycerophosphate
0.05% Triton X 100
500uM DTT
100uM $NaVO_4$
EDTA protease-free inhibitor
(60% of 1 tablet in 30ml solution C)
1mM PMSF
75mM NaCl
dH_2O to make up volume

Solution D
20mM Hepes pH 7.9
2.5mM $MgCl_2$
100uM EDTA
20mM β-glycerophosphate
0.05% Triton X 100
500uM DTT
100uM $NaVO_4$
EDTA protease-free inhibitor
(60% of 1 tablet in 30ml solution C)
1mM PMSF
75mM NaCl
dH_2O to make up volume

Laemmli buffer
63mM Tris HCl
10% glycerol
2% SDS
0.0025% bromophenol blue
pH 6.8

Separating gel
4.9ml dH_2O
2.5ml of 1.5M Tris HCl, pH8.8
50µl 20% SDS
2.5ml acrylamide
50µl 10% APS
20µl TEMED constitutes enough for a single gel

Stacking gel
3.75ml dH_2O
1.5ml 0.5M Tris HCl, pH6.8
30µl 20% SDS
0.75ml acrylamide
40µl 10% Ammonium persulphate
20µl TEMED constitutes enough for a single gel

Running buffer
0.025M Tris-HCl
0.19M Glycine
0.1% SDS, pH 8.6

Transfer buffer
25mM Tris-HCl
192mM glycine

20% methanol, pH 8.3

TBS-T

0.02M Tris-HCl
0.14M NaCl
0.1% Tween-20
pH7.6